

***IN SITU* GREEN SYNTHESIS OF RED WINE SILVER NANOPARTICLES FOR
THE PRODUCTION OF ANTIMICROBIAL COTTON FABRICS AND THE
INVESTIGATION OF THEIR BIOMEDICAL EFFECTS**

ALEXANDRIA ERASMUS



A thesis submitted in fulfilment of the requirements for the degree of Magister Scientiae in the Department of Biotechnology, University of the Western Cape.

Supervisor: Prof. Abram Madiehe

Co-supervisor: Dr. Nicole Sibuyi

September 2024

KEYWORDS

Antimicrobial activity

Antimicrobial resistance

ESKAPE

Nanotechnology

Silver nanoparticles (AgNPs)

Anti-cancer

Antioxidant

Red wine

Cotton

In situ synthesis

ABSTRACT

***In situ* green synthesis of red wine silver nanoparticles for the production of antimicrobial cotton fabrics and the investigation of their biomedical effects**

A. Erasmus

MSc Thesis, Department of Biotechnology, University of the Western Cape

Microbial infections, particularly those caused by pathogenic bacteria, pose a significant barrier in the treatment of infectious diseases. In addition, overuse of antibiotics has resulted in the development of antimicrobial resistance (AMR). AMR is a growing global health concern that can cause serious complications in common infections and chronic wounds infected with AMR microbes. Conventional therapeutic approaches previously used in these conditions (wounds and microbial infections) become ineffective and their life cycle are prolonged. Hence, it is crucial to create innovative and alternative antimicrobial treatment strategies.

The field of biomedicine can benefit from the application of nanotechnology to produce alternative or enhanced pharmaceutical products and therapies. Silver nanoparticles (AgNPs) have demonstrated strong antimicrobial properties and have shown to be beneficial in treating AMR infections. Their added benefit in chronic wounds is their ability to promote the wound healing process by stimulating angiogenesis, cell proliferation, and collagen synthesis, among others. These properties are enhanced in AgNPs synthesized by using medicinal plant extracts. Although green synthesis using this route is rapid, easy and cheap; it can often be limited by low solubility and aggregation after purification. *In situ* synthesis of nanoparticles offers advantages like enhanced stability, better uniformity, reduced contamination, cost-effectiveness, and tailored functionality, especially when nanoparticles need to be directly integrated into a matrix. This synthesis approach has a wide range of applications, including textiles and wound healing dressings. Cotton has been utilised in medical applications since the Middle Ages, primarily as a material for dressing wounds, whereas red wine is recognised for its elevated levels of resveratrol – a phenolic chemical molecule that possesses strong antioxidant and anti-inflammatory qualities.

This study reports on the green synthesis of AgNPs using freeze-dried red wine extract (RW) (RW-AgNPs), the fabrication of RW-AgNP-loaded cotton fabrics (RW-ALC), and the investigation of their antimicrobial, antioxidant, and cytotoxic properties. RW-AgNPs were green-synthesized by optimizing pH, silver nitrate (AgNO₃) concentration, and RW extract

concentration under hydrothermal conditions and characterized using several physicochemical techniques including Ultraviolet-visible (UV-vis) Spectroscopy, Dynamic Light Scattering (DLS) using a Zetasizer, High-Resolution Transmission Electron Microscopy (HR-TEM), Scanning Electron Microscopy (SEM) and Fourier-Transform Infrared (FTIR) Spectroscopy. The RW-ALC were synthesized *in situ* under hydrothermal conditions for one hour using RW extract at a concentration of 6.25 mg/ml and pH 10, and AgNO₃ at a concentration of 3 mM. Assessment of antioxidant activity of the RW and RW-AgNPs was conducted using the ABTS and DPPH scavenging assays. Varying quantities of RW, RW-AgNPs, and the positive control ascorbic acid (ranging from 0.78 to 100 µg/ml) were used in the assays. The antibacterial activity of the RW-ALC and RW-AgNPs was evaluated using the agar disc diffusion and broth microdilution assays against the human pathogens *S. aureus*, MRSA, *E. coli*, *E. cloacae*, *K. pneumoniae*, *P. aeruginosa*, and *A. baumannii*. In the disc diffusion assay, RW-ALC samples synthesized with varying concentrations of RW (ranging from 1.56 to 25 mg/ml) were employed as the treatment. A standard cotton piece served as the negative control. The positive control was prepared by applying 50 µl of a 15 µg/ml Ciprofloxacin solution to a clean cotton piece, except for the *E. coli* samples, where a 10 µg/ml Ciprofloxacin concentration was used instead. The Mueller-Hinton agar (MHA) plates were incubated at 37 °C for 24 hours. The effect of pretreatment with 2-mercaptoethanol on the antibacterial efficacy of the RW-ALC was also investigated. For the microdilution assay, bacterial cultures were subjected to treatment for 24 hours using RW-AgNPs at serially diluted concentrations of 25, 12.5, 6.25, 3.125, 1.56, 0.78, 0.39, and 0.195 µg/ml. The negative control consisted of 50 µl of Mueller-Hinton broth (MHB) added to the well. For the positive control, 50 µl of a solution containing 10 µg/ml of Ciprofloxacin was introduced into each well, with the exception of *E. coli*, for which a concentration of 5 µg/ml of Ciprofloxacin was used. Cytotoxic properties of the RW-AgNPs on five cancerous (MCF-7, Caco-2, PC-3, Panc-1, MIA-Paca-2) and one non-cancerous (KMST-6) human cell lines was assessed using the WST-1 cell viability assay. Cell lines were treated for 24 hours with RW and RW-AgNPs at concentrations ranging from 0 – 100 µg/ml. 5 % DMSO was utilised as a positive control.

The RW-AgNPs were spherical with a core size of 8.7 ± 1.3 nm, hydrodynamic size of 104.30 ± 5.51 nm, PDI value of 0.344 ± 0.2 and ζ -potential of -21.3 ± 6.16 mV. RW-AgNPs exhibited minimum inhibitory concentrations and minimum bactericidal concentrations against *S. aureus* (0.195 µg/ml and 0.78 µg/ml), MRSA (1.56 µg/ml and 3.125 µg/ml), *K. pneumoniae* (0.78 µg/ml and 1.56 µg/ml), *A. baumannii* (0.78 µg/ml and 1.56 µg/ml), *E. cloacae* (3.125

$\mu\text{g/ml}$ for both), *E. coli* (0.78 $\mu\text{g/ml}$ for both), and *P. aeruginosa* (3.125 $\mu\text{g/ml}$ and 6.25 $\mu\text{g/ml}$). Characterisation of the cotton showed polydispersed RW-AgNPs on the surface at a concentration of 80.2 $\mu\text{g/ml}$. The results of the DPPH antioxidant assay demonstrate that the scavenging activity of RW-AgNPs is dose-dependent within the concentration range of 3.125 – 100 $\mu\text{g/ml}$. No significant activity was observed at concentrations between 0.78 and 1.56 $\mu\text{g/ml}$. While RW-AgNPs exhibited considerable antioxidant activity, their efficacy was lower compared to that of RW and ascorbic acid. Conversely, in the ABTS assay, RW, RW-AgNPs, and ascorbic acid (used as a positive control) showed a dose-dependent reduction of the ABTS $\bullet+$ radical. Notably, within the concentration range of 0.78 to 50 $\mu\text{g/ml}$, RW-AgNPs exhibited superior scavenging activity compared to the positive control. RW-ALC exhibited significant antibacterial activity, with zones of inhibition ranging from 12.33 ± 1.15 mm to 23.5 ± 5.15 mm in comparison to 10 $\mu\text{g/ml}$ Ciprofloxacin (between 10 ± 3 mm – 19.17 ± 1.39 mm). Preincubation with 2-mercaptoethanol abrogated the antibacterial activity of RW-ALC, indicating that the antibacterial properties are attributed to silver's ability to bind to sulfhydryl groups. Furthermore, RW-AgNPs showed significant cytotoxicity towards the cancer cell lines: MCF-7; PC-3; Caco-2; MIA-Paca-2; Panc-1 cells with half maximal inhibitory concentration (IC_{50}) values of 11.47 $\mu\text{g/ml}$, 10.98 $\mu\text{g/ml}$, 6.76 $\mu\text{g/ml}$, 7.89 $\mu\text{g/ml}$, and 3.76 $\mu\text{g/ml}$, respectively. Reduced cytotoxicity was observed against the normal human fibroblast KMST-6 cell line (IC_{50} of 27.7 $\mu\text{g/ml}$), suggesting that the RW-AgNPs can be effectively employed in the treatment of bacterial infections and cancer with minimal detrimental effects to healthy mammalian cells.


This study demonstrated that RW can be used to synthesize AgNPs and AgNP-loaded textiles *in situ* under hydrothermal conditions. Furthermore, when evaluating the biological effects of the resultant RW-AgNPs and RW-ALC *in vitro*, both had potent antibacterial and anticancer effects. The RW-ALC could be useful in treating infectious diseases, including bacteria infected chronic wounds. However, cytotoxic effects of these RW-AgNPs require further investigation to ensure their biocompatibility at concentrations that are minimally detrimental to mammalian cells yet still toxic to bacteria and cancer cells. Further studies are underway to elucidate the anticancer mechanisms of the RW-AgNPs. These could then be transformed into novel affordable remedies for chronic non-healing wounds and cancer.

DECLARATION

I declare that “*In situ* green synthesis of red wine silver nanoparticles for the production of antimicrobial cotton fabrics and the investigation of their biomedical effects” is my own work, that it has not been submitted for any degree or examination in any other university, and that all the sources I have used or quoted have been indicated and acknowledged by complete references.

Full name: Alexandria Erasmus

Date: 17th September 2024

Signed: 

ACKNOWLEDGEMENTS

All thanks, glory and honour to my Lord and Saviour, who has carried me through each new day. His grace alone has allowed me to conquer every challenge, and I know that I am highly favoured. **Psalms 46:5**. *“God is in the midst of her; she shall not be moved”*.

To Prof. Abram Madiehe – thank you for your patience, support, and invaluable mentorship. It has not always been easy, but you have taught me the power of resilience and dedication. Being under your supervision is a privilege I cherish.

Dr. Nicole Sibuyi, I am immensely grateful for the time and effort you’ve invested into ensuring that I achieve my full potential and for all of your words of reassurance; they’ve helped me more than you know.

Thank you to Prof. Mervin Meyer, whose assistance and support have been vital in my postgraduate journey.

To my friends in the Department of Biotechnology, Jessica Morrow, Miché Hess, Darin Holmon, Alice Kanyerere, and Junaid Mia – our friendship has been a great source of strength and courage and has carried us through three degrees. Here’s to the next!

To all my lab-mates in the DSI/MINTEK Nanotechnology Innovation Centre, thank you for being the most amazing colleagues any scientist could ask for. Thank you for all your help, your kindness, and your advice. Our culture is one I am thankful for every day. A special thanks to Jodi Couert; you are the big brother I’ve always wanted, and your positivity and warmth has brought me joy when I needed it most. And, to Thendo Mabuda, there’s so much to thank you for. But above all, thank you for believing in me, even when I didn’t believe in myself.

To my parents, Ashley Erasmus and Alicia Sawyer, thank you for all the sacrifices you have made to ensure that I could become the best possible version of myself. I am the best of both of you, and everything I accomplish is all thanks to you. To my siblings, Seth, Leah, and Sophia, thank you for being my pride and joy; I hope I make you just as proud. I love you more than words can say.

Clayé, thank you for being my rock. I would not be where I am – or who I am – today without your unconditional love and support. You are my biggest blessing. Thank you.

Lastly, I would like to extend my heartfelt gratitude and thanks to the Department of Science and Innovation-Mintek Nanotechnology Innovation Centre Biolabels Node for providing me

with the financial support needed to further my studies, and to the NBRG lab, Department of Biotechnology, and the University of the Western Cape for the resources to do so.

DEDICATION

This thesis is lovingly dedicated to my family, whose boundless support and encouragement have been my guiding light. To my parents, whose sacrifices and unwavering belief in my potential have shaped who I am today—I owe this achievement to you. To my friends, who provided comfort, laughter, and perspective when I needed it most, and to my mentors, whose wisdom and guidance have inspired and challenged me—thank you for believing in me even when I doubted myself. This work is a tribute to your love, faith, and endless patience.

CONFERENCE CONTRIBUTIONS

Erasmus A., Sibuyi, N.R.S., Meyer, M., and Madiehe, A.M. “*In situ* green synthesis of red wine silver nanoparticles on cotton fabrics and investigation of their biological effects” at the 2024 NanoAfrica Conference at Sun City, North-West Province, South Africa, 20-24 October 2024. **Poster presentation (First prize).**

TABLE OF CONTENTS

KEYWORDS.....	i
ABSTRACT.....	ii
DECLARATION.....	v
ACKNOWLEDGEMENTS	vi
DEDICATION.....	viii
CONFERENCE CONTRIBUTIONS.....	ix
LIST OF ABBREVIATIONS.....	xiii
LIST OF TABLES.....	xvi
LIST OF FIGURES.....	xvii
CHAPTER 1: LITERATURE REVIEW	1
1.1 Introduction.....	1
1.2 Human Bacterial Infections.....	2
1.2.1 Antimicrobial resistance (AMR)	5
1.2.2 AMR in South Africa	11
1.2.3 Current AMR treatments and their limitations	13
1.3 Green nanotechnology and plant-based therapy as alternative treatment for AMR.....	14
1.4 Nanotechnology in medicine.....	15
1.4.1 History of nanotechnology	16
1.4.2 Types of nanoparticles (NPs)	17
1.4.3 Ag-based agents in the fight against AMR	19
1.4.3.1 Synthesis of AgNPs.....	19
1.4.3.1.1 Green synthesis of AgNPs.....	21
1.4.3.1.2 Biosynthesis of AgNPs from microorganisms	24
1.4.3.1.3 Biosynthesis of AgNPs from plant material	25
1.4.3.2 Biomedical applications of AgNPs	26
1.4.3.2.1 AgNPs as drug-delivery systems.....	26
1.4.3.2.2 AgNPs for wound healing.....	27
1.4.3.2.3 Anti-cancer effects of AgNPs.....	29

1.4.4 AgNPs as antibacterial agents.....	31
1.4.5 Production of AgNP-loaded antimicrobial textiles.....	33
1.4.6 Antibacterial mechanism of AgNPs.....	34
1.5 Red grapes and red wine.....	36
1.5.1 Resveratrol.....	38
1.5.2 Antimicrobial Compounds Derived from Grape By-Products.....	40
1.5.3 Wine By-Products in the fight against antibiotic resistance.....	42
1.6 Detailed research proposal.....	43
1.6.1 Problem statement.....	43
1.6.2 Aims and objectives.....	43
1.6.3 Hypothesis.....	44
CHAPTER 2: MATERIALS AND METHODS.....	45
2.1. Materials – Reagents, Equipment, and Suppliers.....	45
2.2. Research Methodology.....	50
2.2.1 Sample Preparation.....	50
2.2.2 Hydrothermal synthesis of RW-ALC and RW-AgNPs.....	50
2.2.2.1 Effect of pH on in situ synthesis of RW-ALC.....	50
2.2.2.2 Effect of AgNO ₃ concentration on the hydrothermal synthesis of RW-AgNPs.....	51
2.2.2.3 Effect of RW concentration on in situ synthesis of RW-AgNPs and RW-ALC.....	51
2.2.2.4 Upscaled synthesis and characterisation of RW-AgNPs and RW-ALC.....	51
2.2.2.4.1 Ultraviolet-visible spectroscopy.....	51
2.2.2.4.2 Dynamic Light Scattering.....	52
2.2.2.4.3 High-resolution Transmission Electron microscopy.....	52
2.2.2.4.4 Scanning Electron microscopy.....	52
2.2.2.4.5 Fourier-transform Infrared spectroscopy.....	52
2.2.2.4.6 Inductively Coupled Plasma Optical Emission Spectrometry.....	53
2.2.3 Stability analysis of RW-AgNPs.....	53
2.2.4 Analysis of phytochemical composition and assessment of antioxidant activity.....	54
2.2.4.1 Total Phenolic Content (TPC).....	54
2.2.4.2 2,2'-azino-di-(3-ethylbenzthiazoline sulfonic acid (ABTS) scavenging assay.....	54
2.2.4.3 2,2-diphenyl-1-picrylhydrazyl (DPPH) scavenging assay.....	54
2.2.5 Antibacterial efficacy of RW-AgNPs and RW-ALC.....	55
2.2.5.1 MacFarland standardising of bacteria culture for microbiological assays.....	55
2.2.5.2 Evaluating the antibacterial activity of RW-ALC using disc diffusion method.....	55
2.2.5.3 Evaluating the effects of 2-mercaptoethanol on the antibacterial activity of RW-ALC.....	56

2.2.5.4 Determination of MIC	56
2.2.5.5 Determination of MBC	56
2.2.6 Effect of RW-AgNPs on human cell lines <i>in vitro</i>	56
2.2.6.1. Cell culture and maintenance	56
2.2.6.2 Cell trypsinisation.....	57
2.2.6.3 Cell cryopreservation	57
2.2.6.4 Cell count: trypan blue exclusion assay	57
2.2.6.5 Cell viability assay: WST-1.....	58
2.2.7 Statistical analysis.....	58
CHAPTER 3: RESULTS AND DISCUSSION.....	59
3.1 Optimization of hydrothermal synthesis of RW-AgNPs	59
3.1.1 Visual observation of synthesis	60
3.1.2 Effect of pH on RW-AgNPs synthesis	61
3.1.3 Effect of AgNO ₃ concentration on hydrothermal synthesis of RW-AgNPs.....	62
3.1.4 Effect of RW concentration on RW-ALC synthesis.....	63
3.2 Upscaled synthesis and characterisation of RW-AgNPs and RALC	66
3.2.1 UV-Vis spectroscopy analysis of RW-AgNPs	66
3.2.2 DLS analysis of RW-AgNPs.....	67
3.2.3 HR-TEM analysis of RW-AgNPs.....	69
3.2.4 SEM analysis of RW-ALC.....	71
3.2.5 FTIR analysis of RW, RW-AgNPs and RW-ALC.....	73
3.3 Stability analysis of RW-AgNPs	77
3.4 Phytochemical composition and antioxidant activity of RW-AgNPs.....	80
3.4.1 TPC of RW and RW-AgNPs.....	80
3.4.2 Antioxidant analysis of RW and RW-AgNPs.....	81
3.4.2.1 DPPH assay	81
3.4.2.2 ABTS assay.....	82
3.5 Antibacterial activity of RW-AgNPs and RW-ALC.....	84
3.5.1 Disc diffusion assay using RW-ALC	84
3.5.1.1 Effect of 2-mercaptoethanol on the antibacterial activity of RW-ALC.....	89
3.5.2 Microdilution assay using RW-AgNPs.....	93
3.6 Cytotoxicity study	96
CHAPTER 4: CONCLUSION.....	102
REFERENCES.....	103

LIST OF ABBREVIATIONS

°C	Degrees Celsius
β	beta
λ	wavelength
λ _{max}	maximum absorbance/absorption maximum
μl	microlitre
ζ-potential	zeta potential
0-D	Zero-dimensional
1-D	One-dimensional
2-D	Two-dimensional
3-D	Three-dimensional
Al	aluminium
Ag	silver
Ag ⁺	silver ion
Ag ⁰	silver atom
AgNP(s)	silver nanoparticle(s)
AgNO ₃	silver nitrate
AMR	antimicrobial resistance
AMU	antimicrobial use
ATCC	American Type Culture Collection
ATR	Attenuated Total Reflectance
Au	gold
BRICS	Brazil, Russia, India, China, and South Africa
BSIs	bloodstream infections
CDC	Centres for Disease Control and Prevention
CFU/ml	colony-forming units per millilitre
Cu	copper
DLS	dynamic light scattering
EDX	energy-dispersive X-ray
ESBLs	Extended Spectrum Beta-Lactamases

ESKAPE	<i>Enterococcus faecium, Staphylococcus aureus, Klebsiella pneumoniae, Acinetobacter baumannii, Pseudomonas aeruginosa, and Enterobacter</i>
FC	Folin–Ciocalteu
FDA	Food and Drug Administration
Fe	iron
FRAP	Ferric reducing antioxidant power
FTIR	Fourier-transform Infrared spectroscopy
g	gram(s)
GP	grape pomace
HCl	hydrochloric acid
HICs	higher-income countries
HR-TEM	High Resolution-Transmission Electron Microscopy
IC ₅₀	Half maximal inhibitory concentration
ICP-OES	Inductively Coupled Plasma Optical Emission Spectrometry
IR	infrared
KBr	Potassium bromide
keV	kiloelectron volt
L	litre
LMICs	low- and middle-income countries
mM	millimolar
mm	millimetre
MBC	minimum bactericidal concentration
mg	milligram
MHA	Müeller-Hinton agar
MHB	Müeller-Hinton broth
MIC	minimum inhibitory concentration
min(s)	minute(s)
ML	material to liquid
ml	millilitre
MNPs	metallic nanoparticles
mV	millivolt

NaOH	sodium hydroxide
NDoH-RSA	National Department of Health of the Republic of South Africa
nm	nanometre
NP(s)	nanoparticle(s)
OD	optical density
PBS	phosphate buffered saline
PDI	polydispersity index
psi	pounds per square inch
Pt	platinum
ROS	reactive oxygen species
rpm	revolutions per minute
RSA	Republic of South Africa
RT	room temperature
RW-AgNPs	red wine silver nanoparticles
RW-ALC	RW-AgNPs-loaded cotton
RW	red wine extract
SAED	selected area electron diffraction
SD	standard deviation
SEM	standard error of the mean
SPR	surface plasmon resonance
Ti	titanium
TPC	total phenolic content
UTIs	urinary tract infections
UK	United Kingdom
USA	United States of America
WHO	World Health Organization
WST-1	water-soluble tetrazolium salt

LIST OF TABLES

Table 1.1: Microbial defence mechanisms to withstand the impact of antibacterial agents.....	9
Table 1.2: The 12 principles of green chemistry.....	22
Table 2.1: Materials and reagents used and their suppliers.....	45
Table 2.2: Equipment used and their manufacturer.....	47
Table 2.3: Type of cell lines used, their sources, species, and biological media.....	48
Table 2.4: Bacterial strains used and their corresponding ATCC numbers.....	49
Table 3.1: FTIR peak values and peak shifts of RW and RW-AgNPs and their respective functional groups.....	75
Table 3.2: TPC of RW and RW-AgNPs.....	81
Table 3.3: ZOI measurements of RW-ALC synthesised with various concentrations of RW against seven human pathogenic bacteria.....	87
Table 3.4: ZOI measurements of RW-ALC before and after incubation with 2-mercaptoethanol against human pathogenic bacteria.....	91
Table 3.5: MIC and MBC values of RW-AgNPs seven human pathogenic bacteria.....	93

LIST OF FIGURES

Figure 1.1: Overview of the most common human bacterial infections and their causative microorganisms.....	3
Figure 1.2: One Health concept outlining the impact of human, animal, and wildlife health on each other and the surrounding environment.....	6
Figure 1.3: Overview of the ESKAPE pathogens and the human organs that are most susceptible to their infections.....	7
Figure 1.4: Main mechanisms of antibiotic resistance.....	8
Figure 1.5: Burden (A) and distribution (B) of ESKAPE pathogens in the public sector of South Africa from 2018-2022.....	12
Figure 1.6: Analysis of worldwide antibiotic consumption and usage in the human population from 2000 to 2018.....	13
Figure 1.7: Size comparison chart illustrating the sizes of various biological entities and objects, ranging from atoms to a grain of salt, at the nanometre scale.....	15
Figure 1.8: Nanomaterials are classified into organic, inorganic and carbon-based NPs.....	17
Figure 1.9: Overview of different approaches and techniques used to synthesise NPs.....	20
Figure 1.10: Schematic illustration of the green synthesis of MNPs.....	23
Figure 1.11: One-step process of AgNP synthesis using plant extract.....	25
Figure 1.12: Mechanisms of antibacterial activity of AgNPs.....	35
Figure 1.13: Grape pomace methods of extraction and by-products.....	37
Figure 1.14: Schematic illustrating the dual role of resveratrol in modulating autoimmune disorders and cancer, which includes the reduction of pro-inflammatory cytokines (e.g., IL-2, IL-6, TNF- α) and the increase of SIRT1 expression.....	40
Figure 3.1: <i>Ex situ</i> and <i>in situ</i> synthesis of RW-AgNPs under hydrothermal conditions. (a) AgNO ₃ , (b) AgNO ₃ mixed with RW, (c) reaction mixture at the end of the synthesis period, (d) cotton fabrics before and (e) after being used in the <i>in situ</i> synthesis of RW-AgNPs.....	60

Figure 3.2: RW-ALC synthesised under hydrothermal conditions using 3 mM AgNO ₃ and 12.5 mg/ml RW at (a) pH 10 and (b) at natural pH (4.3). (c) UV-Vis spectra of RW-AgNPs showing the effect of various pH levels with 3 mM AgNO ₃ and 12.5 mg/ml RW	62
Figure 3.3: UV-Vis spectra of RW-AgNPs showing the effect of various AgNO ₃ concentrations with 12.5 mg/ml RW.....	63
Figure 3.4: RW-ALC synthesised under hydrothermal conditions using 3 mM AgNO ₃ and various concentrations of RW at pH 10. (a) RW-ALC deposited on 250 mg of cotton and (b) UV-Vis spectra of RW-AgNPs showing the effect of various RW concentrations at pH 10 with 3 mM AgNO ₃	65
Figure 3.5 UV-Vis spectra of RW-AgNPs synthesised under hydrothermal conditions using optimal conditions (6.25 mg/ml RW at pH 10 and 3 mM AgNO ₃).....	66
Figure 3.6: Hydrodynamic size (a) and ζ-potential (b) distribution curves of RW-AgNPs.....	68
Figure 3.7: HR-TEM image analysis of RW-AgNPs. (A) TEM image (scalebar - 30 nm), (B) core size distribution, and (c) Selected area electron diffraction (SAED) pattern of the RW-AgNPs.....	70
Figure 3.8: SEM analysis of the RW-ALC. (a, b); the cotton fabric covered in RW-AgNPs and the control (c).....	72
Figure 3.9: EDX spectra (a) and % weight (b) displaying the composition of the RW-ALC at pH 10 and the presence of a peak at 3 keV characteristic for Ag, as determined by the AgLα lines.....	73
Figure 3.10: FTIR spectra of RW and RW-AgNPs.....	74
Figure 3.11: FTIR spectra of cotton fabric and RW-ALC	77
Figure 3.12: Stability of RW-AgNPs in biological media (ddH ₂ O, PBS, DMEM and MHB)..	79
Figure 3.13: Gallic acid calibration standard curve for determining the TPC of RW and RW-AgNPs.....	80
Figure 3.14: DPPH radical scavenging ability of RW, RW-AgNPs, and ascorbic acid.....	82
Figure 3.15: ABTS radical scavenging ability of RW, RW-AgNPs, and ascorbic acid.....	83
Figure 3.16: Antibacterial activity of RW-ALC using agar disc diffusion assay.....	86

Figure 3.17: Antibacterial activity of RW-ALC using agar disc diffusion assay.....92

Figure 3.18: Investigation of bactericidal effects of RW-AgNPs on Gram-positive (*S. aureus* and MRSA) and Gram-negative (*E. coli* and *P. aeruginosa*) human pathogenic bacteria.....94

Figure 3.19: Screening of the cytotoxic effects of RW and RW-AgNPs using WST-1 assay on human cells: (a) MIA-Paca-2, (b) Panc-1, (c) PC-3, (d) MCF-7, (e) Caco-2, and (f) KMST-6.....97

CHAPTER 1: LITERATURE REVIEW

1.1 Introduction

AMR poses a significant threat to global public health, with *Enterococcus faecium*, *Staphylococcus aureus*, *Klebsiella pneumoniae*, *Acinetobacter baumannii*, *Pseudomonas aeruginosa*, and *Enterobacter* species (ESKAPE) pathogens classified by WHO as a major concern (Murray *et al.*, 2022), necessitating new treatments (Chetty *et al.*, 2019). These pathogens are responsible for many healthcare-associated infections, highlighting the need for new antimicrobial agents. South Africa faces significant challenges with AMR, exacerbated by overuse and misuse of antibiotics (Browne *et al.*, 2021). Current treatments for AMR include antibiotics, which are becoming less effective due to drug resistance (Anees Ahmad *et al.*, 2020). AMR occurs when bacteria evolve to resist antibiotics, making infections harder to treat. This resistance leads to higher medical costs, prolonged hospital stays, and increased mortality. Efforts to combat AMR include improving antibiotic stewardship and developing new antimicrobial agents, such as AgNPs (Anees Ahmad *et al.*, 2020). Nanomaterials are being investigated as potential antibacterial agents (De Oliveira *et al.*, 2020). Inorganic NPs, including metal-based nanoparticles (MNPs) have unique optical and electrical properties, making them essential in various biological and pharmacological applications (Haleem *et al.*, 2023). AgNPs have remarkable antibacterial activity (Almatroudi, 2020) and are suitable for biological applications (Burduşel *et al.*, 2018), this is motivated by the medical history of silver (Ag) for over 2000 years as an antimicrobial agent (Chernousova and Epple, 2013). AgNPs can be synthesized in various forms, dimensions, and sizes for specific biomedical uses. Spherical AgNPs are primarily used in the treatment of bacterial infections and cancer due to their ease of synthesis and absorption by target cells (Riaz *et al.*, 2021). They can also be chemically modified for targeted drug delivery (KJ, 2017).

AgNPs have demonstrated significant antibacterial properties, making them potential candidates for treating bacterial infections (Delgado-Beleño *et al.*, 2018). Their unique properties allow them to disrupt bacterial cell membranes and interfere with cellular processes, leading to bacterial death. AgNPs exert their antibacterial effects through multiple mechanisms, including generating reactive oxygen species (ROS), disrupting cell membranes, and interacting with bacterial DNA (Anees Ahmad *et al.*, 2020). These mechanisms make them effective against a broad spectrum of bacteria, including antibiotic-resistant strains. AgNPs-

loaded wound dressings are being developed to enhance the healing process and prevent infections (Hebeish *et al.*, 2014). These dressings leverage the antibacterial properties of AgNPs to reduce the risk of microbial infection and promote tissue regeneration in the wound healing process (Hasibuan *et al.*, 2021). Furthermore, AgNPs have shown potential in cancer treatment due to their cytotoxic effects on cancer cells (Mahmud *et al.*, 2023). They can induce apoptosis, inhibit cell proliferation, and enhance the efficacy of chemotherapy drugs (Wang *et al.*, 2017). Current cancer treatments include surgery, radiation, and chemotherapy, which have limitations such as side effects and resistance. AgNPs offer a promising alternative with their ability to target cancer cells selectively. AgNPs exhibit anticancer activity through various mechanisms, including inducing oxidative stress, disrupting cellular structures, and enhancing the efficacy of existing cancer treatments (Mahmud *et al.*, 2023). Green nanotechnology is one of the strategies that has been successful in addressing their potential toxicity issues (Simon *et al.*, 2022).

Green synthesis of AgNPs is sustainable, cost-effective, and has minimal environmental impact (Dikshit *et al.*, 2021). Various biological systems such as bacteria, fungi, plant extracts, and small biomolecules (e.g., vitamins, amino acids) have been employed to enhance the production of AgNPs with specific sizes (Parveen *et al.*, 2016). Green-synthesized AgNPs possess antimicrobial properties, making them valuable for treating and preventing bacterial and fungal infections (Rafique *et al.*, 2017). Studies have shown that AgNPs synthesized from plant extracts like *Aloe vera* and *Thuja orientalis* exhibit significant antibacterial and antifungal activities (Burange *et al.*, 2021). Red grapes and RW contain resveratrol and other antimicrobial compounds (Kuršvietienė *et al.*, 2016) that have shown potential in fighting antibiotic resistance. Wine by-products are being explored as alternative treatments against antibiotic-resistant bacteria (Silva *et al.*, 2018). This study seeks to perform the green synthesis and characterisation of AgNPs using RW. Additionally, it aims to create cotton fabrics loaded with RW-AgNPs (RW-ALC) and investigate the antibacterial, antioxidant, and cytotoxic properties of these two nanomaterials.

1.2 Human Bacterial Infections

The skin microbiome comprises a diverse array of bacterial species that serve to safeguard the skin and its host from the external environment and potentially harmful microorganisms (Lambrechts *et al.*, 2022). The human body coexists harmoniously with its own microbiota, and while the relationship is intended to be commensal and mutualistic under physiological

conditions, these microbes can invade and establish colonies within the human body, become pathogenic and cause severe illnesses (Ayres, 2021; Cano *et al.*, 2020). Additionally, bacteria can be spread to people via food, water, air, or living vectors. All human organs are susceptible to bacterial infection as shown in **Figure 1.1**, although particular species have a preference for specific organs (Cano *et al.*, 2020; Mayla and Gohar, 2010).

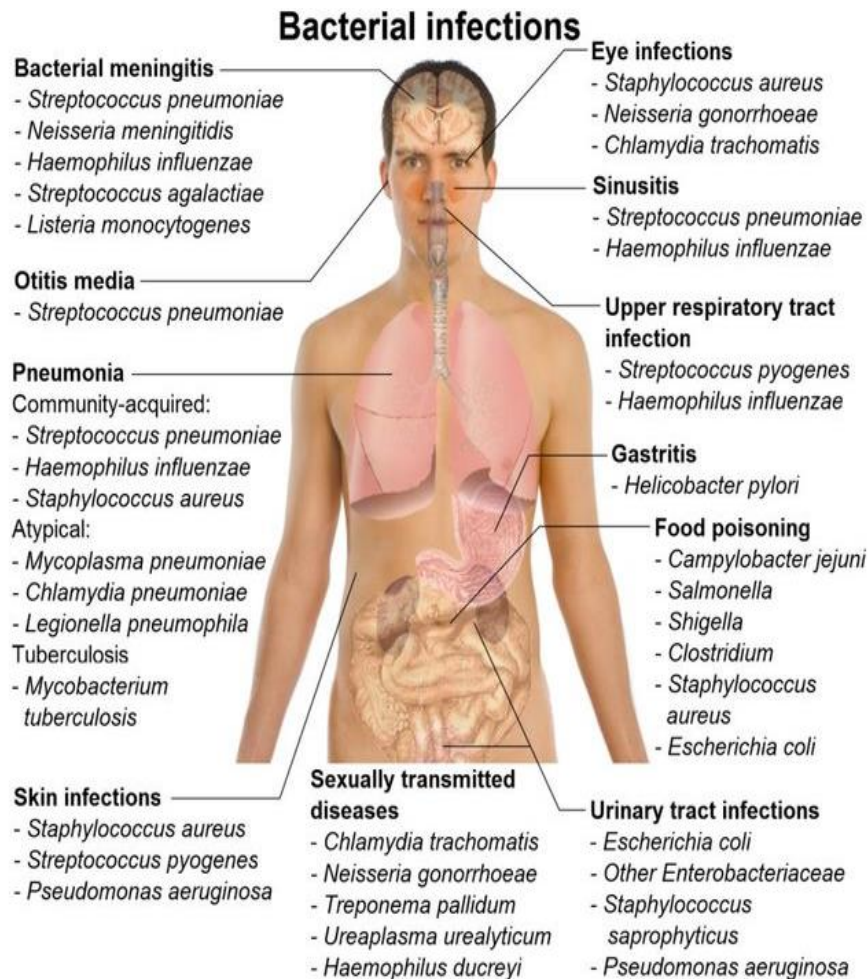


Figure 1.1: Overview of the most common human bacterial infections and their causative microorganisms (adapted from Mayla and Gohar, 2010)

Infectious illnesses claim the lives of more than 17 million individuals annually (Cano *et al.*, 2020). Drug-resistant microorganisms, including bacteria, viruses, parasites, and fungi, are responsible for causing 700,000 fatalities annually on a global scale (Rappuoli *et al.*, 2017). Abundant commensal microbes reside in and on living organisms and provide protection to the host against infections (Lambrechts *et al.*, 2022). However, changes in the external and cutaneous environment lead to an imbalance of these potentially beneficial bacteria. This

change in conditions enables opportunistic microbes to flourish, ultimately resulting in a range of maladies (Lambrechts *et al.*, 2022).

Bacterial infections exert a significant influence on public health, accounting for approximately 9.7 % of global mortality (Cano *et al.*, 2020). Tuberculosis has been ranked as the leading cause of mortality among bacterial infections, accounting for 2.3 % of global fatalities. It is followed by diarrheal bacterial diseases at 2 %, meningitis at 0.5 %, and bacterial sexually transmitted diseases such as syphilis, chlamydia, and gonorrhoea at 0.2 %. Encephalitis also accounts for 0.2 % of global deaths (Cano *et al.*, 2020). The issue of human bacterial infections is exacerbated by the high prevalence of nosocomial infections; as stated by the World Health Organisation (WHO), healthcare-associated illnesses result in around 40,000 fatalities annually (WHO, 2021; Lemiech-Mirowska *et al.*, 2021). In developing nations, the incidence of nosocomial infections can increase by as much as 25 % each year, while in developed countries, it ranges from 5 % to 15 % (Lemiech-Mirowska *et al.*, 2021). Nosocomial infections are a common cause of sepsis, with around 49 % of sepsis patients in intensive care units developing the illness during their hospital stay (WHO, 2020).

Human bacterial infections place a huge burden on the global healthcare system, as they result in extended hospitalization of patients, exorbitant medical costs, and recalcitrant infections (Rappuoli *et al.*, 2017). Infected wounds significantly prolong healing time and can lead to severe complications, including amputation and, in extreme cases, death. Microbial infections are particularly deadly in burn and diabetic wound cases, where they are the leading cause of mortality (Kalantari *et al.*, 2020). Burns are especially prone to infections, severe sepsis, and multiple organ failure due to the loss of the protective skin barrier and the systemic inflammatory response that compromises the immune system. If an infection remains unregulated, it can transform from an acute condition into a chronic one, persisting for months or even years (Hoversten *et al.*, 2020).

Recent trends indicate a significant increase in chronic illnesses such as vascular dysfunction, obesity, and diabetes, which has, in turn, led to a rise in the prevalence of chronic wounds (Kushwaha *et al.*, 2022). Diabetic patients, in particular, have a 15–25 % risk of developing chronic abscesses associated with their condition (Spampinato *et al.*, 2020). Moreover, certain skin conditions, including malignant skin tumors, sporotrichosis, autoimmune skin diseases, dermatomyositis, and physical skin diseases, further heighten individuals' vulnerability to chronic wounds (Wang *et al.*, 2021). Chronic, non-healing wounds expose underlying tissues

to external environments for prolonged periods, increasing susceptibility to complications such as bleeding and osteomyelitis, thereby raising mortality risks in critical cases. Furthermore, chronic infections severely diminish patients' quality of life, escalate financial burdens, and inflict significant mental and psychological stress (Kushwaha *et al.*, 2022).

1.2.1 Antimicrobial resistance (AMR)

Antimicrobial resistance (AMR) poses a significant risk to global public health and development (World Health Organisation, 2021). AMR occurs when microorganisms (bacteria, fungi, parasites, and viruses), develop the ability to resist the effects of antimicrobial agents commonly used to treat these diseases (Tang *et al.*, 2023). The key factor contributing to the occurrence of AMR is the excessive or needless use of antibiotics, coupled with the scarcity of novel antimicrobial therapies and medications (Prestinaci *et al.*, 2015). Without any intervention, it is widely believed that AMR will emerge as the leading cause of mortality globally by the year 2050 (Tang *et al.*, 2023). The discovery of antibiotics is one of the greatest feats in medical history. The formulation of drugs with antimicrobial properties has significantly lowered mortality rates and aided in the management and treatment of infectious diseases in humans and animals alike (Aminov, 2010). Since the discovery of the first antibiotic, i.e., penicillin, by Sir Alexander Fleming in 1928, the average human life expectancy has risen by 23 years (Hutchings *et al.*, 2019). Fleming is credited with launching the “golden era” of antibiotics, as his discovery marked the beginning of a period of extensive antibiotic research and development (Hutchings *et al.*, 2019). However, shortly thereafter, it became apparent that some types of bacteria were resistant to antibiotics and could produce penicillinase, which in turn rendered penicillin ineffective for medical use (Lobanovska and Pilla, 2017). This is a serious problem considering that penicillin and its derivatives are the main class of antibiotics still being used today to treat bacterial infections. Over 150 new antibiotics have been identified and utilised since the "golden era", however, their excessive usage has led to increased resistance and the emergence of multi-drug resistant (MDR) microbes, also known as "superbugs" (Lobanovska and Pilla, 2017). Antibiotic resistance by bacteria poses a significant challenge (Tang *et al.*, 2023) and is exacerbated by the reduced rate of discovery of new and effective antibiotics since the early 1990s. Between 2017 and 2019, only 11 novel antimicrobial agents were approved by the US FDA (De Oliveira *et al.*, 2020). AMR is a natural biological process that takes place when microorganisms acquire mechanisms to counteract the effects of the antibiotic (Aljeldah, 2022). This could be attributed to alterations

in the structure or composition of the bacterial envelope, as well as the synthesis of enzymes that degrade the drugs (Konop *et al.*, 2016).

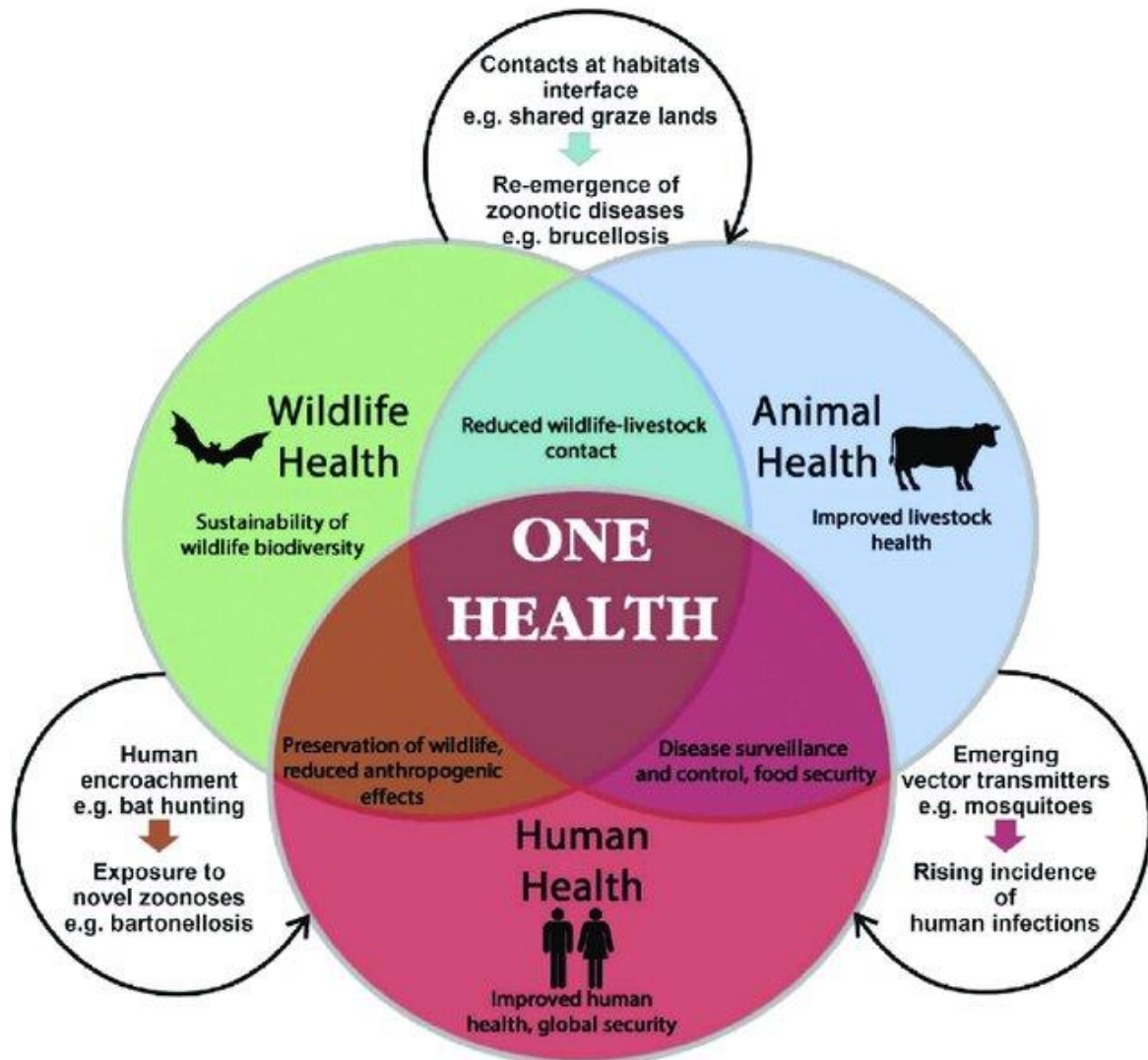


Figure 1.2: One Health concept outlining the impact of human, animal, and wildlife health on each other and the surrounding environment (adapted from Tang *et al.*, 2023)

In order to combat AMR, the “One Health” global approach was established (Figure 1.2) which clearly shows the interdependence of human and animal health with the surrounding environment (Soto, 2021). Animals and humans can be infected by the same bacteria and diseases and consequently, use the same antibiotics (Centers for Disease Control and Prevention, 2024a). As such, AMR has become one of the most pressing “One Health” issues, as AMR can spread across all aspects of human and animal health, such as the food chain and healthcare settings. This makes it extremely difficult to control various infectious diseases in humans and animals (Centers for Disease Control and Prevention, 2024a). Given the fast emergence of AMR, constant monitoring of infection and mortality rates associated with AMR

is necessary. There was a total of 4.95 million deaths worldwide in 2019 that were associated with AMR, 1.27 million were specifically caused by bacterial AMR (Murray *et al.*, 2022). The annual mortality rate attributed to AMR is projected to increase to 10 million by 2050.



Figure 1.3: Overview of the ESKAPE pathogens and the human organs that are most susceptible to their infections (Pulgar, 2019)

The regions with the greatest estimated mortality rates include Asia and Africa, mostly due to their enormous populations and lack of legislation regarding the prevention of AMR (Tang *et al.*, 2023). Sub-Saharan Africa has the highest all-age death rate estimated by the Global Burden of Diseases that is specifically associated with or connected to AMR. In contrast, Australasia had the lowest incidence of AMR-related mortality in 2019 (Murray *et al.*, 2022). AMR in pathogenic microorganisms has emerged as a major peril to public health. As this problem persists, it has given rise to multidrug-resistant organisms (MDROs) (Magiorakos *et al.*, 2012). MDROs are categorised based on their resistance to several antimicrobial agents, and the infections they cause are frequently associated with unfavourable patient outcomes. In

2017, the WHO released a list of pathogens that urgently need new antibacterial drugs in order to promote the advancement of research and development of novel antibiotics (De Oliveira *et al.*, 2020). Out of the listed pathogens, seven were given "priority status" (**Figure 1.3**).

These pathogens include *Enterococcus faecium*, *Staphylococcus aureus*, *Klebsiella pneumoniae*, *Acinetobacter baumannii*, *Pseudomonas aeruginosa*, and *Enterobacter* species (De Oliveira *et al.*, 2020). The abbreviation 'ESKAPE' is widely used to refer to them; aptly so, as they are able to “escape” the killing mechanism of antimicrobial agents (Pulgar, 2019).

ESKAPE pathogens pose the highest risk of death and illness, particularly in low- and middle-income countries (LMICs), leading to a significant worldwide economic burden (Tang *et al.*, 2023). These bacteria have obtained mobile genetic elements (MGEs) and genetic alterations that allow them to avoid the effects of antimicrobial treatments such as lipopeptides, tetracyclines, oxazolidinones, macrolides, β -lactams, β -lactam- β -lactamase inhibitor combos, and fluoroquinolones (De Oliveira *et al.*, 2020). The resistance mechanisms of these pathogens involve drug inactivation, modification of the antibiotic's target site, reduced drug accumulation, and the development of new cellular processes that bypass the antibiotic's target (**Figure 1.4**) (Deda, n.d.).

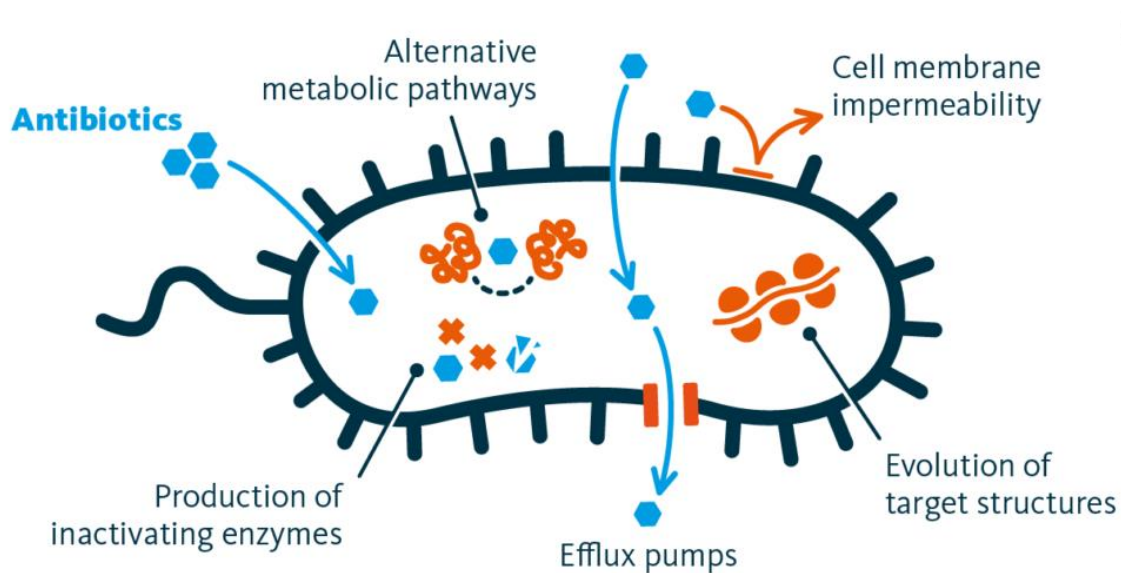


Figure 1.4: Main mechanisms of antibiotic resistance (adapted from Deda, n.d.)

Microorganisms use a variety of defence strategies to mitigate or overcome the activities of antimicrobials, as outlined in **Table 1.1** (Centers for Disease Control and Prevention, 2024b). The formation of biofilms is another way in which pathogens physically inhibit antibiotics. Biofilms are distinguished by a confined environment formed through the attachment of

microbial cells to one another and the production of an extracellular polymeric substance that constructs a shielding matrix (Jorge *et al.*, 2019). Biofilm generation is a critical process for the development of virulence in many bacterial pathogens that are medically important (Jorge *et al.*, 2019). In addition, biofilms exacerbate the occurrence of AMR by promoting persistent infections and shielding latent cells that are tolerant to antibiotics. This, in turn, contributes to the difficulty in treating AMR-related infections. Every pathogen included in the WHO priority list has demonstrated the capacity to develop biofilms (Jorge *et al.*, 2019).

Table 1.1: Microbial defence mechanisms to withstand the impact of antibacterial agents. (Adapted from Centers for Disease Control and Prevention, 2024b)

Resistance Mechanisms	Description
Limit the accessibility of the antibiotic	Microbes impede access by altering the entry points or reducing their amount. Gram-negative bacteria possess an outer membrane that serves as a protective barrier against their surroundings. These bacteria possess the ability to utilise their membrane to selectively prevent the entry of antibiotics.
Elimination of the antimicrobial agents	Microorganisms eliminate antibiotics by employing efflux pumps located in their cell membranes to expel the antibiotics that infiltrate the cell. Certain strains of <i>P. aeruginosa</i> possess efflux pumps that enable them to expel many crucial antibiotics, such as fluoroquinolones, β -lactams, chloramphenicol, and trimethoprim.
Alter or eradicate the antibiotic	Microorganisms alter or degrade antibiotics via enzymes and proteins that dismantle the medication. <i>Klebsiella pneumoniae</i> secrete carbapenemases, which enzymatically degrade carbapenems as well as the majority of other β -lactam medications.

<p>Modify the targets for the anti-microbial</p>	<p>Several antibiotics are engineered to specifically target and eliminate particular components of a bacterium. Microorganisms undergo genetic mutations that alter the target for antibiotics, rendering the medicine incapable of binding and carrying out its intended function. <i>E. coli</i> with the <i>mcr-1</i> gene have the ability to modify the outer surface of their cell wall, preventing colistin from binding to it.</p>
<p>Counteract the impact of the antibiotic</p>	<p>Microorganisms undergo cellular adaptations that enable them to circumvent the specific target of the antibiotic. Certain strains of <i>S. aureus</i> have the ability to circumvent the pharmacological impact of trimethoprim.</p>

Although *E. coli* is not officially classified as one of the ESKAPE pathogens, it is common in bloodstream infections (BSIs) and urinary tract infections (UTIs), especially those caused by antibiotic-resistant *E. coli* strains (De Oliveira *et al.*, 2020). These infections frequently progress to sepsis. *E. coli* commonly acquires resistance genes from other members of the *Enterobacteriales* through horizontal gene transfer and is the predominant Gram-negative bacteria found in blood and urine cultures in Australian inpatient and emergency department settings. *E. coli* is a frequent cause of infections in surgical wounds and was found to be the second most prevalent (21 %) bacterial pathogen among surgical patients by the University hospital in Iran (Rahim *et al.*, 2017). According to reports, 46 % of *E. coli* isolates that cause wound infections are resistant to ampicillin, 25 % are resistant to tetracycline, and 21 % are resistant to fluoroquinolones (Alharbi *et al.*, 2019). Currently, AMR *E. coli* is a significant clinical challenge that has a detrimental effect on both human and animal well-being. To prevent exacerbating these issues, it is imperative to categorise this bacterium as a crucial public health issue (De Oliveira *et al.*, 2020). In 2019, the six primary disease-causing microorganisms that were resistant to treatment and resulted in the most deaths were *Escherichia coli*, *Staphylococcus aureus*, *Klebsiella pneumoniae*, *Streptococcus pneumoniae*, *Acinetobacter baumannii*, and *Pseudomonas aeruginosa*. These pathogens were responsible

for a total of 929,000 deaths directly caused by AMR and an additional 3.57 million deaths associated with AMR (Murray *et al.*, 2022). If the problem of AMR is not tackled, numerous species that do not currently pose a significant threat may become more dangerous in the future due to the spread of AMR (Murray *et al.*, 2022). The impact of AMR is felt worldwide, but it poses the greatest risk to human health in LMICs in Sub-Saharan Africa and South Asia (Murray *et al.*, 2022).

1.2.2 AMR in South Africa

In South Africa, there is a growing prevalence of infectious diseases primarily caused by bacteria. The prevalence of ESKAPE organisms causing BSIs in the public sector during a five-year period (2018-2022) was reported by the National Department of Health Republic of South Africa (NDoH-RSA) from the National Health Laboratory Service data files (NDoH-RSA, 2024). The total number of consecutive blood cultures examined rose from 3,610,401 in 2018 to 4,207,656 in 2022. The proportion of ESKAPE organisms detected in all positive blood cultures with antibiotic susceptibility results declined during the five years, ranging from 41 % to 37 % (**Figure 1.5A**) (NDoH-RSA, 2024). During this period, the most frequently cultured organisms were *K. pneumoniae* and *S. aureus*, with *E. coli* and *A. baumannii* following closely behind (**Figure 1.5B**). Between 2020 and 2022, there was a surge in the incidence of *A. baumannii*, *E. faecalis*, and *E. faecium* infections (NDoH-RSA, 2024). *K. pneumoniae* was a prevalent pathogen found in blood samples from both private and public healthcare sectors in South Africa, while *E. coli* ranked as the second most prevalent Gram-negative bacteria (NDoH-RSA, 2024). Although the data does not distinguish between infections acquired in the community and those acquired in hospital settings, the presence of *E. coli* may indicate community-acquired illnesses specifically related to UTIs. There has been a steady decrease in the prevalence of methicillin-resistant *S. aureus* (MRSA) over the years, dropping from 23 % in 2018 to 16 % in 2022 (NDoH-RSA, 2024). However, the level of resistance varies among different regions. Active surveillance conducted in specific locations within two provinces has revealed that less than 8 % of MRSA bacteraemia cases were acquired from the community, in contrast to some other nations, where more than 50 % of MRSA cases originate from the community (Perovic *et al.*, 2017). According to the 2022 national data, 15 % of *P. aeruginosa* isolates showed resistance to piperacillin/tazobactam, while 23 % showed resistance to meropenem (NDoH-RSA, 2024). *E. faecalis* is highly responsive to ampicillin, which is still the preferred treatment with a 7 % resistance rate in 2022. However, ampicillin resistant *E. faecium* was observed in over 95 % of isolates, consistent with its worldwide prevalence.

According to the NDoH-RSA analysis, the provinces of Free State and North West exhibited more resistance to ampicillin in 2022 compared to other provinces (NDoH-RSA, 2024).

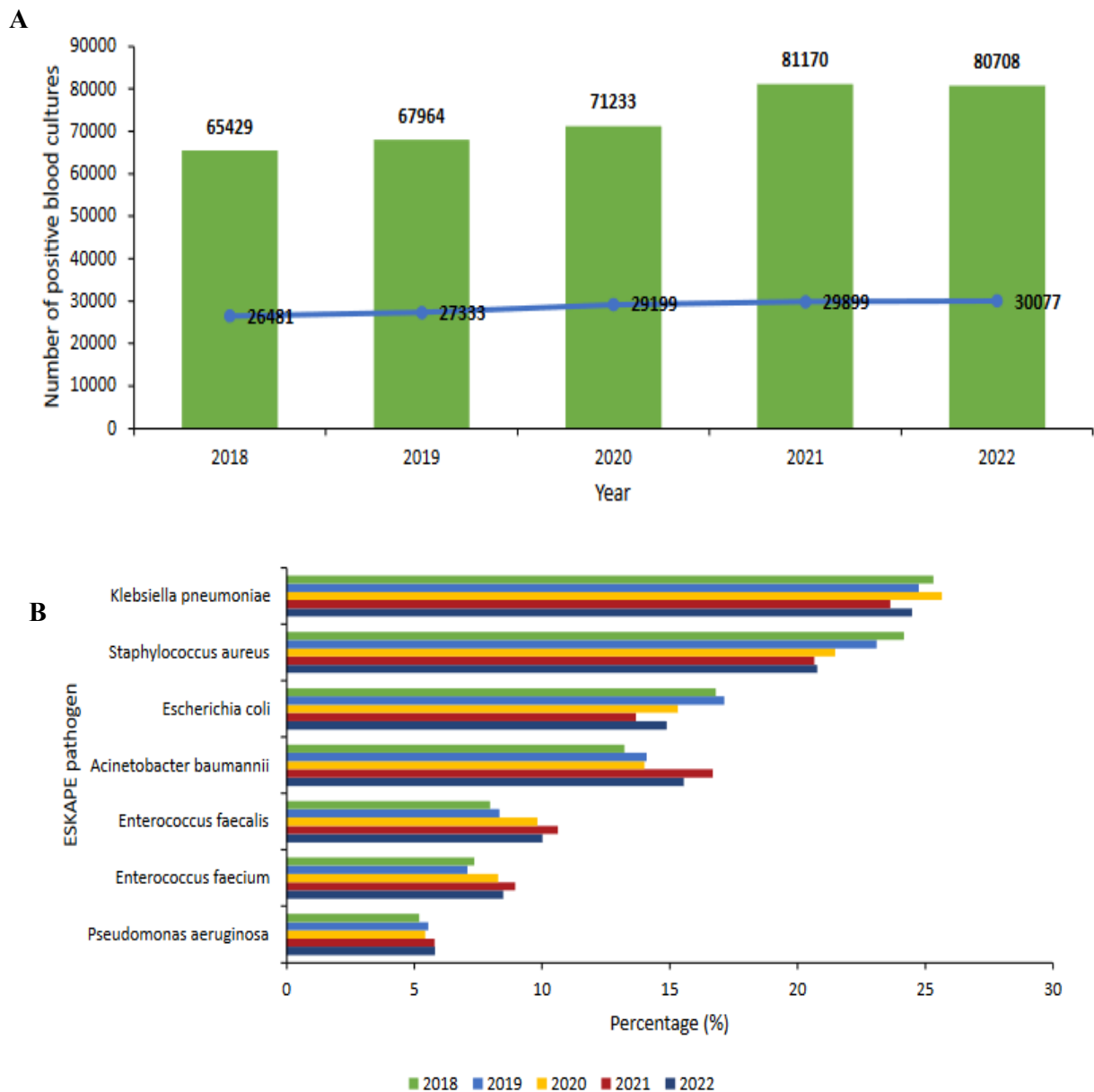


Figure 1.5: Burden (A) and distribution (B) of ESKAPE pathogens in the public sector of South Africa from 2018-2022 (NDoH-RSA, 2024).

The proliferation of AMR worldwide can be attributed to various factors (Tang *et al.*, 2023). However, in South Africa, the misuse of antibiotics is widespread due to a clear lack of awareness and understanding of appropriate antimicrobial usage (AMU) (Chetty *et al.*, 2019). Based on the 2018 data from the global AMU study, South Africa's antimicrobial consumption was calculated to be 17.9 defined daily doses per 1000 people per day (Browne *et al.*, 2021).

The consumption estimate for this country was lower compared to other African countries, such as Algeria (36.8), Tunisia (38), Egypt (24), and Tanzania (25). While it exhibited similarities to other Brazil, Russia, India, China, and South Africa (BRICS) countries, its level was still below that of the majority of HICs (**Figure 1.6**) (NDoH-RSA, 2024). The fundamental concern is that if AMR is not addressed swiftly and successfully, it could lead to a return to the pre-antibiotic era. Even simple illnesses, such as the common cold might become fatal. Hence, novel approaches are required to combat the problem of AMR (Tang *et al.*, 2023).

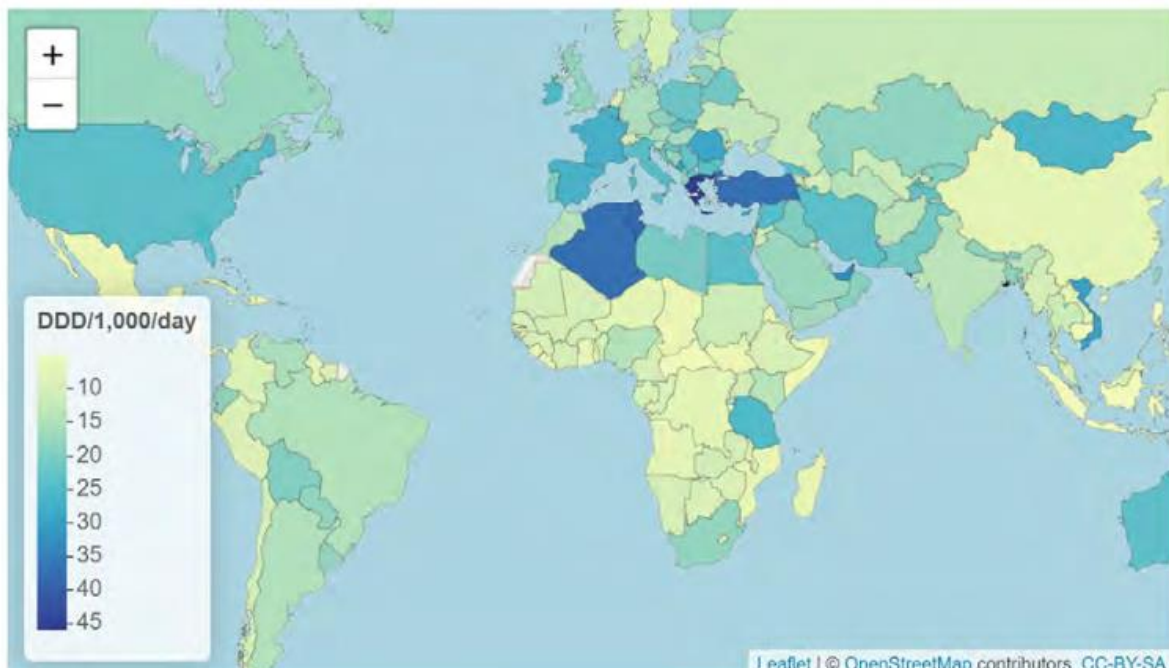


Figure 1.6: Analysis of worldwide antibiotic consumption and usage in the human population from 2000 to 2018 (Browne *et al.*, 2021)

1.2.3 Current AMR treatments and their limitations

It is obvious that to properly tackle a disease as pervasive and lethal as AMR, a range of treatment options must be used, including innovative antimicrobial medicines, enhanced diagnostics, and better management (Alghamdi, 2021). However, antibiotic therapy continues to be the standard treatment for bacterial infections. While antibiotics have proven to be one of the greatest advances in medical history, their utility in treating microbial illnesses is limited (Zhang *et al.*, 2020). The most notable of these restrictions is the development of bacterial antibiotic resistance. Additionally, unpleasant side effects such as abdominal pain, nausea, and disruption of the natural gut microbiota, as well as the antibiotics' limited availability and high cost, are also important considerations (Zhang *et al.*, 2020). The overuse and overprescription

of antibiotics further nullify its effectiveness. General practitioners prescribe the vast majority of antibiotics used in medicine (Llor and Bjerrum, 2014). In fact, primary care accounts for 80-90 % of all antibiotic prescriptions in Europe, with most antibiotics taken for respiratory tract illnesses. It has been demonstrated that there is a direct association between antibiotic use and resistance (Tang *et al.*, 2023).

Countries with increased antibiotic consumption have higher rates of resistance. Excessive use of antibiotics is associated with a range of problems, in addition to the rise of resistance. Antibiotics expose individuals to the possibility of experiencing adverse consequences and contribute to more than 20 % of all emergency room visits linked to drugs in the US (Llor and Bjerrum, 2014). While allergic responses make up more than 80 % of these visits, commonly prescribed antibiotics can also lead to gastrointestinal, neurologic, and mental complications. Most of these adverse effects are insignificant, but a few have the potential to be lethal, such as hepatotoxicity resulting from the combination of amoxicillin and clavulanate. Excessive prescription of antibiotics has increased patients returning for further medical attention by treating conditions that would naturally resolve on their own (Llor and Bjerrum, 2014).

Although antibiotic therapy carries inherent hazards, it continues to be the prevailing and undisputed standard practice. It is undeniable that antibiotics are very successful in treating the majority of bacterial infections today (Hu *et al.*, 2020). Utilising antibiotics in a judicious manner, including implementing reasonable control measures and reducing antibiotic dosages, is crucial for mitigating the detrimental effects of AMR and impeding its development (Llor and Bjerrum, 2014). Recently introduced antibiotics, including ceftobiprole, ceftaroline, tedizolid, and delafloxacin, have proven efficacy against multidrug-resistant gram-positive bacteria (Hu *et al.*, 2020). However, it is important to note that these antibiotics may also lead to the development of antimicrobial resistance. Thus, it is advisable to prioritise the utilisation of non-antibiotic treatments (Tang *et al.*, 2023).

1.3 Green nanotechnology and plant-based therapy as alternative treatment for AMR

Due to its remarkable antibacterial and therapeutic properties, silver has been utilised in the treatment and control of various microbial ailments since ancient times (Almatroudi, 2020). There is ample evidence to suggest that Ag ions and Ag-based compounds possess a strong ability to kill microorganisms, making Ag-based products a valuable alternative for AMR treatment (Almatroudi, 2020). Furthermore, natural medicines, such as plant-based remedies and herbal therapy, have been used to treat bacterial infections, frequently in conjunction with

antibiotics and other conventional medications, to improve their efficacy through a synergistic approach (Zhang *et al.*, 2020). Plant-based therapies have antimicrobial and antibiofilm properties, and they help relieve infection symptoms due to their anti-inflammatory, antipyretic, and analgesic effects. Plant-based medications, when used instead of antibiotics, are less expensive, more accessible, and safer, with fewer adverse effects. They can also minimise the risk of AMR and other side effects associated with antibiotic use (Zhang *et al.*, 2020).

1.4 Nanotechnology in medicine

Nanotechnology has had a significant impact on global industries, particularly in recent years. It has cemented itself as the most promising technology of the modern century, with particular effort being focused into implementing nanotechnology techniques and products into the field of medicine (Haleem *et al.*, 2023). Nanoscience incorporates a wide variety of disciplines, including biology, chemistry, engineering, physics, and material sciences, all of which could potentially aid in the development of novel biomedical and pharmaceutical applications (Malik *et al.*, 2023). Nanotechnology involves the manipulation of particles at the nanoscale, to produce novel devices, products, or systems (Dikshit *et al.*, 2021). The nanoscale range is displayed in **Figure 1.7**, with NPs in the same scale range as biomolecules such as DNA (1 nm) and viruses (100 nm) (Bayda *et al.*, 2020). “Nano” is a prefix derived from “*nanos*”, which is the Greek word for “dwarf” (Omran *et al.*, 2017). A nanometre (nm) is equivalent to a billionth of a meter (10^{-9}), which is smaller than a single strand of human hair that is approximately 80,000 nm (Mazayen *et al.*, 2022).

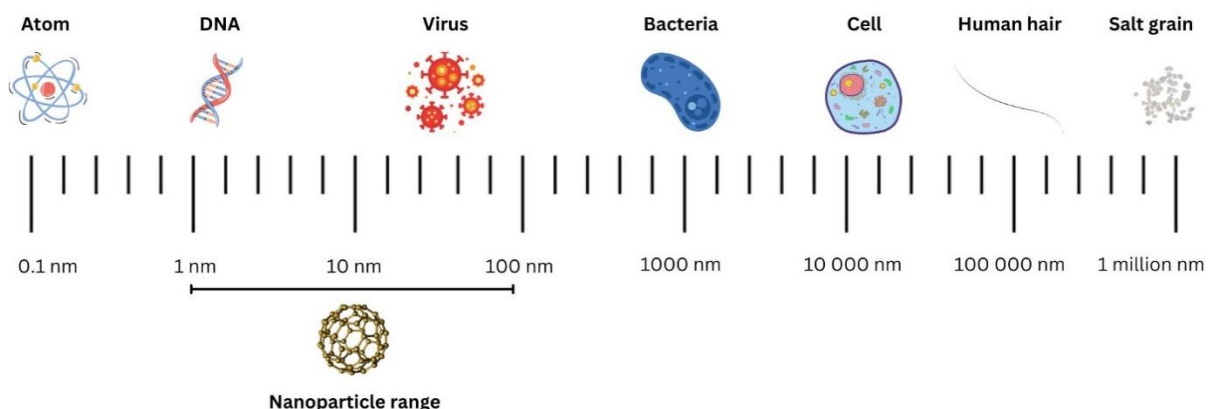


Figure 1.7: Size comparison chart illustrating the sizes of various biological entities and objects, ranging from atoms to a grain of salt, at the nanometre scale. (adapted from Bayda *et al.*, 2020)

Nanomaterials are tiny particles that typically fall within the 1 – 100 nm diameter range. At the nanoscale, particles exhibit distinct physicochemical and structural characteristics due to the influence of quantum laws, rather than the conventional laws of physics (Thomford *et al.*, 2018). Quantum phenomena have the ability to modify the optical, mechanical, electrical, magnetic, thermal, and catalytic properties of nanomaterials (Joudeh and Linke, 2022). The dimensions, configuration, and surface structure of nanomaterials can impact their inherent qualities by facilitating the emergence of novel or enhanced traits (Haleem *et al.*, 2023).

1.4.1 History of nanotechnology

It is believed that nanotechnology began in Asia between the fourth and fifth century BC (Paul *et al.*, 2010). Traditional healers across India were able to synthesise gold colloids – known as “Swarna Bhasma” – that possessed therapeutic activity. Over in Europe, it has been reported that mental disorders and syphilis were treated with gold colloids during the Middle Ages, while in Africa, there is evidence that the ancient Egyptians were able to produce cosmetic products using lime, lead oxide, and water (Joudeh and Linke, 2022; Paul *et al.*, 2010). Despite evidence supporting the foundation of nanoscience in ancient times, the Nobel laureate Dr. Richard Feynman is credited as the “father of nanotechnology” (Joudeh and Linke, 2022). Feynman delivered a revolutionary lecture in 1959, titled “There’s Plenty of Room at the Bottom” at the California Institute of Technology in the USA, wherein he introduced the concept of manipulating and controlling materials at a very tiny scale – the nanoscale (Dawadi *et al.*, 2021; Feynman, 1960). The lecture was the launching pad for the inception of multiple top-down approaches to miniaturising materials, and during the 1950s and 1960s, numerous studies were undertaken on MNPs. However, the term “nanotechnology” had not yet been coined (Joudeh and Linke, 2022) and was first introduced in 1974 by Dr. Norio Taniguchi of Tokyo Science University while working on the creation of nanosized materials (Sharon *et al.*, 2012). The multitude of innovations in the advancement of nanotechnology since the 1980s have served as evidence of Feynman's foresight in 1959 (Joudeh and Linke, 2022). From the 1990s to the early 2000s, there was a significant surge in the interest and investment in nanotechnology from researchers and the scientific community as a whole (Dawadi *et al.*, 2021). Novel approaches in the manufacturing of nanomaterials like carbon nanotubes and quantum dots have created new possibilities for the fields of energy, health, technology, and agriculture (Bayda *et al.*, 2020). One of the most notable breakthroughs in nanotechnology came in 1986, when Gerd Binnig and Heinrich Rohrer invented the scanning tunnelling microscope (Bayda *et al.*, 2020). The invention earned them the Nobel Prize in Physics and

was the dawn of modern nanotechnology. Ten years later in 1996, Richard Smalley, Harold Kroto, and Robert Curl were also awarded Nobel Prizes, this time for their discovery of a group of carbon molecules known as fullerenes (Malik *et al.*, 2023). The field is advancing swiftly, with continuous research being undertaken to develop novel nanomaterials, nanosystems, and nanodevices with enhanced and unprecedented abilities (Malik *et al.*, 2023).

1.4.2 Types of nanoparticles (NPs)

Nanomaterials serve as the fundamental building blocks for all nanotechnology applications. Nanomaterials are materials characterised by having at least one dimension of less than 100 nm (Joudeh and Linke, 2022). Nanomaterials in the nanoscale range are classified into one of four classes based on the number of dimensions they possess (Kolahalam *et al.*, 2019). Zero-dimensional nanomaterials, known as 0-D nanomaterials, are materials that have all three of their dimensions within the nanoscale range. The most prevalent examples of these materials include quantum dots, NPs, and fullerenes. Nanomaterials that possess a single dimension outside the nanoscale range, such as nanotubes, nanorods, and nanofibers, are categorised as one-dimensional (1-D). Two-dimensional nanomaterials (2-D) are nanomaterials that have two dimensions outside of the nano range; this includes nanosheets and nanofilms. Three-dimensional (3-D) nanomaterials, also known as bulk nanomaterials, lack any dimensions that fall inside the nanoscale range.

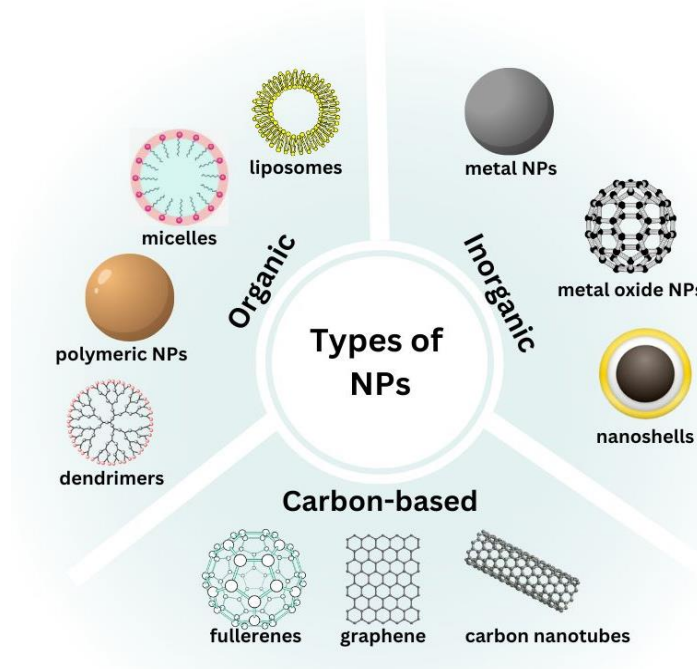


Figure 1.8: Nanomaterials are classified into organic, inorganic and carbon-based NPs. (adapted from Spirescu *et al.*, 2021)

These substances usually consist of NPs dispersions, clusters of nanowires, and bulk powders (Kolahalam *et al.*, 2019). NPs exhibit a diverse range of sizes, shape, and chemical structures, and can exist as either uniform entities or as assemblies with several layers (Bayda *et al.*, 2019). NPs are classified into three categories based on their composition: organic, inorganic, and carbon-based (**Figure 1.8**) (Spirescu *et al.*, 2021)

NPs that are composed of proteins, lipids, polymers, carbohydrates, or other organic substances are categorised as organic NPs (Pan and Zhong, 2016). This class include liposomes, micelles, and protein complexes. Organic NPs are typically non-toxic and biodegradable. However, they are susceptible to the effects of heat and light (Joudeh and Linke, 2022). They are usually created through non-covalent intermolecular interactions, which enables them to be eliminated from the human body (Ng and Zheng, 2015). The chemical makeup, durability, and surface morphology of organic NPs play a crucial role in determining their specific uses. In recent times, they have been extensively utilised in the field of biomedicine, particularly in the areas of targeted drug administration and cancer treatment (Gujrati *et al.*, 2014).

Carbon-based NPs such as fullerenes or carbon quantum dots consist exclusively of carbon atoms (Joudeh and Linke, 2022). Fullerenes have a symmetrical structure that is closed and cage-like, whereas carbon quantum dots consist of discrete carbon NPs that are quasispherical and smaller than 10 nm (Mauter and Elimelech, 2008; Dresselhaus *et al.*, 1993). Due to their carbon-based composition, this category of NPs combines the distinct characteristics of sp²-hybridized carbon bonds with the unusual physicochemical properties observed at the nanoscale (Khan *et al.*, 2019; Oh *et al.*, 2010). Carbon-based NPs are utilised in drug delivery, bioimaging, and energy storage because of their exceptional conductivity, durable nature, electron affinity, and optical and thermal characteristics (Oh *et al.*, 2010).

Inorganic NPs are composed of materials other than carbon or organic matter (Joudeh and Linke, 2022). The most prevalent examples of this category include metallic, ceramic, and semiconductor NPs. MNPs consist exclusively of metal precursors and can exist as monometallic, bimetallic, or polymetallic structures (Toshima and Yonezawa, 1998). These NPs possess distinct optical and electrical capabilities as a result of their localised surface plasmon resonance (SPR) features from multiple precursors (Khan *et al.*, 2019). In addition, MNPs exhibit unique thermal, magnetic, and biological properties (Joudeh and Linke, 2022); and have become a crucial component in the advancement of nanodevices used in a wide range of biological and pharmacological applications (Mody *et al.*, 2010). MNPs can be produced

using several metal precursors, such as Ag, gold (Au), copper (Cu), platinum (Pt), iron (Fe), aluminium (Al), and titanium (Ti) (Khan *et al.*, 2019). The size and shape of MNPs play a vital role in the development of ground-breaking materials (Dreaden *et al.*, 2012). MNPs synthesised from alkali and noble metals, such as Ag and Au, exhibit a wide absorption range in the visible region of the solar electromagnetic spectrum. Noble NPs exhibit a prominent UV-Vis excitation band that is absent in the spectrum of bulk metal (Khan *et al.*, 2019). AgNPs are among the widely studied MNPs due to their antimicrobial effects and are investigated in the current study.

1.4.3 Ag-based agents in the fight against AMR

Due to its extensive array of homoeopathic qualities and therapeutic capacities, Ag has been utilised for medicinal purposes for more than 2000 years (Almatroudi, 2020). Ag has preservative properties, as evidenced by its historical use by ancient civilizations such as the Egyptians, Romans, and Greeks for the storage of food and beverages (Park, 2014). It was a widespread custom among ancient empires, as Ag was thought to possess extraordinary antibacterial powers. Ag has been utilised for therapeutic purposes from at least 1850 B.C., specifically for the healing and control of wounds, as recorded by Paladini and Pollini in 2019. In addition, historical textbooks documented the application of AgNO₃ for treating ulcers during the 17th and 18th centuries. However, the elucidation of Ag's antibacterial properties was not made until the 19th century (Paladini and Pollini, 2019). Subsequently, Ag became the main substance used for antibacterial treatment until the advent of antibiotics in the early 1900s (Srikar *et al.*, 2016).

Ag stands out among other noble metals due to its distinctive optical qualities, chemical stability, exceptional electrical conductivity, and antibacterial activity (Dawadi *et al.*, 2021). AgNPs are highly significant and captivating nanomaterials that play a crucial role in various applications, alongside other MNPs. AgNPs have a significant impact on the fields of nanoscience and nanotechnology, namely in the area of nanomedicine (Zhang *et al.*, 2016). AgNPs' favour lies in their localised SPR and unique physicochemical properties, which enable them to be utilised as diagnostic and therapeutic tools for numerous diseases. Biological activities of AgNPs include antidiabetic, antimicrobial, antioxidant, and anticancer (Lethongkam *et al.*, 2023; Salve *et al.*, 2022; Tyavambiza *et al.*, 2022; Saratale *et al.*, 2021).

1.4.3.1 Synthesis of AgNPs

There are two predominant approaches to synthesising NPs – the “top-down” and the “bottom-up” principles. In the “top-down” approach, nanoscale materials are manufactured by the

physical fragmentation of bulk materials into smaller nanomaterials of a desired shape (**Figure 1.9**) (Patra and Baek, 2014). On the other hand, the “bottom-up” approach involves the use of various chemical and biological techniques to synthesise nanomaterials from atomic-sized particles that cluster together to form NPs. Mode of synthesis is wholly dependent on the technology and reducing agents used, and a plethora of physical, chemical, biological, and hybrid methods have been designed to synthesise AgNPs (Patra and Baek, 2014; Rafique *et al.*, 2017).

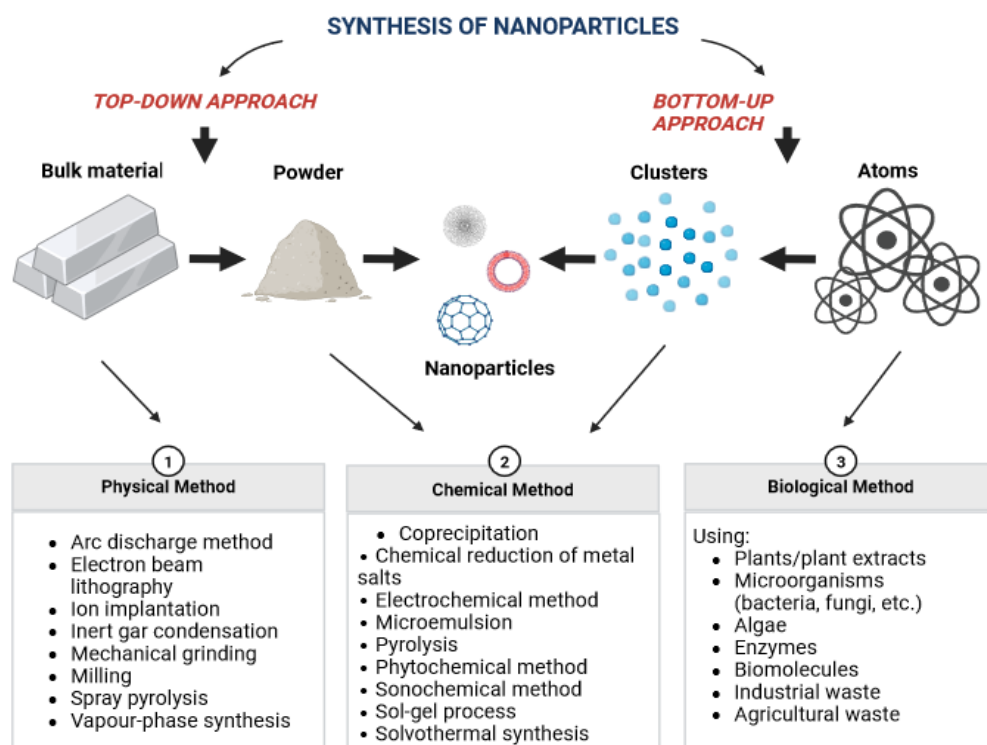


Figure 1.9: Overview of different approaches and techniques used to synthesise NPs (adapted from Patra and Baek, 2014)

Conventional approaches used to the synthesize NPs involve physicochemical techniques that require chemicals, energy, microwaves, light, sound, and lasers (Dawadi *et al.*, 2021). Physical synthesis methods include arc discharge, electron beam lithography, ion implantation, mechanical grinding, ball milling, spray pyrolysis, and vapour-phase synthesis (Patra and Baek, 2014). NP synthesis via chemical methods includes co-precipitation, chemical reduction of metal salts, microemulsion, pyrolysis, and solvothermal synthesis (Rafique *et al.*, 2017).

The employment of physical and chemical techniques for NP manufacturing frequently produces harmful and dangerous byproducts to humans and the environment, making them

unsustainable (Gonzalez-Ballesteros *et al.*, 2018). These processes also demand significant amounts of energy, employ expensive chemicals, and rely on high levels of reducing and stabilising agents, all of which have negative impacts on the environment. Moreover, both physical and chemical synthesis procedures are lengthy processes (Rafique *et al.*, 2017). In addition, physical techniques do not consistently achieve homogeneity of nanomaterial (Park, 2014). As a result of concerns about sustainability, toxicity, and environmental pollution caused by current physical and chemical procedures utilised for NP synthesis, there is an increasing demand for a clean, environmentally friendly, biocompatible, cost-effective strategy for synthesis of AgNPs (Park, 2014). Biological methods offer a potential solution to the issues caused by physical and chemical methods (Dawadi *et al.*, 2021).

1.4.3.1.1 Green synthesis of AgNPs

The primary cornerstone on which the green synthesis of NPs is built involves, amongst others, the usage of non-toxic capping, reducing agents, and environmentally sound solvents (Amid *et al.*, 2018). For this reason, biological (green) synthesis of NPs is preferred over physical and chemical routes and is built on sustainable green chemistry principles. The 12 principles of green chemistry (**Table 1.2**) were introduced in 1998 by Anastas and Warner in the inaugural textbook on green chemistry - “Green Chemistry: Theory and Practice” (Anastas and Warner, 1998). Implementing these regulations in the realm of green nanotechnology can result in the production of inherently safer NPs and a reduction in the production of toxic waste (Gonzalez-Ballesteros *et al.*, 2018). These have aided researchers worldwide in reducing their use of hazardous material and developing less harmful by-products (Parveen *et al.*, 2016). The principles of green chemistry are applied across every stage of the life cycle of nanomaterials to optimise the design framework (Soni *et al.*, 2022). A benign target particle or molecule has the potential to be transformed into a life-saving medicinal treatment that can benefit society. However, it can also cause harm and environmental contamination at the end of its life cycle (Soni *et al.*, 2022).

Table 1.2: The 12 principles of green chemistry (adapted from Anastas and Warner, 1998)

1. Preventing waste is more advantageous than treating or remedying waste after its formation.
2. The design of synthetic methods should aim to optimise the integration of all materials utilised in the process into the end product.
3. Whenever possible, synthetic approaches should be developed to utilise and produce substances that have minimal or no harmful effects on human health and the environment.
4. The design of chemical products should prioritise the preservation of their effectiveness while minimising their toxicity.
5. Whenever feasible, the need for auxiliary substances such as solvents and separation agents should be eliminated, and when they are utilised, they should be harmless.
6. It is important to acknowledge the environmental and economic consequences of energy needs and strive to reduce them. It is advisable to carry out synthetic procedures under normal temperature and pressure conditions.
7. Whenever technically and economically feasible, the raw material used as feedstock should be renewable rather than diminishing.
8. Avoid unnecessary derivatization, such as the use of blocking groups, protection/deprotection, or temporary modification of physical/chemical processes, if feasible.
9. Catalytic reagents, which aim to be as selective as possible, are more advantageous than stoichiometric reagents.
10. Chemical items should be designed such that they do not persist in the environment and instead degrade into harmless degradation products after their intended purpose is met.

11. There is a need to enhance analytical approaches in order to provide real-time monitoring and control during the production process, before the creation of dangerous compounds.

12. When selecting substances and their form for a chemical process, it is important to choose in a way that reduces the likelihood of chemical accidents, such as releases, explosions, and fires.

Green nanotechnology emerged as a result of incorporating the principles of green chemistry and focused on the creation of environmentally friendly methods that minimises the possible hazards to the environment and human health associated with the production of nanomaterials (Soni *et al.*, 2022). Green nanotechnology seeks to substitute existing products with nanoproducts with environmentally benign characteristics that are sustainable and are devoid of harmful ingredients (Dikshit *et al.*, 2021). Several studies have produced biogenic AgNPs with specific sizes using various biological systems such as bacteria, fungi, plant extracts, and small biomolecules like vitamins and amino acids as highlighted in **Figure 1.10** (Golpour *et al.*, 2024; Burange *et al.*, 2021; Jiang *et al.*, 2018).

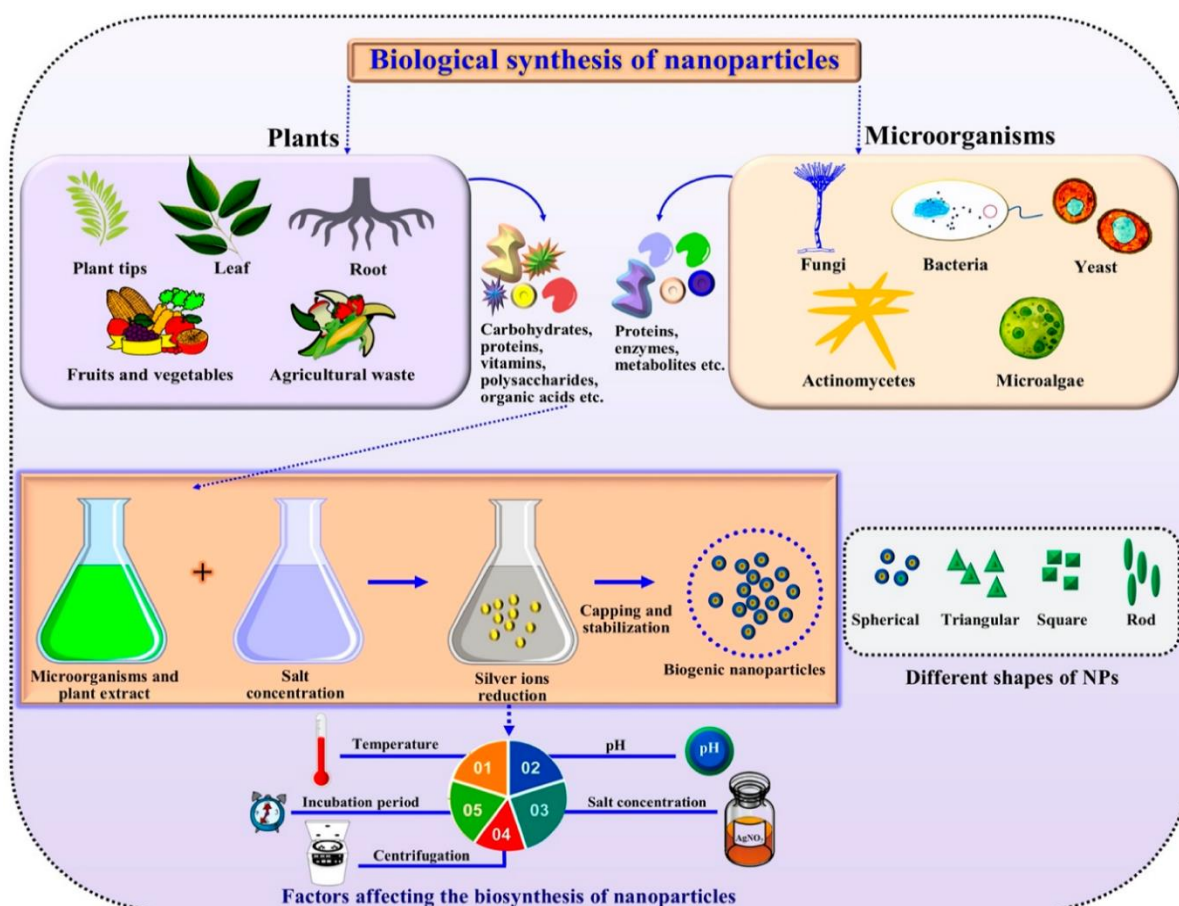


Figure 1.10: Schematic illustration of the green synthesis of MNPs (Ali *et al.*, 2020)

This approach serves as an alternative to chemical methods and is not only used for AgNPs but also for the synthesis of other types of MNPs (Algotiml *et al.*, 2022). The biologically assisted synthesis of NPs is a simple, cost-effective, dependable, and environmentally benign process (Ovais *et al.*, 2016).

1.4.3.1.2 Biosynthesis of AgNPs from microorganisms

Microorganisms, including bacteria, fungi, algae, and viruses, are increasingly being studied for their ability to act as reducing agents in the synthesis of MNPs (Aboyewa *et al.*, 2021). Microbes possess the capacity to produce inorganic substances that can aid in bioreduction of metal precursors through intracellular and extracellular processes. In the intracellular process the ion transport mechanism of the microbes plays a key role. The negatively charged bacterial cell wall exhibits electrostatic attraction towards positively charged metal ions. The bacterial metabolites, especially enzymes catalyse the reduction of metal ions into their corresponding NPs (Ovais *et al.*, 2018). In the extracellular method, the microbes release the metabolites such as reductases into the media that are employed in the bioreduction of metal ions, resulting in the formation of the corresponding MNPs directly in the medium (Ali *et al.*, 2020). The bacterial strains such as *Pseudomonas stutzeri*, *P. aeruginosa*, *Thiobacillus ferrooxidans*, and *E. coli* were employed to produce uniformly dispersed MNPs that possess exceptional biological properties (Salem and Fouda, 2021; Smitha *et al.*, 2009). The production of NPs by fungi offers several advantages compared to bacteria. Fungi can be utilised to produce NPs that exhibit greater uniformity compared to those synthesised by bacteria (Das *et al.*, 2017). Microorganisms have unquestionably produced MNPs with substantial antibacterial and anticancer characteristics (Salem and Fouda, 2021). Yet, the complex experimental methods involved in isolating, preparing, and maintaining cultures have placed a burden on this methodology (Simon *et al.*, 2022). This constraint, along with others, has led to an increase in the production of MNPs using plant sources. Plant-mediated synthesis is increasingly dominant, providing a faster and more controllable method compared to microbial sources (Dikshit *et al.*, 2021).

1.4.3.1.3 Biosynthesis of AgNPs from plant material

Synthesis of AgNPs using plants and plant extracts has several advantages over microbes, including simplicity, cost-effectiveness, speed, and non-pathogenicity (Aboyewa *et al.*, 2021). It is a faster and simpler process, a one-step and ecologically friendly method (Ovais *et al.*, 2016). A solution containing Ag metal ions, and a biological reducing agent are required for the green synthesis of AgNPs in a simple, one-step reaction, as depicted in **Figure 1.11**. During the process of synthesising nanoparticles from plant extracts, the plant extract is combined with a solution of metal salt at ambient temperatures (Malik *et al.*, 2014). The process is rapidly completed within a short period of time. Through biological reduction, the metals undergo a conversion from their oxidation states of either mono or divalent to a state of zero-valence (Malik *et al.*, 2014). The occurrence of nanoparticle production is visually evidenced by the observed change in colour. During the process of bio-reduction and nucleation, smaller particles undergo mechanical interactions to create larger particles that are thermodynamically more stable, leading to a growth phase (Aboyewa *et al.*, 2021). This approach generally does not necessitate conditions such as elevated temperatures, excessive energy consumption, intense pressure, or hazardous chemicals (Rafique *et al.*, 2017). The risks, costs, and labour-intensive procedures involved in isolating, growing, and purifying NPs synthesized by microbes are completely avoided when using plant extracts (Saratale *et al.*, 2021; Rafique *et al.*, 2017). The biomolecules found in plant extracts serve as both reducing and stabilizing/capping agents (Bhardwaj *et al.*, 2020). A wide range of primary and secondary plant metabolites, such as phenolics, tannins, alkaloids, terpenoids, saponins, vitamins, polysaccharides, proteins, amino acids, and enzymes, are some of the phytochemicals that have the ability to reduce and stabilise NPs (Saratale *et al.*, 2021).

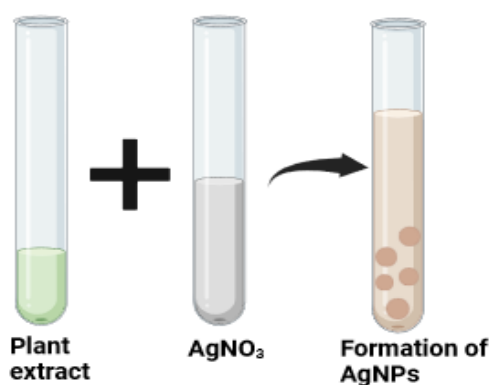


Figure 1.11: One-step process of AgNP synthesis using plant extract (adapted from Rafique *et al.*, 2017)

Phytochemicals can be extracted from a variety of plant parts, including leaves, roots, stems, and fruits (**Figure 1.10**) (Ali *et al.*, 2020). Plants produce a variety of primary and secondary metabolites, including carbohydrates, proteins, vitamins, polysaccharides, and organic acids, which can function as both reducing agents and stabilisers (**Figure 1.10**) (Ali *et al.*, 2020; Soltys *et al.*, 2021). The therapeutic capabilities of bioactive compounds can be incorporated into AgNPs (Rigo *et al.*, 2013b), leading to improvement in the biological activities (Gnanajobitha *et al.*, 2013). Furthermore, by optimising the parameters for biological synthesis, specifically by adjusting the amounts of metal precursor salts, reducing and stabilising agents, temperature, and pH, it becomes possible to easily control the shape, size, and functions of NPs (Zhang *et al.*, 2016). Biologically synthesised NPs have a wide range of characteristics including increased stability and ideal shapes and sizes (Parveen *et al.*, 2016). Numerous studies have shown that plant extracts can act as precursors for synthesis AgNPs (Simon *et al.*, 2022). Extracts from *Curcuma Longa* (turmeric), *Allium cepa* (onion), and *Solanum lycopersicum L.* (tomato) (Chand *et al.*, 2020), have been used to successfully reduce AgNO₃ to Ag⁰ in the formation of AgNPs (Simon *et al.*, 2022). Certain green-synthesised AgNPs can exhibit antimicrobial properties, which could afford them a role in the treatment or prevention of bacterial and fungal infections (Salve *et al.*, 2022). Burange *et al.* (2021) reported that AgNPs synthesised from *Aloe vera* and *Thuja orientalis* leaf extracts displayed antibacterial and antifungal activity (Burange *et al.*, 2021; Kalantari *et al.*, 2020).

1.4.3.2 Biomedical applications of AgNPs

The abundant use of AgNPs in the biological field can be attributed to their versatility. While their physicochemical characteristics greatly determine their biological use, the modification or control of their other properties can alter or determine their role in biological applications. Morphology is a characteristic that can be altered, and AgNPs can be produced in different forms, dimensions, and arrangements that make them appropriate for a particular biomedical use (Zhang *et al.*, 2016). Spherical AgNPs are commonly used in the treatment of bacterial infections and cancer, as they are easily absorbed by the target cells (Jebali *et al.*, 2013).

1.4.3.2.1 AgNPs as drug-delivery systems

The inherent therapeutic effects of prescription drugs in medicine are equally as significant as their pharmacokinetics and pharmacodynamics (Ramezanpour *et al.*, 2016). Due to the significant focus on improving present healthcare practices, the targeted delivery and effectiveness of therapeutic agents have become a highly researched area. As a result, NPs have

gained considerable interest for their potential in designing and developing advanced drug-delivery systems (Jahangirian *et al.*, 2017). AgNP-based nanosystems were assessed as effective carriers for a range of therapeutic compounds, such as anti-inflammatory (Jiang *et al.*, 2018; Karthik *et al.*, 2018), antioxidant (Arumai Selvan *et al.*, 2018; Soni and Dhiman, 2017), antibacterial (Al-Obaidi *et al.*, 2018; Kaur *et al.*, 2018), and anticancer (Petrov *et al.*, 2016) agents (Tiwari *et al.*, 2012). In order to develop new and improved drug-delivery systems that can respond to changes in temperature, light, or pH and target inflammatory, infectious, and malignant diseases, hybrid molecular units containing AgNPs were developed. AgNPs can undergo chemical modifications to facilitate the attachment and transport of biomolecules to specific cells (Jebali *et al.*, 2013). This modification is commonly achieved by conjugating bioactive molecules (or drugs) on the surface of the AgNPs (Barbieri *et al.*, 2017). AgNPs were chosen due to their excellent biocompatibility and suitability for nanoscale-based therapeutic applications (KJ, 2017). They have been proven to be useful in delivering anti-tumour pharmaceuticals, serving as either passive (Patra *et al.*, 2015) or active (Poudel *et al.*, 2018; Ding *et al.*, 2017) carriers for anticancer medications (Yang *et al.*, 2018; Díaz-Cruz *et al.*, 2016; Hefni *et al.*, 2016). Recently, there has been a significant focus on developing drug-delivery platforms using AgNP due to its unique characteristics. These include its ability to bind various organic molecules, its adjustable and strong absorption properties, and its low toxicity. Recent studies have demonstrated the potential application of AgNPs as carriers for vaccines and drugs, allowing for targeted delivery to specific cells or tissues (Rai *et al.*, 2014).

1.4.3.2.2 AgNPs for wound healing

Wound infections are a significant clinical problem that greatly affects patient health and can lead to death. They also have significant economic consequences (Wilkinson *et al.*, 2011). Ensuring the prevention of wound dehiscence and surgical-site infection is a difficult but crucial feature of modern clinical practice (Chowdhury *et al.*, 2014). The skin, being the largest and one of the most intricate organs in the human body, is susceptible to various detrimental environmental insults (You *et al.*, 2017). Both physically and chemically produced lesions on the skin can greatly disrupt its structure and function at various stages. The severity of the injury determines whether it will result in lifelong handicap or even death (Zulkifli *et al.*, 2017). Over the past few years, wound infections caused by opportunistic pathogenic microorganisms have become a significant concern in clinical practice (Gong *et al.*, 2018). The ultimate goal for managing infected wounds is to achieve rapid tissue healing, along with maximum restoration of functionality and minimal formation of scar tissue (Hendi, 2011).

The wound healing process, like any intricate pathophysiological mechanism, consists of distinct stages, including coagulation, inflammation, cellular proliferation, and matrix and tissue remodelling (Hendi, 2011). Throughout history, Ag-based chemicals and materials have been utilised to effectively combat various illnesses in an unconventional way (Hebeish *et al.*, 2011). Nanosilver has unique physicochemical properties and biological characteristics that make it highly effective in killing a wide variety of anaerobic and aerobic bacteria, including both Gram-negative and Gram-positive strains. It is widely recognised that bacterial and mammalian cells have limited ability to absorb metallic or elemental silver, mostly because it becomes chemically inactive. Hence, in order to exert targeted antibacterial properties in the presence of bodily fluids or secretions, the process of Ag ionisation is necessary. Once Ag ions (Ag^+) enter cells, they interact with both enzymatic and structural proteins (Konop *et al.*, 2016). AgNPs or Ag^+ , when employed in wound dressings, have the ability to interact with and eliminate the pathogens present in exudate (Yang and Hu, 2015). A recent study revealed the following facts concerning the absorption of AgNPs through the skin: (i) there is abundant scientific evidence regarding the penetration of NPs through the skin in laboratory settings, and (ii) there is a significant increase in penetration when the skin is damaged (Larese *et al.*, 2009). When naturally occurring biopolymers such as chitosan or collagen are used in NP synthesis, they showed great promise for creating new and improved platforms for effective wound healing applications (Larese *et al.*, 2009). Acticoat™ and Bactigras™ (Smith & Nephew), Aquacel™ (ConvaTec), PolyMem Silver™ (Aspen), and Tegaderm™ (3M) are examples of biopolymercomposites that have been altered with ionic Ag and have received US Food and Drug Administration (FDA) approval for use in wound dressings (Burduşel *et al.*, 2018). Promising outcomes have been observed when AgNPs are incorporated into innovative and naturally derived biomaterials for improved wound healing management. These materials include modified cotton fabrics, bacterial cellulose, chitosan, and sodium alginate (Burduşel *et al.*, 2018). Using AgNPs and Ag^+ carriers is an effective approach for healing of diabetic wounds, as these wounds often come with multiple secondary infections. AgNPs can aid diabetic patients in the initial stages of wound healing, while also reducing the formation of small scars (Mishra *et al.*, 2008). In addition, an *in vivo* test conducted on rats with second-degree burns showed a remarkable 98.97 % enhancement in recovery after 28 days, surpassing the effectiveness of its commercially available alternatives. Therefore, the findings indicate that the developed composite nanofiber has great potential for use in wound healing, as it helps to improve the process of skin regeneration (Karami *et al.*, 2023). Given the effective and improved antibacterial properties demonstrated by AgNPs and their significant effects in

wound treatment and medical-device coatings, it is crucial to extensively investigate their biocompatibility and safety aspects (Rigo *et al.*, 2013a).

The use of NPs in wound healing has various advantages, including their potential to resist bacterial infections, accelerate the healing process, and prevent the creation of excessive scarring. These advantages provide compelling justification for introducing nanomaterials into healthcare settings (Mihai *et al.*, 2019). AgNPs have been widely investigated in numerous clinical trials for the treatment of wounds, particularly burns and chronic wounds such as diabetic ulcers. The market for nanotechnology-based products, specifically AgNPs, is quickly growing. Following the discovery of MNPs' antibacterial capabilities, AgNPs emerged as the frontrunners in this field, entering the market for the first time in 2016 (Mihai *et al.*, 2019). According to Sánchez-López *et al.* (2020), the market for AgNPs is expected to exceed US\$3 billion by the end of 2024. Because of the broad antibacterial capabilities of Ag and AgNPs, commercially available products such as Ag-based lotions and ointments, as well as biomedical products incorporating AgNPs, such as wound dressings, have been developed (Sánchez-López *et al.*, 2020; Paladini and Pollini, 2019). AgNPs are currently widely commercialised, with 55.4 % of all nanomaterial-based consumer items (313 out of 565 products) using AgNPs in some way (Paladini and Pollini, 2019). Clinical studies show that using Acticoat™ wound dressing with Ag sulphadiazine and chlorhexidine digluconate cream can effectively prevent infections in burn wounds (Mihai *et al.*, 2019). Other materials that have shown promising results for wound healing and incorporate AgNPs include modified cotton, bacterial cellulose, chitosan, and sodium alginate (Paladini and Pollini, 2019).

1.4.3.2.3 Anti-cancer effects of AgNPs

Cancer is one of the leading causes of death globally, with a total of 18.1 million recorded cases in 2020 (World Cancer Research Fund International, 2024). Cancer is defined as the excessive and unregulated growth of cells (Afzal *et al.*, 2021). Free radicals often trigger cell proliferation and impair proper cellular function, research has demonstrated that excessive cellular proliferation can be managed, governed and regulated by NPs (Salve *et al.*, 2022). NPs have the ability to regulate the generation of free radicals, which in turn allows them to inhibit excessive cell growth (Salve *et al.*, 2022; van der Meel *et al.*, 2019). The progression and growth of cancer are greatly impacted by the tumour microenvironment, which includes the impacts of macrophages and stromal cells that promote the growth of new blood vessels and allow cancer cells to evade the immune system (Sun *et al.*, 2017).

Conventional cancer therapies often employ one or a combination of three modalities - surgical intervention, chemotherapy, and radiation therapy (Hamdi *et al.*, 2021). Although these treatments are often effective, they do have a variety of drawbacks and restrictions. Surgery is recommended when the cancer or tumours are confined to a specific area and have not spread to other parts of the body (Obidiro *et al.*, 2023). This approach may not be suitable for tumours situated in inaccessible areas or if the cancer has already metastasized (Dey *et al.*, 2023). In the case of chemotherapy, the medication may also harm normal and non-cancerous cells resulting in undesirable consequences such as alopecia, emesis, and other associated medical conditions (Dey *et al.*, 2023). Moreover, cancer cells can develop resistance to chemotherapy, thereby rendering the treatment ineffective (Dey *et al.*, 2023; Ferraz da Costa *et al.*, 2020). Radiation therapy is typically combined with surgery and chemotherapy and use high-energy beams to eliminate cancer cells (Dey *et al.*, 2023). This treatment can also result in negative side effects such as fatigue, alterations in the patient's skin, and harm to other organs (Medina *et al.*, 2020). Moreover, specific cancers may exhibit resistance to radiation therapy or necessitate dosages that exceed acceptable limits, as they pose a potential threat to adjacent healthy tissues (Obidiro *et al.*, 2023). Scientists have turned their attention to nanotechnology as a possible remedy for the issue of inadequate cancer treatment (Mahmud *et al.*, 2023; Obidiro *et al.*, 2023). Nanomaterials has the potential to revolutionise the future of cancer as treatment or drug delivery systems (Dadwal *et al.*, 2018). NP-drug conjugates can be developed to encapsulate, attach, or adsorb cancer-therapeutic agents to the NPs (Moharil *et al.*, 2017). AgNPs are a desirable tool for the diagnosis and treatment of cancer. The reason for this is mostly due to the long-standing integration of Ag into biomedical applications (Fadaka *et al.*, 2022). AgNPs have the capacity to infiltrate cancer cells, consequently impeding cell growth and inducing DNA damage (Mahmud *et al.*, 2023). A study conducted by Yuan *et al.* (2018) assessed the combined effect of AgNPs and the powerful anticancer agent Camptothecin (CPT) on human cervical cancer (HeLa) cells. Their study showed that using a combination of CPT and AgNPs effectively reduced the ability of HeLa cells to remain viable and proliferate. This suggested that using AgNPs in cancer treatment may have more benefits compared to monotherapy (Yuan *et al.*, 2018). Fadaka *et al.* (2022) investigated the cytotoxic effects of AgNPs synthesised using gum arabic (GA), and the research demonstrated that the GA-AgNPs had excellent anti-proliferative and cytotoxic activity against colon cancer (Caco-2 and HT-29) cell lines. This study, along with similar ones, has shown that the presence of phytochemicals and secondary metabolites in the plant extract resulted in NPs with enhanced cytotoxic effects (Golpour *et al.*, 2024; Fadaka *et al.*, 2022; Salve *et al.*, 2022).

1.4.4 AgNPs as antibacterial agents

Traditional methods of preventing and treating microbial infections typically require the use of antibiotics, either applied directly to the affected area or via ingestion. However, these procedures can result in ineffective therapy or the development of antibiotic resistance (Jiang *et al.*, 2022). Various nano-formulations with antibacterial properties have been created and used in the treatment of infections, particularly in infected wounds, where they play a crucial role in managing the infection (Jiang *et al.*, 2022). Due to their distinctive chemical and physical characteristics and high ratio of surface area to volume, AgNPs exhibit several biological effects, such as antibacterial (Dube *et al.*, 2020), antifungal (Rai *et al.*, 2014), anti-inflammatory (Tyavambiza *et al.*, 2021), antiviral (Rai *et al.*, 2015), anti-angiogenic (Simon *et al.*, 2022), and anticancer (Mahmud *et al.*, 2023) activities (Rai *et al.*, 2014). Utilising AgNPs as a novel class of antimicrobial agents is an appealing and economical solution to combat the issue of drug resistance observed in both Gram-negative and Gram-positive bacteria (Gurunathan *et al.*, 2014).

Substituting standard antibiotics with AgNPs is an appealing approach, as MNPs do not contribute to AMR (Kumar *et al.*, 2018). AgNPs have been widely used in clinical settings and medical investigations, and AgNP-based wound therapy products have been commercially accessible for decades (Sibbald *et al.*, 2007). AgNPs eradicate microorganisms and viruses by generating a constant supply of Ag⁺ that interact with nucleic acids and proteins, leading to molecular abnormalities (Chernousova and Epple, 2013). Multiple investigations have demonstrated the favourable potential of AgNPs as antiseptics. Luna-Hernández *et al.* (2017) discovered that the utilisation of a blend of functional chitosan and Ag nanocomposites had antibacterial properties against *S. aureus* and *P. aeruginosa* in burn injuries. Furthermore, the composite dressing resulted in significantly reduced silver buildup in mice compared to the clinically used AcasinTM nanosilver dressing (Luna-Hernández *et al.*, 2017). Haidari *et al.* (2021) demonstrated that AgNPs hydrogel acts as a versatile platform, providing numerous benefits such as antibacterial efficacy, exudate absorption, affordability, compatibility with living tissues, compatibility with blood, and improved healing for long-lasting wounds (Haidari *et al.*, 2021). Yin *et al.* (2021) created a microneedle patch with an organic framework that included AgNPs. The medicine was administered transdermally and proved effective in avoiding infections caused by *S. aureus*, *E. coli*, and *P. aeruginosa* in diabetic wounds (Yin *et al.*, 2021). Furthermore, various commercially available products containing AgNPs have been developed for clinical use (Jiang *et al.*, 2022). The products include ActicoatTM, Allevyn[®] Ag,

Aquacel® Ag Surgical, Atrauman Ag, Biatain® Silicone Ag, Flaminal®, Mepilex® Transfer Ag, SILVERCEL™, and Urgo Clean Ag (Jiang *et al.*, 2022).

Given the potent antibacterial activities of AgNPs and the significant attention they have received for their potential use as coatings on medical devices and in wound care, it is imperative to promptly establish their safety and biocompatibility (Rigo *et al.*, 2013a). The biological efficacy of NPs is governed by their physicochemical characteristics, such as size and shape (Mihai *et al.*, 2019). The biochemical characteristics of NPs, including their interaction with biological targets, hydrophobicity, and tissue penetration at deeper levels, can be easily modified by altering their material, size, shape, and electrical charge (Hamdan *et al.*, 2017). Multiple studies have demonstrated that various forms of nanomaterials have exhibited encouraging outcomes in terms of their antibacterial properties. Utilising nanomaterials to combat microbial drug resistance has been identified as a highly promising approach (Okkeh *et al.*, 2021). Before AgNP-based antimicrobial treatments can be approved for clinical use, they need to be evaluated via a multitude of laboratory-based assays (Rigo *et al.*, 2013a). *In vitro* experimental models, or laboratory-based testing, are important tools in drug development. *In vitro* techniques are inexpensive and simple, making them widely used for the testing of novel antibacterial and wound dressing materials based on NPs (Kalantari *et al.*, 2020). These assays provide significant information about the effect of various test materials on cells (Kalantari *et al.*, 2020). Several *in vitro* and *in vivo* investigations have established the antibacterial activity of AgNPs derived from various biological sources. For example, a study demonstrated that Aloe vera-conjugated AgNPs (Av-AgNPs) exhibited growth inhibitory effects on various strains, such as the Gram-positive *S. aureus*, Gram-negative *E. coli*, *A. baumannii*, *P. aeruginosa*, and the fungus *Candida albicans* (*C. albicans*) (Arshad *et al.*, 2022). In the same study, when filter paper coated with Av-AgNPs was used as a filtration medium for a sample of polluted drinking water, a significant decrease in the number of colony-forming units (CFU) of *E. coli* was detected (Arshad *et al.*, 2022). A separate investigation found that *Cotyledon orbiculata*-derived AgNPs demonstrated antibacterial properties, with the most significant effect shown against *P. aeruginosa* (Tyavambiza *et al.*, 2021). Gurunathan *et al.* (2014) demonstrated that the inclusion of *Allophylus cobbe*-AgNPs enhances the antibacterial activity of certain antibiotics against bacterial test strains. In their investigation, the activity of ampicillin was more potent against Gram-negative bacteria such as *P. aeruginosa* and *Shigella flexneri*, whereas vancomycin showed greater efficacy against Gram-positive bacteria including *S. aureus* and *Streptococcus pneumoniae*. Remarkably, the cotreatment of low doses

of antibiotics with *Allophylus cobbe*-AgNPs resulted in a substantial augmentation of cell death and an enhanced production of ROS compared to the individual effects of antibiotics or AgNPs alone. The findings indicate that AgNPs have the potential to serve as an adjunct in the treatment of diverse infectious diseases caused by both Gram-negative and Gram-positive bacteria (Gurunathan *et al.*, 2014). Karami *et al.* (2023) created two-layer nanofibers by combining polyvinyl alcohol–chitosan–gelatin/polyacrylonitrile (PVA–CS–Gel/PAN) with mupirocin in the bottom layer and *Capsella bursa-pastoris*-AgNPs in the top layer. The optimised nanofibers (Mu/1 % AgNPs) exhibited favourable biocompatibility and displayed synergistic effects against *E. coli* and *S. aureus* (Karami *et al.*, 2023).

1.4.5 Production of AgNP-loaded antimicrobial textiles

AgNPs have strong antibacterial properties and are widely used in the medical, agricultural, and environmental sectors. They can be incorporated with other systems to develop innovative nanomaterials for application in the aforementioned fields. Consequently, the use of AgNPs to modify textile (cellulosic) materials has become an appealing approach for developing alternative treatments for microbial diseases (Novoa *et al.*, 2022). Cotton has been a fundamental material in medical applications for centuries, with its usage documented as far back as the Middle Ages, when it was predominantly employed as a wound dressing (Tang *et al.*, 2013). The inherent properties of cotton, including its softness, breathability, and high absorbency, have rendered it an indispensable resource in wound care (Zhou *et al.*, 2017). Historically, cotton was utilized primarily for its physical attributes in protecting wounds from external contaminants, thus facilitating the healing process. As medical science advanced, particularly with the emergence of antiseptic practices and the germ theory of disease, the role of cotton in medical applications expanded significantly (Novoa *et al.*, 2022). Cotton's versatility allowed for its incorporation into a wide array of medical products, including sterile gauze, bandages, and surgical dressings. These applications capitalized on cotton's ability to serve as a barrier against microbial contamination while effectively managing wound exudates (Mpofu *et al.*, 2023). The hypoallergenic nature of cotton further underscores its suitability in medical contexts, particularly for patients with sensitive skin or those prone to allergic reactions (Hebeish *et al.*, 2014). This characteristic, combined with its biodegradability and natural origin, positions cotton as a preferable choice over synthetic materials, especially in the context of increasing environmental and sustainability concerns within healthcare (Jain *et al.*, 2022).

Recent advancements in cotton processing and treatment have led to the development of innovative medical textiles that retain the traditional benefits of cotton while incorporating

modern technological enhancements (El-Naggar *et al.*, 2016). Several methods have been developed to protect cotton from damage caused by microorganisms by adding antimicrobial agents. Out of these methods, the process of modifying cotton with AgNPs has gained significant attention for biomedical applications (Tang *et al.*, 2013).

Cotton has been primarily utilised for the *in situ* synthesis of fabric loaded with AgNPs (El-Naggar *et al.*, 2016). These fabrics demonstrate antibacterial properties by releasing Ag⁺ that penetrates the microbial cell and interferes with the replication of DNA. The gradual release of the AgNPs can provide certain characteristics, such as long-lasting antibacterial action (Novoa *et al.*, 2022). Tang *et al.* (2013) synthesised AgNPs-loaded fabrics that had potent and durable antibacterial properties. In another study, *Azadirachta indica* leaf extract was used in the *in situ* synthesis of eco-friendly and durable AgNPs cotton fabrics (Jain *et al.*, 2022). An evaluation was conducted to determine the efficiency of the fabric against antibiotic-resistant strains of Gram-positive and Gram-negative bacteria. The antibacterial efficiency was highest against *Bacillus licheniformis*, with a 93.3 % inhibition rate, whereas it was moderate against *K. pneumoniae* (20 %) and *E. coli* (10 %). Furthermore, the fabrics exhibited UV protection activity, with UV protection factors ranging from 33.4 – 89.9 (Jain *et al.*, 2022). *Aloe vera* leaf extract (AVE) was also utilised for the synthesis of AgNP cotton fabric *in situ* (Zhou *et al.*, 2017). These AgNP-fabrics demonstrated significant UV protection, antimicrobial activity, and durability. The UV protection factor in this instance was 148. the AVE-AgNPs-loaded cotton was effective against *E. coli* and *S. aureus* using (Zhou *et al.*, 2017).

The utilisation of plant extract in the production of AgNPs by green synthesis is regarded as a secure, economical, and ecologically friendly method for creating antibacterial finishes and fabrics, and AgNPs-functionalized cotton fabrics show great promise for use in the biomedical field (Hebeish *et al.*, 2011). Additional knowledge regarding the mechanisms that control the enhanced *in situ* green synthesis of AgNPs on fabric, particularly under hydrothermal conditions, is required to increase comprehension and explore potential applications (Zhang *et al.*, 2019).

1.4.6 Antibacterial mechanism of AgNPs

There is abundant evidence that show and proves that Ag and Ag-based compounds are highly toxic and can successfully kill a wide spectrum of microorganisms (Kalantari *et al.*, 2020). Ag antibacterial effects are caused by the release of Ag⁺ which interacts with proteins, enzymes, and thiol groups in microbes. Ag⁺ induces the release of potassium ions from bacteria, hence

the cytoplasmic or plasma membrane is an important site for Ag^+ activity (Anees Ahmad *et al.*, 2020). Ag^+ have antibacterial properties, hence the release of ions from AgNPs is expected to contribute to their antimicrobial qualities. There have been reports that exposure to Ag^+ alters the physiology and morphology of bacteria. The modifications include cytoplasm shrinkage and cell wall detachment, DNA condensation and localization in an electron-light region in the cell's centre, and cell membrane collapse, which allows intracellular components to be released (Kalantari *et al.*, 2020). Although the exact method by which AgNPs affect bacteria is not clear, there are three widely acknowledged routes of action (Dawadi *et al.*, 2021). There are numerous hypotheses about interactions between AgNPs and bacterial cells. **Figure 1.12** depicts how AgNPs interact with bacterial cells through electrostatic interactions between positively charged NPs and negatively charged cell membranes (Anees Ahmad *et al.*, 2020).

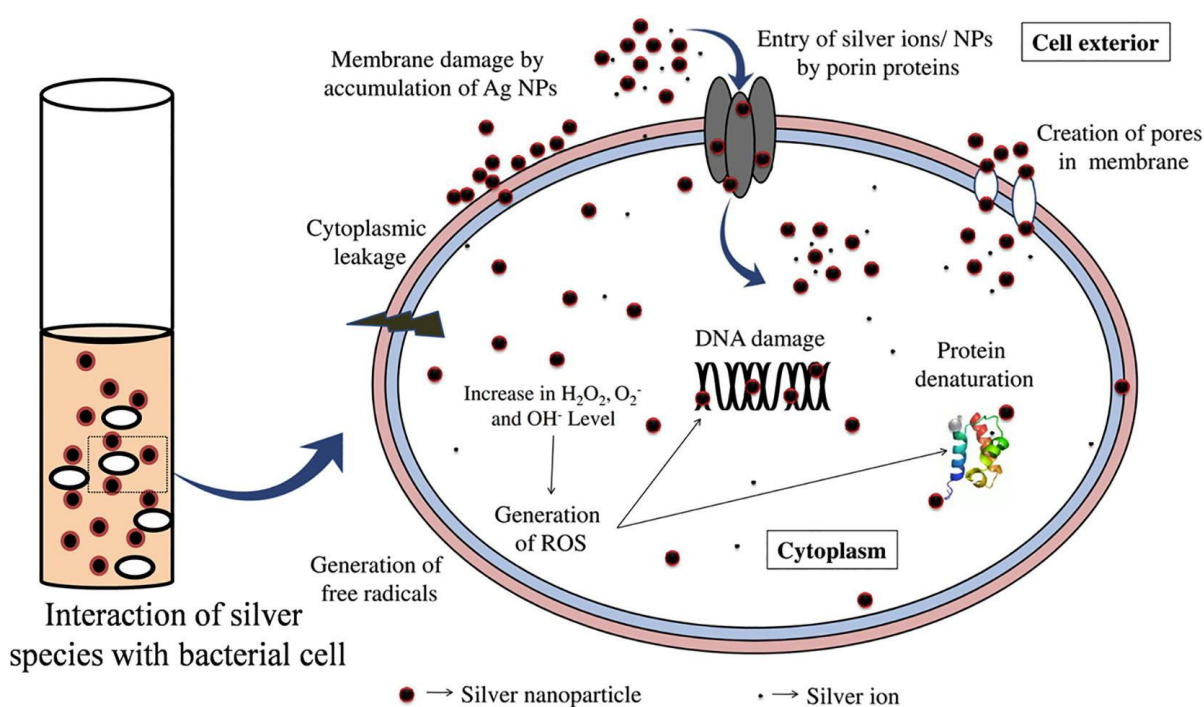


Figure 1.12: Mechanisms of antibacterial activity of AgNPs (adapted from Anees Ahmad *et al.*, 2020)

Upon absorption, the AgNPs release Ag^+ which then interferes with ATP synthesis and DNA replication. This is followed by the production of ROS by AgNPs and Ag^+ , and the direct disruption of cell membranes caused by the action of AgNPs (Dawadi *et al.*, 2021). ROS are by-products of cellular metabolism that occur naturally in respiring organisms. The cells' defence against antioxidants can regulate decreased amounts of ROS, but high levels can lead to oxidative stress (Kalantari *et al.*, 2020). The interaction between AgNPs and certain biomolecules such as thiols or enzymes involved in superoxide-radical scavenging, including

superoxide dismutases, is likely to disrupt respiratory chain enzymes in bacteria, leading to the formation of ROS (Paladini and Pollini, 2019). They have the ability to interact with proteins containing sulphur and phosphorus, such as DNA. It has been postulated that proteins containing sulphur may serve as favourable sites for interaction between AgNPs and cell membranes, similar to how Ag interacts with thiol groups in the respiratory chain and transport proteins, interrupting their normal function (Kalantari et al., 2020). The presence of damaged protein membranes on bacteria after exposure to AgNPs has been confirmed using bioluminescent bacteria, making this process more plausible than electrostatic attraction. It is vital to highlight that proteins rapidly attach to AgNPs (Paladini and Pollini, 2019). As a result, it is critical to investigate the interaction between the protein corona produced on the NPs and the cell. According to research, unlike other antibacterial therapies, a small amount of positive Ag⁺ generated from AgNPs can more easily attract bacteria with negatively charged cell membranes. Ag⁺ immobilise and penetrate the bacteria, causing respiratory failure and, eventually, bacterial death (Kalantari et al., 2020).

1.5 Red grapes and red wine

Grapes have the second-largest global crop yield, following oranges (Friedman, 2014). The Food and Agricultural Organisation of the United Nations estimated the global grape production at >67 million tonnes per annum. The main purpose of grapes is to be utilised in the production of wine (Saratale *et al.*, 2021). There are two primary classifications of wine: i) table wines, which have an alcohol content of less than 14 %, and ii) dessert wines, which are produced from grapes with high sugar and low acid levels (Friedman, 2014). Around 40 % of grapes become waste after the process of wine production (Saratale *et al.*, 2021; Friedman, 2014). Grapes are composed of organic compounds that can aid plants in protecting themselves against harmful plant diseases such as 3,5-dihydroxybenzoic acid, protocatechuic acid, and 4-hydroxy-5-(phenyl)valeric acid (Friedman, 2014), and together with their products red grapes and wine can also combat various human diseases (Ferraz da Costa *et al.*, 2020).

Grape pomace (GP), which includes seeds, skins, stems, and leaves, is a rich source of low-cost antioxidant phenolic compounds that are commonly found in winery leftovers (Friedman, 2014). These chemicals have beneficial health effects, such as cardioprotective and neuroprotective properties, etc. tannin, a polyphenolic compound, has a beneficial impact on human health due to its heightened antioxidant capacity (Saratale *et al.*, 2021). Due to the limited methods available for utilising the significant amounts of GP, it accumulates as a waste

product in close proximity to wineries, resulting in disposal and environmental challenges (Saratale *et al.*, 2021). Due to the low efficiency of extraction in winemaking, substantial quantities of condensed tannins remain as residue. GPs possess high levels of phenolic compounds due to inadequate extraction during the winemaking process (Gonzalez-Ballesteros *et al.*, 2018). This indicates that the pomace extract has the potential to be a cost-effective and eco-friendly source of natural antioxidants. GP is an inexpensive resource for obtaining phytochemicals that can be used in the culinary, cosmetic, and pharmaceutical industries, as well as for improving human health (Charalampia and Koutelidakis, 2016). González-Ballesteros *et al.* (2018) demonstrated a cost-effective and environmentally sustainable method for producing gold and AgNPs using an aqueous extract of GP. This is a substantial and sustainable use for grape remains. The researchers found that the GP extract had a higher total phenolic content and reducing activity compared to the raw materials used in wine production. In addition, the skin and seeds of berries constitute the main portion of the GP generated during winemaking as the leftover residue from fermentation. Despite this, the GP contain significant amounts of polyphenols, as a result of a partial extraction process that occurs during maceration. **Figure 1.13** depicts several extraction processes and by-products derived from GP (Ilyas *et al.*, 2021).

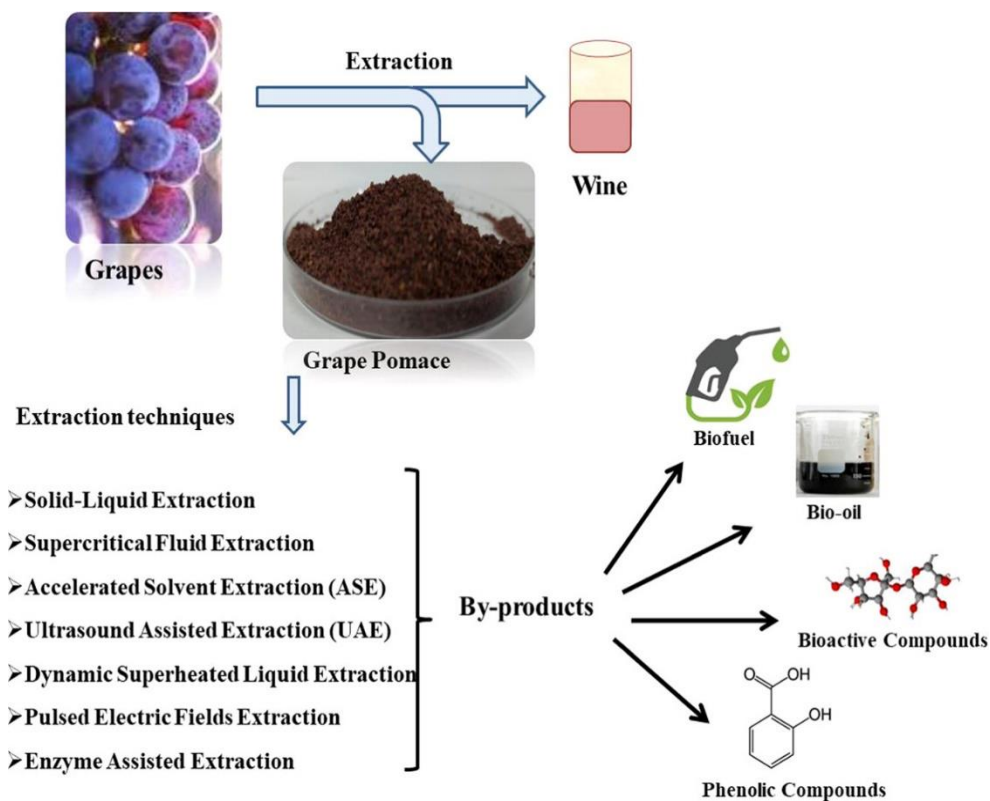


Figure 1.13: Grape pomace methods of extraction and by-products (Ilyas *et al.*, 2021)

GP extracts have been investigated as a potential source of natural antioxidants since they contain substantial levels of monomeric phenolics such as catechin, as well as dimeric, trimeric, and tetrameric procyanidins, among other compounds (Charalampia and Koutelidakis, 2016). Grapes and wine include two main forms of polyphenols: phenolic acids (hydroxybenzoic and hydroxycinnamic acids) and flavonoids (flavan-3-ols, flavonols, and anthocyanins). Few studies have specifically pinpointed the biomolecules that are necessary for the synthesis of NPs (Gonzalez-Ballesteros *et al.*, 2018). The specific biomolecules involved were identified by Gas Chromatography-Mass Spectrometry in the extracts before and after synthesis. The main components were phytols, terpenoids, and antioxidants such as 1,4-eicosadiene, δ -stan-3,5-diene, and vitamin E (Gonzalez-Ballesteros *et al.*, 2018; Charalampia and Koutelidakis, 2016). Resveratrol is one of the main phytochemicals in grapes and has been widely studied due to its many biological activities (Gianhecchi and Fierabracci, 2020).

1.5.1 Resveratrol

Resveratrol, a polyphenol known as trans 3,5,4'-trihydroxystilbene, is naturally synthesised by several plant species such as blueberries, rhubarb, peanuts, and certain types of red grapes (Kuršvietienė *et al.*, 2016). Red wine is rich in resveratrol, which is mostly found in the skin of red grapes, with concentrations ranging from 0.1 to 15 mg/L (Muqbil *et al.*, 2012). This polyphenol serves a function in safeguarding against detrimental circumstances such as pathogenic assaults, injury, and environmental strain. Resveratrol was initially identified in 1939 by Takaoka in the white hellebore (*Veratrum grandiflorum*), and subsequently categorised as a phytoalexin (Gianhecchi and Fierabracci, 2020; Muqbil *et al.*, 2012). The presence of resveratrol in RW was discovered by Siemann in 1992, and also contributed to the "French Paradox", where low levels of mortality from coronary heart disease were observed in certain parts of France, despite the population's consumption of high fat and cholesterol diet (Siemann and Creasy, 1992). The ability of resveratrol to impede the proliferation of cancer cells was discovered in 1997 by Jang and his associates (Muqbil *et al.*, 2012). Resveratrol has several advantages due to its cardioprotective, immunomodulatory, anti-inflammatory, chemopreventive (Varoni *et al.*, 2016), antibacterial, antioxidant, and anti-neurodegenerative properties (Gianhecchi and Fierabracci, 2020), which operate through distinct mechanisms.

In recent years, substantial research has significantly enhanced the knowledge of the molecular pathways that are responsible for the anticancer activities of resveratrol (Varoni *et al.*, 2016). Resveratrol's chemopreventive characteristics are specifically linked to its ability to hinder the activation of different carcinogens and promote their detoxification. It also inhibits oxidative

damage to the DNA of target cells, reduces inflammation, and inhibits the proliferation of cancer cells. The efficacy of resveratrol in treating cancer is maintained in both *in vitro* and *in vivo* due to its ability to decrease resistance to chemotherapy and inhibit the processes of angiogenesis and metastasis in cancer progression (Varoni *et al.*, 2016; Riehemann *et al.*, 2009). Resveratrol modulates many pathways, such as the PI3K/Akt/mTOR and the mitogen-activated protein kinase pathways, to promote the programmed cell death (apoptosis) of specific premalignant or cancerous cells (Barkat *et al.*, 2020; Varoni *et al.*, 2016). The preventive measures and the efficacy of resveratrol in combating autoimmune illnesses and cancer are depicted in **Figure 1.14**. The known characteristics of resveratrol can be summarised as follows: it hinders the cell cycle, causing cancer cells to undergo apoptosis, by disrupting the activity of nitric oxide synthase produced by tumours (Giancetti and Fierabracci, 2020). Additionally, it halts the growth and movement of cancer cells, safeguards DNA from damage that can lead to tumour development through its antioxidant properties and regulates the activation of nuclear factor kappa-B (Barkat *et al.* 2020; Giancetti & Fierabracci 2020; Varoni *et al.* 2016; Muqbil *et al.* 2012).

Prior to using resveratrol in clinical therapy, further investigation in human subjects is necessary, despite its notable efficacy in combating several types of cancer and reversing multidrug resistance in tumour cells (Giancetti and Fierabracci, 2020; Varoni *et al.*, 2016). The use of resveratrol in combination with pterostilbene effectively restricted the growth of triple-negative breast cancer (TNBC) tumours, which make up about 10-20 % of all breast malignancies. The expression of Silent information regulator 1 (Sirtuin 1, SIRT) was reduced, a type III histone deacetylase involved in various molecular processes such as cancer and immunological tolerance, as well as the regulation of peripheral T cell tolerance and DNA methyltransferases enzymes (Giancetti and Fierabracci, 2020). Subsequent research revealed that combining resveratrol and pterostilbene could potentially restore the expression of Oestrogen Receptor (ER) in breast cancer cells that do not have ER expression. These cells are known to be more aggressive and resistant to typical hormone-directed therapy. The findings corroborated the notion that dietary factors have the ability to regulate gene expression. Moreover, the adverse consequences of traditional medications employed to reinstate ER expression can be circumvented by employing these dietary constituents in combination therapy. Most clinical trials conducted thus far have primarily examined the safety, bioavailability, pharmacokinetics, and tolerance of resveratrol. Only a limited amount of study has been dedicated to investigating its potential anticancer properties. In addition, there have

been no clinical studies conducted or currently in progress that examine the combined use of resveratrol and other anticancer drugs (Giancetti and Fierabracci, 2020).

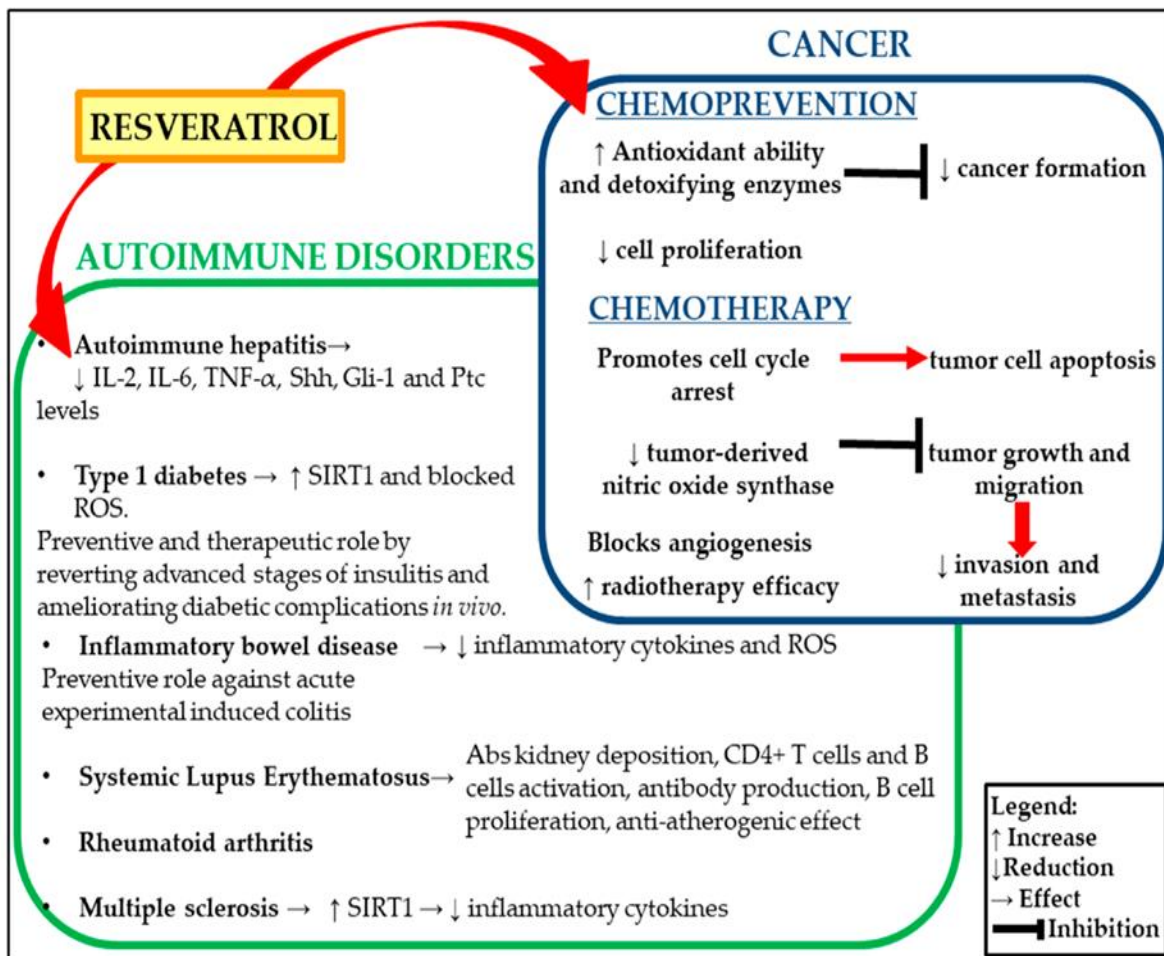


Figure 1.14: Schematic illustrating the dual role of resveratrol in modulating autoimmune disorders and cancer, which includes the reduction of pro-inflammatory cytokines (e.g., IL-2, IL-6, TNF- α) and the increase of SIRT1 expression (Giancetti and Fierabracci, 2020).

1.5.2 Antimicrobial Compounds Derived from Grape By-Products

Naturally occurring products are vital in the search for alternative antimicrobial agents (Alvarez-Martinez *et al.*, 2020; Wright, 2019; Thomford *et al.*, 2018; Atanasov *et al.*, 2015). Polyphenols found in plants and plant-derivatives are the most promising when it comes to compounds with notable biological properties including antimicrobials (Efenberger-Szmechtyk *et al.*, 2021; Brenes *et al.*, 2016; Jara-Palacios *et al.*, 2015). Moreover, these compounds can also increase the efficacy of antibiotics, potentially reducing the dose needed to inhibit or eradicate pathogenic microorganisms, or even combating their antibiotic resistance

(Alvarez-Martinez *et al.*, 2020). Even though the antibacterial activity of polyphenols has been established, the mode of action is not thoroughly understood. It is suspected that polyphenols attack various constituents of bacterial cells, including the cell membrane and bacterial proteins, upset the equilibrium of metabolites and ions, prevent biofilm formation, disrupt the proton gradient needed for oxidative phosphorylation, and disturb the synthesis of nucleic acid and the regulation of gene expression (Alvarez-Martinez *et al.*, 2020; Górnjak *et al.*, 2018; Brenes *et al.*, 2016). In addition, they could potentially reduce virulence (AlSheikh *et al.*, 2020). The cell wall of the bacteria appears to be the primary target for the antimicrobial action of phenolic compounds, as they compromise cell wall integrity, in turn causing deformation of the cell and increasing permeability (Alvarez-Martinez *et al.*, 2020). Gram-positive bacteria may be more susceptible to the effects of polyphenols than Gram-negative bacteria, since Gram-negative bacteria possess an outer membrane in the cell wall, which interrupts the uptake of polyphenols (Efenberger-Szmechtyk *et al.*, 2021).

Certain classes of polyphenols exhibit a higher affinity for cell membranes, particularly in Gram-positive bacteria. These polyphenols modify the membrane's thickness and fluidity, resulting in increased permeability (Alvarez-Martinez *et al.*, 2020; Górnjak *et al.*, 2018; Langeveld *et al.*, 2014). Polyphenols are also able to bond with vital bacterial proteins, either covalently or non-covalently, with certain compounds modifying gene expression and causing significant metabolic changes as a result (Alvarez-Martinez *et al.*, 2020). The precise mechanisms of this modification are currently unknown; however, it is suspected that it could be accomplished either by direct interaction with the bacterial DNA or by epigenetic mechanisms i.e., the alteration of the activity of transcription factors (Alvarez-Martinez *et al.*, 2020). Furthermore, polyphenols hinder several enzymes responsible for nucleic acid synthesis, a characteristic that substantially contributes to their antimicrobial action (Górnjak *et al.*, 2018). Biofilms aid bacteria in their pathogenicity by enabling them to survive in unsuitable environments (Roy *et al.*, 2018). However, these biofilms can be rendered ineffective via the action of polyphenols, which disrupt bacterial motility and adhesion (Górnjak *et al.*, 2018). The existence of free -OH groups on phenolic compounds enable them to function as antioxidants to hinder the production of reactive oxygen species and scavenge free radicals, thereby reducing redox potential and influencing microbial growth (Gyawali and Ibrahim, 2014).

Multiple studies have shown the antimicrobial abilities of extracts from the by-products of winemaking (Silva *et al.*, 2018; Xu *et al.*, 2016; Xu *et al.*, 2014; Cheng *et al.*, 2012; Cueva *et*

al., 2010; Katalinić *et al.*, 2010). These phenolics are, namely, phenolic acids, quinones, saponins, flavonoids, tannins, coumarins, terpenoids, and alkaloids (Brenes *et al.*, 2016; Gyawali and Ibrahim, 2014). Although all these polyphenols display antimicrobial activity, the difference in the structural makeup of these bioactive compounds could potentially cause variations in their antimicrobial action. Numerous factors need to be considered when discussing the antimicrobial effects of the by-products of winemaking. Some factors that have been proven to affect antimicrobial activity are the extraction process (including the solvent used), the pomace fraction, and the variety of grape (Oliveira *et al.*, 2013; Cheng *et al.*, 2012). In most reports, grape variety seems to have a huge impact on antibacterial activity (Xu *et al.*, 2016; Cheng *et al.*, 2012; Serra *et al.*, 2008). It has also been reported that by-products from red grapes had higher minimum inhibitory concentrations than that of white grapes (Katalinić *et al.*, 2010).

1.5.3 Wine By-Products in the fight against antibiotic resistance

Plant extracts are comprised of an abundance of antimicrobial compounds and as such, can be used to inhibit the growth of microbial pathogens, or even adjuvants in therapeutic applications as moderators of bacterial virulence (Efenberger-Szmechtyk *et al.*, 2021). The wide range of activity of extracts made from biological material – particularly winemaking by-products – offers a promising research avenue for the production of novel antimicrobials. Polyphenol-rich extracts from winemaking by-products have potential applications as antimicrobials, particularly in combination therapy as antibiotic adjuvants (Langeveld *et al.*, 2014; Oliveira *et al.*, 2013). Combination therapy offers a strategy to overcome bacterial resistance to antibiotics by avoiding the use of a single drug, broadening the range of effectiveness, increasing their ability to kill or inhibit bacterial growth, and preventing the development of antibiotic-resistant strains. This has the potential to reverse the progression of illnesses that do not react to traditional antibiotic treatment, including those caused by strains resistant to several drugs (Oliveira *et al.*, 2013). These by-products have the ability to decrease multidrug resistance, which can enhance the effectiveness of existing antibiotics (Friedman, 2014; Oliveira *et al.*, 2013; Cheng *et al.*, 2012).

Understanding of the mode-of-action of plant polyphenols-antibiotic synergy is still in its infancy. Knowledge thus far indicates that there are four primary processes involved: (i) alteration of the active sites in and on the bacterial cell, (Alvarez-Martinez *et al.*, 2020); (ii) hindrance of bacterial enzymes responsible for the antibiotic modification or degradation of antibiotics, (Siriwong *et al.*, 2016); (iii) improved membrane permeability (Alvarez-Martinez

et al., 2020); and (iv) inhibition of antibiotic efflux pumps (Alvarez-Martinez *et al.*, 2020). An *in vitro* study has shown that GP extracts can enhance the effectiveness of several classes of antibiotics against multidrug-resistant clinical isolates of *E. coli* and *S. aureus* (Sanhueza *et al.*, 2017). However, the identification of *in vitro* bioactive characteristics only marks the initial stage of the extensive and complex process of drug development. The bioavailability, toxicity, route of distribution, and interaction with other components or medications in a therapeutic environment are equally important (Górniak *et al.*, 2018). Furthermore, the current lack of information regarding the combined effects of winemaking by-products and their interactions with bacteria and antibiotics is a significant obstacle, necessitating further research. The absence of standardised analytical procedures used to assess antibacterial activity and synergism in various research is a further barrier that hinders a comprehensive understanding of the potential uses of winemaking by-products as antimicrobials and/or antibiotic adjuvants (AlSheikh *et al.*, 2020; Barbieri *et al.*, 2017).

1.6 Detailed research proposal

1.6.1 Problem statement

Microbial infections, especially those caused by pathogenic bacteria, pose a substantial challenge due to their potential to disrupt normal biological processes and contribute to disease progression. These infections can impair the functioning of various systems and complicate the overall management of health conditions. Moreover, antibiotic overuse can lead to antimicrobial resistance (AMR), creating new problems for infectious chronic wounds, with AMR posing a major global threat to human and animal health. Traditional treatment methods for wounds and microbial infections do not present favourable outcomes. It is therefore imperative that novel, alternative therapies are developed.

1.6.2 Aims and objectives

The aim of this project was to investigate the antimicrobial, antioxidant, and cytotoxic potential of AgNPs synthesized using RW and RW-AgNPs-loaded on cotton fabrics *in vitro*.

The research objectives were as follows:

- To synthesise RW-AgNPs and RW-AgNP-loaded cotton fabrics *in situ* using an aqueous RW.
- To characterise the RW-AgNPs and RW-ALC
- To evaluate the stability of the RW-AgNPs in various biological media.

- To examine the antioxidant potential of the RW-AgNPs.
- To investigate the antibacterial activity of the RW-AgNPs and RW-ALC human pathogenic bacteria.
- To assess the cytotoxic and anti-cancer effects of the RW-AgNPs against various human cell lines.

1.6.3 Hypothesis

Using RW in green synthesis will produce RW-AgNPs and AgNP-loaded cotton fabrics with enhanced antioxidant, antibacterial, and cytotoxic properties.

CHAPTER 2: MATERIALS AND METHODS

2.1. Materials – Reagents, Equipment, and Suppliers

Table 2.1: Materials and reagents used and their suppliers

Materials and Reagents	Supplier	Supplier Location
(2,2-azino-bis(3-ethylbenzthiazoline-6-sulphonic acid)) (ABTS)	ThermoFisher (Kandel) GmbH	Kandel, Germany
2,2-diphenyl-1-picrylhydrazyl (DPPH)	Sigma-Aldrich	Missouri, USA
2,4,6-Tris(2-pyridyl)-s-triazine (TPTZ)	Sigma-Aldrich	Missouri, USA
2-mercaptoethanol	Sigma-Aldrich	Missouri, USA
Acetic acid (CH ₃ COOH)	Kimix	Cape Town, Republic of South Africa (RSA)
Ascorbic acid (C ₆ H ₈ O ₆)	Saarchem	Gauteng, RSA
Cell culture flasks (25 cm ²)	SPL Life Sciences	Kyonggi-do, South Korea
Ciprofloxacin	Sigma-Aldrich	Missouri, USA
Conical tubes (15 ml and 50 ml)	SPL Life Sciences	Kyonggi-do, South Korea
Dimethyl sulphoxide (DMSO)	Sigma-Aldrich	Missouri, USA
Disposable cuvette (DTS0012)	Malvern Instruments	Worcestershire, United Kingdom (UK)
Disposable folded capillary cell (DTS1070)	Malvern Instruments	Worcestershire, UK
Dulbecco's Modified Eagle's Medium (DMEM)	Lonza	Basel, Switzerland
Fetal Bovine Serum (FBS)	Thermo Scientific (Gibco)	New York, USA
Hydrochloric acid (HCl)	Merck	New Jersey, USA
Millipore Ultra-purified distilled water (18.2 MΩ cm at 25 °C)	ThermoFisher Scientific	Massachusetts, USA
Müeller Hinton agar (MHA)	Sigma-Aldrich	Missouri, USA
Müeller Hinton broth (MHB)	Sigma-Aldrich	Missouri, USA
Nitric Acid (HNO ₃)	Kimix	Cape Town, RSA
Phosphate buffered saline (PBS)	Lonza	Basel, Switzerland

Polystyrene 96-well microtiter™ plates	Greiner (Lasec)	Bio-One	Cape Town, RSA
Potassium persulfate (K ₂ S ₂ O ₈)	Sigma-Aldrich		Missouri, USA
Silver nitrate (AgNO ₃)	Merck		Gauteng, RSA
Silver ICP standard	Sigma-Aldrich		Missouri, USA
Sodium acetate (C ₂ H ₃ NaO ₂)	Sigma-Aldrich		Missouri, USA
Sodium hydroxide (NaOH)	Lasec		Cape Town, RSA
Sterile cotton swabs	Lasec		Cape Town, RSA
Sterile loops	Sigma-Aldrich		Missouri, USA
Trypan blue	Sigma-Aldrich		Missouri, USA
Trypsin 2X	Sigma-Aldrich		Missouri, USA
Trypsin-EDTA	Sigma-Aldrich		Missouri, USA
Water soluble Tetrazolium salt (WST-1)	Roche		Mannheim, Germany

Table 2.2: Equipment used and their manufacturer

Equipment	Supplier	Supplier Location
Analytical weighing balance	Ohaus Adventurer	New Jersey, USA
Centrifuge 5415D	Eppendorf	Hamburg, Germany
Countess® Automated Cell Counter	ThermoFisher Scientific	Massachusetts, USA
Countess™ chamber slide	ThermoFisher Scientific	Massachusetts, USA
EC4.5-6.50 CP centrifuge	Eins-Sci	Johannesburg, RSA
Evos XL Core inverted microscope	ThermoFisher Scientific	Massachusetts, USA
Forma series II Water Jacketed CO2 incubator	ThermoFisher Scientific	Massachusetts, USA
Fourier-Transform Infrared Spectrophotometer	Perkin Elmer Spectrum 400	Waltham, USA
High-Resolution Transmission Electron Microscope (FEI Tecnai G2 20 FEG)	ThermoFisher Scientific	Massachusetts, USA
FEI Nova NanoSEM	FEI	Oregon, USA
IncoTherm Oven	Labotec	Cape Town, RSA
Incubator	ThermoFisher Scientific	Massachusetts, USA
Laminar flow hood	ThermoFisher Scientific	Massachusetts, USA
pH meter – Crison Basic 20	Lasec	Cape Town, RSA
POLARstar Omega Plate Reader	BMG Labtech	Ortenberg, Germany
Varian 710-ES Inductively Coupled Plasma Optical Emission Spectrometer	Varian	California, USA
Zetasizer – Nano-ZS90 System	Malvern Instruments	Worcestershire, UK

Table 2.3: Type of cell lines used, their sources, species, and biological media

*Cell Line	Type	Species and Source	Media
KMST-6	Normal	Human – Skin fibroblast	Complete DMEM
MCF-7	Cancer	Human – Breast tissue	Complete DMEM
Caco-2	Cancer	Human – Colon tissue	Complete DMEM
PC-3	Cancer	Human – Prostrate issue	Complete RPMI-1640
Panc-1	Cancer	Human – Pancreatic ductal tissue	Complete DMEM
MIA-Paca-2	Cancer	Human – Pancreatic tissue	Complete DMEM

*All cell lines were purchased from American Type Culture Collection (ATCC, Manassas, VA, USA)

Table 2.4: Bacterial strains used and their corresponding ATCC number

*Bacterial strain	ATCC number	Gram reaction
<i>Escherichia coli (E. coli)</i>	35218	Gram-negative
<i>Enterobacter cloacae (E. cloacae)</i>	13047	Gram-negative
<i>Acinetobacter baumannii (A. baumannii)</i>	19606	Gram-negative
<i>Staphylococcus aureus (S. aureus)</i>	25923	Gram-positive
<i>Klebsiella pneumoniae (K. pneumoniae)</i>	13883	Gram-negative
Methicillin-resistant <i>Staphylococcus aureus (MRSA)</i>	33591	Gram-positive
<i>Pseudomonas aeruginosa (P. aeruginosa)</i>	27853	Gram-negative

*All bacterial strains were purchased from ATCC.

2.2. Research Methodology

2.2.1 Sample Preparation

RW was previously prepared by Prof. AM Madiehe (DSI/MINTEK NIC Biolabels Research Node, University of the Western Cape). An aliquot of the RW was dried by rotary evaporation and the resulting paste was dried overnight in a 50 °C oven. The extract was then concentrated by freeze-drying. Stock solutions of 100 mg/ml of the RW were prepared in deionized water and stored at 4 °C until further use.

2.2.2 Hydrothermal synthesis of RW-ALC and RW-AgNPs

The synthesis of RW-AgNP-loaded cotton fabrics (RW-ALC) was performed as per a method described by Jain *et al.* (2022), with modifications. Plain woven, bleached, mercerized and scoured cotton fabric was purchased from Rivatex East Africa Limited in Eldoret, Kenya and gifted for use in this study by Ms. Nonsikelelo Mpofo. RW at a concentration of 6.25 mg/ml at pH 10 and AgNO₃ were mixed in a volume ratio of 1:10 (v/v) in a final reaction volume of 10 ml. Pieces of cotton fabric were cut at 5 mm x 5 mm and were added to the reaction mixture to achieve a material-to-liquid (ML) ratio (volume of reaction mix to weight of the fabric) of 40. A reaction mixture was also prepared without cotton fabrics, using the same conditions. The reaction mixtures were incubated in an autoclave under standard conditions (121° C, 15 psi) for 20 minutes to allow for the hydrothermal synthesis of RW-ALC and RW-AgNPs, respectively. Various parameters such as RW concentration, pH of RW and AgNO₃ concentrations were investigated for the synthesis of RW-ALC and RW-AgNPs; these parameters were altered for each set of reactions, one at a time. To avoid photoactivation of AgNO₃, the samples were wrapped in aluminium foil to prevent light exposure during synthesis. The successful *in situ* synthesis of RW-ALC was identified by the colour change of the cotton from white before the reaction to light yellow/brown after the reaction. Similarly, the successful formation of RW-AgNPs was confirmed by the change in colour from light yellow to brown. The degree of colour alteration in the cotton fabrics was directly proportional to the quantity of RW-AgNPs deposited on the surface during the synthesis process.

2.2.2.1 Effect of pH on in situ synthesis of RW-ALC

AgNO₃ at 3 mM was mixed with 12.5 mg/ml RW at its natural pH (3.4) and pH 10 at 9:1. Cotton fabrics cut into 5 mm x 5 mm were added to each vial. The samples were autoclaved at standard conditions (121° C, 15 psi) for 20 minutes. Following incubation, the reaction mixture

was cooled to room temperature (RT) after which the cotton fabrics were removed, rinsed thoroughly with deionised H₂O and allowed to dry.

2.2.2.2 Effect of AgNO₃ concentration on the hydrothermal synthesis of RW-AgNPs

Various concentrations (1 mM, 2 mM, and 3 mM) of AgNO₃ at 9 ml was mixed with 1 ml of 12.5 mg/ml RW at previously optimised pH 10. The samples were autoclaved under standard conditions (121° C, 15 psi) for 20 minutes. Following incubation, the reaction mixture was cooled to RT, and the reaction mixture was centrifuged for 30 minutes at 13 200 rpm. The supernatant was removed and discarded, and the pelleted RW-AgNPs were resuspended in equal volumes of deionised H₂O.

2.2.2.3 Effect of RW concentration on in situ synthesis of RW-AgNPs and RW-ALC

Various concentrations (1.56, 3.125, 6.25, 12.5, 15.75, 19, 22.25, and 25 mg/ml) of RW (1 ml) at pH 10 were mixed with 9 ml of 3 mM AgNO₃. Cotton fabrics cut into 5 mm x 5 mm were added to each vial. Control samples were prepared without the addition of cotton fabrics. The samples were placed in an autoclave and subjected to incubation under standard conditions (121° C, 15 psi) for 20 minutes. Following incubation, the reaction mixture was cooled to RT after which the cotton fabrics were removed, rinsed thoroughly with deionised H₂O and allowed to dry. The reaction mixture containing RW-AgNPs was centrifuged for 30 minutes at 13 200 rpm. The supernatant was removed and discarded, and the pelleted RW-AgNPs were resuspended in equal volumes of deionised H₂O.

2.2.2.4 Upscaled synthesis and characterisation of RW-AgNPs and RW-ALC

A large-scale synthesis of RW-AgNPs and RW-ALC was performed using the previously optimised conditions in a final reaction volume of 50 ml. The resulting RW-AgNPs and RW-ALC were characterised using a range of analytical techniques, including Ultraviolet-Visible (UV-Vis) Spectroscopy, Dynamic Light Scattering (DLS), High-Resolution Transmission Electron Microscopy (HR-TEM), Scanning Electron Microscopy, Inductively Coupled Plasma Optical Emission Spectroscopy (ICP-OES), and Fourier Transform Infrared (FTIR) Spectroscopy.

2.2.2.4.1 Ultraviolet-visible spectroscopy

The confirmation of RW-AgNPs formation was achieved through the utilisation of UV-Vis spectroscopy, which involved the observation of the SPR features of the biogenic AgNPs. The absorbance spectra were measured within the wavelength (λ) range of 300 to 800 nm using a

POLARstar Omega microplate reader. The RW-AgNPs samples were diluted with sterile deionised H₂O in a 1:10 ratio (v/v) in a final volume of 300 µl in a 96-well flat-bottom microtiter plate. The results obtained was analysed by Omega Mars and Microsoft Excel software.

2.2.2.4.2 Dynamic Light Scattering

The hydrodynamic size, polydispersity index (PDI), size distribution, and zeta potential (ζ -potential) of the RW-AgNPs were analysed by Malvern Zetasizer Nano ZS90. RW-AgNPs samples were diluted with sterile deionised H₂O in a ratio of 1:10 (v/v) and then transferred onto a 10 mm optical density square polystyrene cuvette. The solution containing RW-AgNPs was examined using DLS at a temperature of 25°C and an angle of 90°. In order to determine the ζ -potential, a volume of 0.7 ml of the diluted RW-AgNPs was added into a disposable foldable capillary cell. The analysis was conducted at a voltage of 4 mV, with the temperature set at 25 °C and the angle at 90°.

2.2.2.4.3 High-resolution Transmission Electron microscopy

The morphology and core size of the synthesised RW-AgNPs were examined using high-resolution transmission electron microscopy (HR-TEM). A single droplet of the diluted RW-AgNPs was deposited onto a carbon-coated copper grid. The grid was subsequently dried using a xenon lamp for a duration of 10 minutes. The dried samples were then examined and observed using an FEI Tecnai G2 20 field-emission gun HR-TEM microscope. The microscope was utilised in a bright field mode with an accelerating voltage of 200 kV. Micrograph images were captured and utilised to determine the core dimensions of the RW-AgNPs by making use of ImageJ analysis software (National Institute of Health, USA) and OriginPro 2021 software.

2.2.2.4.4 Scanning Electron microscopy

Scanning electron microscopy was used to analyse the dispersion and deposition of RW-AgNPs on the cotton fabrics. RW-ALC on a 5 mm x 5 mm cotton was affixed to the sample stub and covered with a thin layer of gold using sputter coating. The deposition of AgNPs on the cotton was then detected using a scanning electron microscope (FEI Nova NanoSEM).

2.2.2.4.5 Fourier-transform Infrared spectroscopy

The functional groups of phytochemicals involved in the synthesis of RW-AgNPs were identified by FTIR. The freeze-dried RW (100 µl), RW-AgNPs (100 µl), and RW-ALC (250 mg) were separately combined and pulverised with potassium bromide (KBr) using a mortar

and pestle. The powdered RW, RW-AgNPs and RW-ALC were compacted into a pellet and examined on an Attenuated Total Reflectance (ATR) element using a Perkin Elmer Spectrum 400 FTIR spectrometer. Background correction was performed using pure KBr. The data was analysed via the Spectrum (v9.5) and OriginPro (v9.8) 2021 software.

2.2.2.4.6 Inductively Coupled Plasma Optical Emission Spectrometry

The amount of silver in the RW-AgNPs and RW-ALC was determined using inductively coupled plasma optical emission spectrometry (ICP-OES). The analysis was conducted using a Varian 710-ES ICP Optical Emission Spectrometer. The RW-AgNPs and RW-ALC were digested in aqua regia. Briefly, 1 ml of RW-AgNPs were centrifuged at 13 200 rpm for 15 minutes at 25°C. A solution of aqua regia, made by mixing 3 parts hydrochloric acid (HCl) with 1 part nitric acid (HNO₃), was added to the RW-AgNPs pellet. The mixture was then heated at 90 °C and left to incubate for 24 hours. Following incubation, the solution was diluted to 10 ml using a 2 % HCl solution. For the RW-ALC samples, a 5 mm x 5 mm piece of cotton was digested in 5 ml of nitric acid (HNO₃) overnight. The sample was centrifuged, and the resulting supernatant was collected and utilised to quantify the silver concentration on the tested fabric. The experiment was conducted in triplicate. The specimens were sent to the Chemistry Department (University of the Western Cape) for subsequent analysis. The reported results were derived using a calibration curve utilising a silver ICP standard (Sigma-Aldrich). The following formula was employed to determine the concentration of silver in the samples:

$$\text{Concentration of silver } (\mu\text{g/ml}) = \text{Amount of silver detected} \times \text{dilution factor}$$

2.2.3 Stability analysis of RW-AgNPs

The stability of the RW-AgNPs was assessed in four different media: MHB, dH₂O, PBS, and DMEM. The RW-AgNPs were diluted with MHB, dH₂O, PBS, and DMEM in a 1:10 (v/v) ratio in a final volume of 1 ml. The samples were placed in an incubator set at 37 °C. An aliquot of 100 µl per sample was placed on a 96-well plate at different time intervals (0, 24, and 48 hours) for UV-Vis spectroscopy analysis read at the 300-800 nm range on a POLARstar Omega microplate reader (BMG Labtech Germany). The stability of the RW-AgNPs was assessed by examining any alterations in the UV-Vis spectra. The experiment was conducted in triplicate.

2.2.4 Analysis of phytochemical composition and assessment of antioxidant activity

2.2.4.1 Total Phenolic Content (TPC)

The TPC of RW and RW-AgNPs was quantified using the Folin-Ciocalteu (FC) assay with gallic acid as the reference standard as described before (Alirezalu *et al.*, 2020). Various concentrations of gallic acid (15.6, 31.25, 62.5, 125, 250, 500 µg/ml) were used. In a 96-well plate, 20 µl of RW, RW-AgNPs, and gallic acid standards were added. Subsequently, 100 µl of a 10 % solution of FC reagent was introduced into each well, followed by an incubation period of 5 minutes. Subsequently, 80 µl of a 7.5 % aqueous Na₂CO₃ solution was added to the wells and the plate was allowed to incubate for 30 minutes at room temperature. The TPC was determined by measuring absorbance at 765 nm. The TPC was quantified as gallic acid equivalent (µg GAE/ml) generated using the gallic acid standard curve. The experiment was conducted in triplicate.

2.2.4.2 2,2'-azino-di-(3-ethylbenzthiazoline sulfonic acid (ABTS) scavenging assay

The antioxidant capacity of RW and RW-AgNPs was assessed using the ABTS (2,2'-azino-di-(3-ethylbenzthiazoline sulfonic acid) assay following a previously described method (Arumai *et al.*, 2018) with some modifications. A solution containing 7 mM of ABTS was prepared using deionized H₂O. This solution was then combined with 2.45 mM of K₂S₂O₈ in a 1:1 ratio. The resulting combination was covered with foil and stored in a dark environment at ambient temperature for a period of 12-16 hours. After this time, a blue-green colour was observed. The blue-green ABTS solution was diluted with ethanol to modify its absorbance to 0.70 at 734 nm. Various concentrations of RW, RW-AgNPs, and the standard ascorbic acid were prepared. Then, 20 µl of RW, RW-AgNPs, and ascorbic acid were combined with 180 µl of ABTS in a 96-well plate. The plate was incubated in a dark environment and kept at room temperature for 6 minutes. The samples were then measured at 734 nm. The ABTS radical scavenging was calculated using the following equation (EQ):

$$\text{EQ 1: Radical scavenging (\%)} = (OD \text{ blank} - OD \text{ sample}) / OD \text{ blank} \times 100 \%$$

2.2.4.3 2,2-diphenyl-1-picrylhydrazyl (DPPH) scavenging assay

The total antioxidant content of the RW and RW-AgNPs was determined using the DPPH scavenging assay as per a study by Baliyan *et al.* (2022), with modifications. Briefly, 100 µl of DPPH solution (0.25 mM in methanol) was added to every well of a 96-well plate. Afterwards, varying quantities of RW, RW-AgNPs, and ascorbic acid (ranging from 0.78 to 100 µg/ml)

were introduced into each well. The plate was placed in a dark environment and kept at room temperature for 1 to 2 hours. The samples were analysed using UV-Vis spectroscopy, measured at 517 nm. The proportion of radical scavenging activity was determined using EQ 1.

2.2.5 Antibacterial efficacy of RW-AgNPs and RW-ALC

2.2.5.1 MacFarland standardising of bacteria culture for microbiological assays

MacFarland turbidity standard was employed for the standardisation of antimicrobial tests conducted according to the method outlined by Balouiri *et al.* (2016). Individual bacterial strains (*E. coli*, *E. cloacae*, *A. baumannii*, *S. aureus*, *K. pneumoniae*, MRSA, and *P. aeruginosa*) were cultured on MHA plates and incubated at 37 °C for 24 hours. Thereafter, single colonies from the separate bacterial cultures were inoculated in 2 ml of MHB and incubated for 2 hours at 37 °C in a shaking incubator at 200 rpm. Afterwards, the spectrophotometer was used to determine the optical density (OD) of the bacterial suspensions at a wavelength of 600 nm. The OD value was calibrated to a range of 0.08-0.12 then diluted 1:150 for all assays, which corresponds to the 0.5 MacFarland turbidity standard, equivalent to approximately 1.5×10^8 colony-forming units per millilitre (CFU/ml).

2.2.5.2 Evaluating the antibacterial activity of RW-ALC using disc diffusion method

The antibacterial activity of the RW-ALC was investigated using the agar disc diffusion method as outlined by Jain *et al.* (2022), with modifications. The bacterial suspensions with a turbidity standard of 0.5 MacFarland were evenly spread onto MHA plates using sterile cotton swabs. Thereafter, eight 5 mm × 5 mm pieces of RW-ALC were carefully deposited on the MHA plates using sterile forceps. Each of the eight RW-ALC pieces was synthesized using various concentrations (ranging from 1.56 – 25 mg/ml) of RW. A standard cotton piece was utilized as the negative control. The positive control was created by applying 50 µl of 15 µg/ml Ciprofloxacin onto a clean piece of cotton, except for *E. coli* where 10 µg/ml Ciprofloxacin was used instead. The MHA plates were incubated at 37 °C for a duration of 24 hours. The diameter of the zone of inhibition was measured with a ruler to evaluate the antibacterial efficacy of the RW-ALC. The experiment was conducted in triplicate and used to ascertain the optimal concentration of RW for synthesizing RW-ALC, namely the concentration that produced RW-ALC with the highest antibacterial activity.

2.2.5.3 Evaluating the effects of 2-mercaptoethanol on the antibacterial activity of RW-ALC

The effect of 2-mercaptoethanol on the antibacterial efficacy of the RW-ALC was investigated using the method outlined in **Section 2.2.5.2**, with modifications. Two pieces of RW-ALC of each concentration (ranging from 1.56 – 25 mg/ml of RW) were used in this investigation – one piece was left unaltered, and the other was pre-incubated with a 10 % solution of 2-mercaptoethanol for 5 minutes, then left to dry before use in the agar disc diffusion assay.

2.2.5.4 Determination of MIC

The microdilution test was used to determine the MIC of the RW-AgNPs. Microbial cultures were prepared according to the MacFarland turbidity standard outlined in **Section 2.2.5.1**, then, 50 µl of the diluted bacterial suspensions was added to a 96-well flat-bottom microtiter™ plate. After that, 50 µl of RW-AgNPs, which were diluted in sterile deionised H₂O, were added to the plate. The concentrations of RW-AgNPs used were 0.195 – 25 µg/ml. In the negative control, 50 µl of MHB was introduced into the well. The positive control involved adding 50 µl of a solution containing 10 µg/ml of Ciprofloxacin for all strains, except for *E. coli* where 5 µg/ml of Ciprofloxacin was employed instead. The plates were hermetically sealed and placed in an incubator set at 37 °C for 24 hours. Following incubation, the plates were examined visually, and the MIC was determined as the lowest concentration at which no microbial growth was observed in the wells. Additionally, spectrophotometry was used to measure the absorbance at 600 nm using a POLARstar Omega microplate reader. The experiment was repeated three times.

2.2.5.5 Determination of MBC

The MBC was determined by subculturing the bacterial culture/RW-AgNPs mixture from the wells that did not display any visible bacterial growth in the microdilution assay (**Section 2.2.5.4**) onto MHA plates. The plates were placed in an incubator set at 37 °C for 24 hours. The MBC was determined as the concentration at which no growth was detected on the MHA plates. The experiment was conducted in triplicate.

2.2.6 Effect of RW-AgNPs on human cell lines *in vitro*

2.2.6.1. Cell culture and maintenance

The panel of cell lines listed in **Table 2.3** were used to investigate the cytotoxic and anti-cancer effects of the RW-AgNPs in this study. All of the cells were purchased from ATCC. Cryovials

of frozen stocks, containing 1-2 ml of cells suspended in freezing media containing 10 % DMSO, were taken out of the cryo-freezer (-80 °C). The cells were thawed and transferred into a 15 ml tube with 5 ml of complete media (DMEM with 10 % FBS and 1 % Pen-strep). They were subsequently centrifuged at 3000 rpm for 5 minutes using an EC4.5-6.50 CP centrifuge. The supernatant was discarded, and the pellet was resuspended in 1 ml of media. This mixture was transferred into T25 cell culture flasks containing their respective media up to 5 ml. The flasks were placed in a Forma series II Water Jacketed CO₂ incubator and kept at a temperature of 37 °C. The cells were routinely examined using an Evos XL Core inverted microscope to monitor their growth and any contamination. The media was replaced at intervals of 2 to 3 days as necessary.

2.2.6.2 Cell trypsinisation

The cells were trypsinized when they reached a confluency of 70-80 %. The media was removed from the flask and the cells were rinsed with 2-5 ml of DPBS. Then, 2 ml of 2X trypsin (KMST-6, Caco-2, PC-3, Panc-1, MIA-Paca-2) or trypsin EDTA (MCF-7) was added into the flasks and incubated at 37 °C. The cells were monitored using an Evos XL Core inverted microscope at intervals of 2-5 minutes to determine if the cells had detached. In order to halt the trypsinization process, 5 ml of growth media was added to the flask. The mixture was transferred into a 15 ml tube and centrifuged for 5 minutes at 3000 rpm. The pellets were reconstituted in 2 ml of complete medium.

2.2.6.3 Cell cryopreservation

The cells underwent trypsinization according to the procedure outlined in **Section 2.2.6.2**. They were then resuspended in DMEM containing 10 % DMSO. Subsequently, 1.5 ml of the mixture was aliquoted into 2 ml cryovials and stored at -80 °C.

2.2.6.4 Cell count: trypan blue exclusion assay

Following the trypsinisation methodology described in **Section 2.2.6.2**, an aliquot of the cell suspension was mixed with an equal amount of 0.4 % trypan blue dye. The resulting mixture was then placed onto a Countess™ chamber slide for cell counting. The quantification of viable cells was performed using the Countess® Automated Cell Counter. The concentration of cells (1×10^5 live cells) was standardized based on the quantity of live cells to be cultured in a 96-well plate.

2.2.6.5 Cell viability assay: WST-1

The cytotoxicity of the RW and RW-AgNPs were evaluated on five cancerous (MCF-7 Caco-2, PC-3, Panc-1, MIA-Paca-2) and one non-cancerous (KMST-6) human cell lines using the water-soluble tetrazolium salt (WST-1) assay following the manufacturer's instructions (Roche). Briefly, 100 µl of cells (1×10^5 live cells) was seeded in 96-well plates, and incubated for 24-hour at 37 °C and 5 % CO₂. Following this incubation, the cells received treatment with different concentrations of RW (ranging from 0.78 – 1000 µg/ml) and RW-AgNPs (ranging from 0.048 – 100 µg/ml). The positive control consisted of DMEM containing DMSO at a ratio of 9:1 (v/v). Untreated cells (DMEM) were utilized as a negative control. The treatments were removed from the wells, and the cells were rinsed with DPBS. Afterwards, 100 µl of DMEM with 10 % WST-1 reagent was added to all wells, except for the interference wells where 100 µl of DMEM only was added. The plate was wrapped in foil and placed in an incubator for 3 hours. Thereafter, the absorbances of the plates were measured at 440 nm, using a reference wavelength of 630 nm. The cell viability was determined by calculating the percentage (%) of viable cells using the EQ 2:

$$\text{EQ 2: Cell viability (\%)} = (\text{Test absorbance at 440 nm} - \text{Absorbance at 630 nm}) / (\text{Negative control absorbance at 440 nm} - \text{Absorbance at 630 nm}) \times 100 \%$$

2.2.7 Statistical analysis

The data was subjected to statistical analysis using the GraphPad Prism version 6 and a One-way ANOVA test. Within each group of assays in this investigation, multiple-comparison analyses were conducted. The assays were performed in triplicates and repeated three times, and the findings were presented as the average \pm standard error of the mean (SEM) of the three repeated experiments. The levels of statistical significance were denoted as follows: * for $p < 0.05$, ** for $p < 0.01$, *** for $p < 0.001$, and **** for $p < 0.0001$. IC₅₀ values were determined using GraphPad Prism v6.

CHAPTER 3: RESULTS AND DISCUSSION

Green nanotechnology originated from the integration of green chemistry principles in the synthesis of multifunctional NPs. Green nanotechnology aims to produce nanomaterials that are environmentally benign and reduces potential risks to the environment and human health during the manufacturing processes and their downstream applications (Soni *et al.*, 2022). The utilisation of biological entities in the synthesis of MNPs has attracted considerable interest owing to a diverse array of features exhibited by the biogenic NPs such as their remarkable optical, chemical, and physical properties (Parveen *et al.*, 2016). Biomolecules have the ability to change the size and shape of NPs, thus influencing their activity for various applications (Kalantari *et al.*, 2020; Parveen *et al.*, 2016). The therapeutic properties of bioactive chemicals can also be integrated into NPs, resulting in enhanced and/or synergistic biological functions of the NPs (Gnanajobitha *et al.*, 2013). In addition, it is possible to readily manipulate the shape, size, and distribution of NPs by fine-tuning the factors involved in biological synthesis, such as the concentration of metal precursor salts, type of reducing and stabilising agents, temperature, and pH (Zhang *et al.*, 2016).

The study presents the green synthesis of RW-AgNPs using the *ex situ* and *in situ* methods, as well as their biological (antibacterial, antioxidant, and cytotoxic) activities *in vitro*. The synthesised RW-AgNPs (*ex situ*) and RW-ALC (*in situ*) were characterised using several techniques including UV-Vis spectroscopy, DLS, electron microscopy (HR-TEM and SEM), ICP-OES, and FTIR. The antibacterial effects of RW-AgNPs and RW-ALC were tested *in vitro* against human pathogenic bacteria associated with antimicrobial resistance (AMR), including *S. aureus*, MRSA, *E. coli*, *P. aeruginosa*, *K. pneumoniae*, *E. cloacae*, and *A. baumannii*. The antioxidant scavenging abilities of RW-AgNPs were assessed through DPPH and ABTS assays. Additionally, the biocompatibility and anticancer/cytotoxic effects of RW-AgNPs were examined using the WST-1 cell viability assay on human skin fibroblast (KMST-6) and human cancer (MCF-7, Caco-2, PC-3, Panc-1, and MIA-Paca-2) cell lines.

3.1 Optimization of hydrothermal synthesis of RW-AgNPs

To ensure that optimal production rate, yield, and stability of the RW-AgNPs are achieved, some reaction parameters were optimized. These parameters can influence the physicochemical characteristics, morphology of the NPs, and their downstream applications (Soltys *et al.*, 2021). The concentration and type of phytochemicals present in the plant extracts, as well as the pH, reaction time, and temperature (Rafique *et al.*, 2017), and the ratio of the metal salt to the plant

extract (Srikar *et al.*, 2016) can have a considerable impact on the quality, size, and shape of the NPs.

3.1.1 Visual observation of synthesis

RW-AgNPs, and subsequently RW-ALC, were synthesised following a green synthesis method whereby an aqueous biological extract (RW) was employed as a reducing and capping agent, and AgNO₃ as an Ag⁺ ion precursor. During the synthesis process, the red-coloured RW was combined with a transparent solution of AgNO₃; the resulting brown solution indicated the presence of RW-AgNPs (**Figures 3.1(a-c)**). Similarly, the *in situ* synthesis of RW-AgNPs on the cotton fabric (RW-ALC) was confirmed by the colour change of the fabric at the end of synthesis (**Figure 3.1(d)**). The fabric's colour changed from white to a yellowish-brown colour, indicating the presence of AgNPs on the surface of the cotton. The colour change can be ascribed to the SPR and the bioreduction of Ag⁺ by phytochemicals found in the RW (Delgado-Beleño *et al.*, 2018). The phenomenon can be attributed to the collective oscillation of electrons in AgNPs, which interacts with light waves and produces a distinct absorption peak at around 400 nm (Hanh *et al.*, 2017). Furthermore, the alteration in colour has been previously documented as an early indication of the presence of AgNPs, as it is anticipated that AgNPs have a distinctive brown hue (Dube *et al.*, 2020).

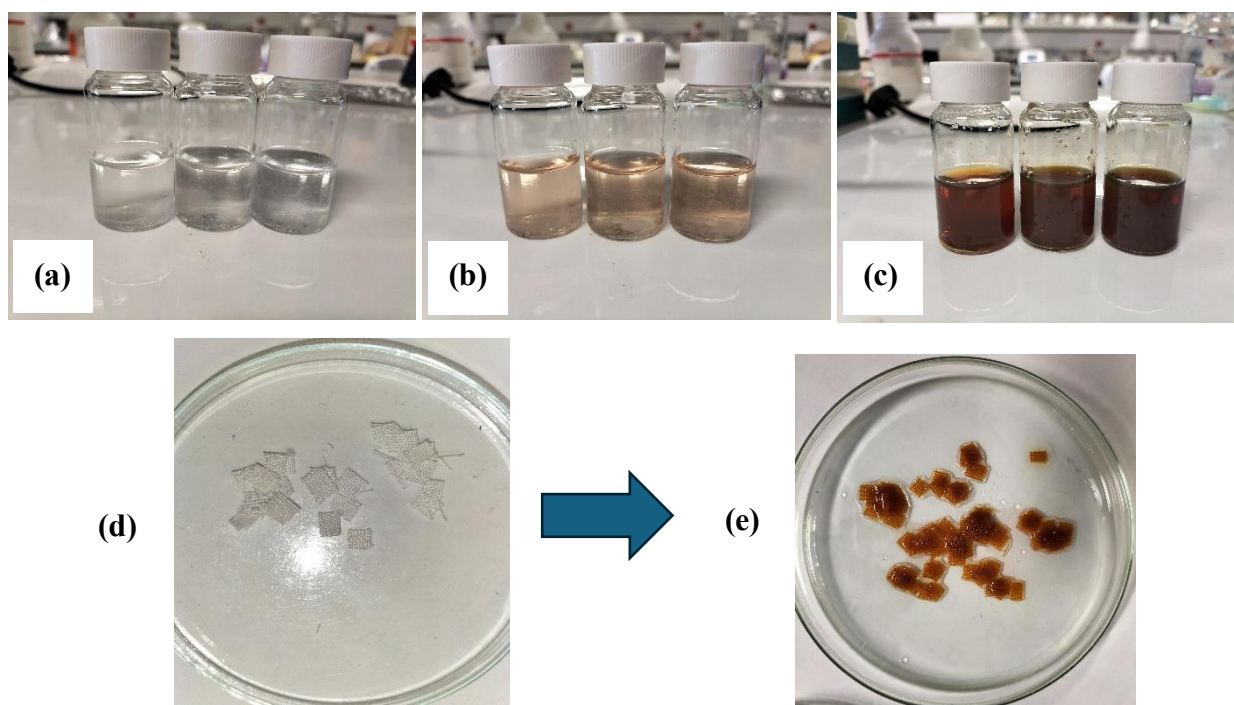


Figure 3.1: *Ex situ* and *in situ* synthesis of RW-AgNPs under hydrothermal conditions. (a) AgNO₃, (b) AgNO₃ mixed with RW, (c) reaction mixture at the end of the synthesis period, (d) cotton fabrics before and (e) after being used in the *in situ* synthesis of RW-AgNPs.

3.1.2 Effect of pH on RW-AgNPs synthesis

Research has demonstrated that altering the pH level of the reaction environment can impact the shape and dimensions of the biogenic AgNPs (Dubey *et al.*, 2010). High pH values can result in the formation of smaller particles in comparison to lower acidic pH values. Adjusting the pH of the reaction mixture alters the charges of the functional groups of the phytochemicals in the plant extract, which in turn affects the local surface charge of NPs in the nucleation and growth stages of the synthesis (Makarov *et al.*, 2014). This change in pH determines how the metal ions and phytochemicals interact, thus affecting the capping and stabilising of NPs, which ultimately affects the size, morphology, and yield of NPs.

The distribution of RW-AgNPs on the cotton fibres was visually detected through colour change from white to brown (**Figure 3.1(d-e)**). The hue of the fabrics after *in situ* synthesis was determined by the quantity of RW-AgNPs that were effectively deposited onto the fabric surface during the reaction. The effect of pH on the hydrothermal synthesis of RW-ALC and deposition of RW-AgNPs onto the cotton fibres was assessed using the RW at natural pH of 4.3 and pH 10. The resulting RW-ALC were visually examined and compared when the reaction was completed (**Figure 3.2(a-b)**). Upon visual examination, the cotton containing RW-ALC at a natural pH appeared to have a more grey-brown colour after the fabrics were rinsed and dried. In contrast, the cotton containing RW-ALC at a pH 10 exhibited a reddish-brown colour. The difference in results can be attributed to the absence of available ions in the natural pH RW, leading to a reduced synthesis of RW-AgNPs and an increased deposition of unreacted silver ions (from AgNO_3) onto the textiles. The confirmation of this was obtained through the UV-Vis analysis of the reaction mixture (**Figure 3.2(c)**). The analysis clearly indicated that RW-ALC produced from the natural pH sample were of poor quality. This is evident from the significantly red-shifted spectra with a SPR (λ_{max}) of 430 nm and a lower absorbance of 0.863, compared to the pH 10 sample which exhibited an absorbance of 2.0 and an SPR of 414 nm.

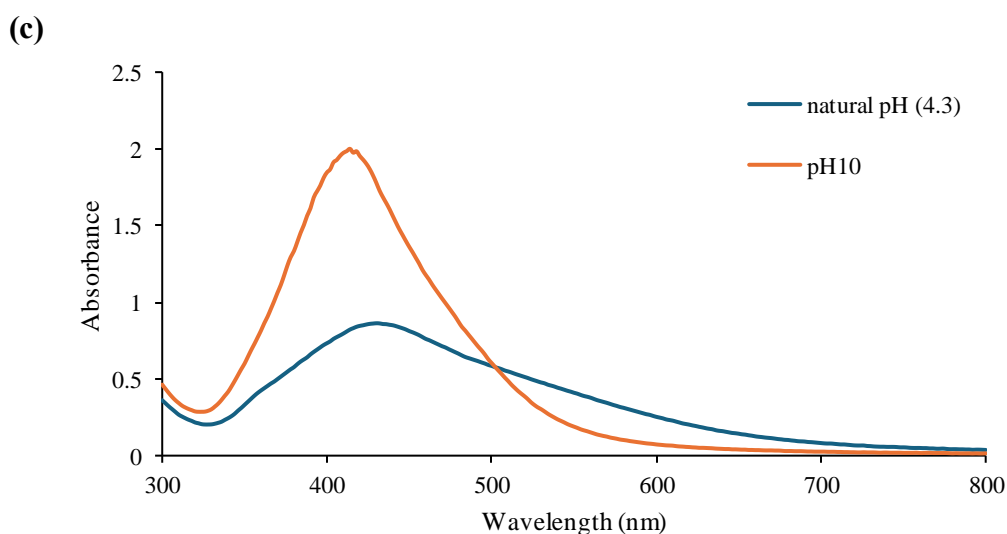
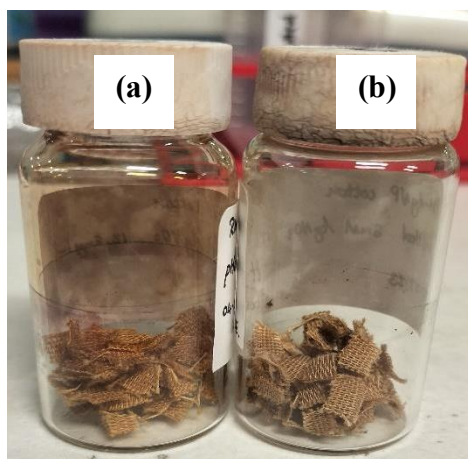


Figure 3.2: RW-ALC synthesised under hydrothermal conditions using 3 mM AgNO₃ and 12.5 mg/ml RW at (a) pH 10 and (b) at natural pH (4.3). (c) UV-Vis spectra of RW-AgNPs showing the effect of various pH levels with 3 mM AgNO₃ and 12.5 mg/ml RW.

3.1.3 Effect of AgNO₃ concentration on hydrothermal synthesis of RW-AgNPs

The AgNO₃ concentration was optimised using the previously optimised pH and RW concentrations, which were pH 10 and 12.5 mg/ml, respectively. The effect of salt concentration on the synthesis of RW-AgNPs is demonstrated in **Figure 3.3**. The UV-Vis spectra demonstrated that the synthesis of RW-AgNP took place at all concentrations of AgNO₃ that were examined and that the absorption peaks increased with an increasing salt concentration. The SPR values for 1 mM, 2 mM, and 3 mM were 412, 412, and 414 nm, respectively. The corresponding absorbance values at SPR were 0.426, 0.817, and 1.244. The 3 mM AgNO₃ produced more RW-AgNPs, their SPR wavelength red-shifted to 414 nm, in comparison to the 412 nm wavelength for 1 and 2 mM samples. The high absorbance value of

1.244 for 3 mM AgNO₃ indicated a higher yield of RW-AgNPs. It is worth noting that the absorbance of AgNPs is directly correlated with the concentration of AgNPs in solution (Mohammadlou *et al.*, 2017). In addition, the RW-AgNPs at 1 mM and 2 mM had wider peaks compared to the ones synthesized with 3 mM, indicating that the RW-AgNPs had non-uniform particle sizes. The peak of RW-AgNPs in the 3 mM sample was more distinct and narrower, indicating that they have a uniform size distribution. Although it is generally observed that increasing the salt concentration in synthesis reactions leads to the formation of larger and more varied NPs, there have been reports of hydrothermal syntheses where NPs formed with lower salt concentrations were large in size (Liu *et al.*, 2022). Therefore, 3 mM AgNO₃ was selected as the optimal concentration, as it resulted in the highest quantity of RW-AgNPs, with a rather uniform size distribution.

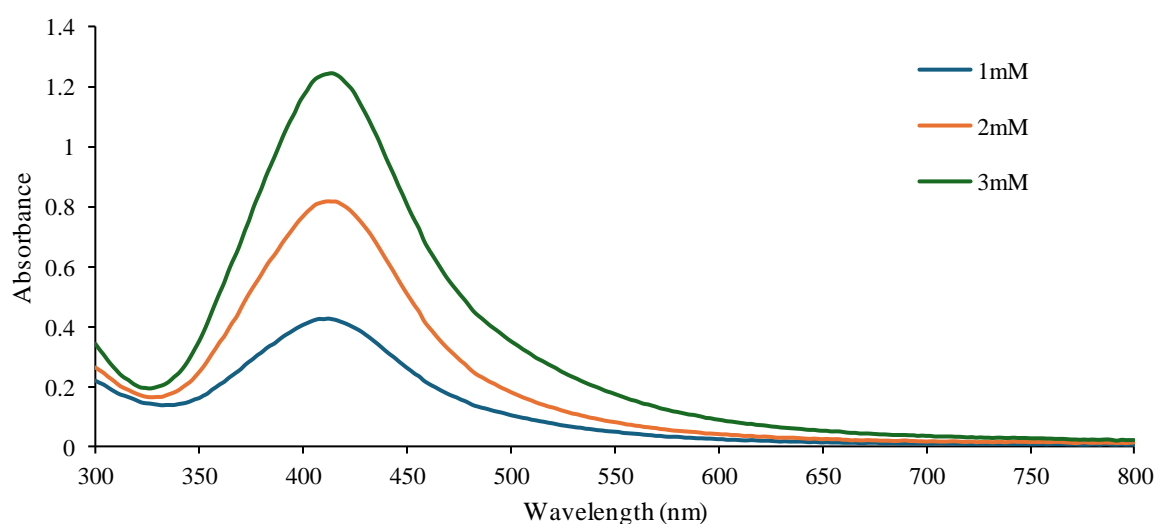


Figure 3.3: UV-Vis spectra of RW-AgNPs showing the effect of various AgNO₃ concentrations with 12.5 mg/ml RW.

3.1.4 Effect of RW concentration on RW-ALC synthesis

The effect of RW concentration on the hydrothermal synthesis of RW-ALC is shown in **Figure 3.4**. The cotton showed considerable deposition of RW-AgNPs at lower concentrations (1.56 and 3.125 mg/ml) than higher concentrations, as evidenced by the brown hue observed after the synthesis (**Figure 3.4(a)**). The UV-Vis spectra also confirmed that the conversion of Ag⁺ to Ag⁰ by RW and the formation of RW-AgNPs occurred at all RW concentrations (**Figure 3.4(b)**). RW-AgNPs produced with 1.56 and 3.25 mg/ml RW exhibited the lowest absorbances.

This can be attributed to the insufficiency of phytochemicals available for the reduction of Ag^+ ions into Ag^0 , resulting in reduced production of NPs (Makarov *et al.*, 2014). This phenomenon can be explained by the scarcity of nucleation sites at lower extract concentrations, which leads to a higher degree of reduction taking place (Ndikau *et al.*, 2017). Consequently, this leads to the formation of bigger NPs. In addition, the spectra generated by the lower concentrations of RW were characterised as wide and lacked a distinct peak, indicating the presence of anisotropy and polydispersed RW-AgNPs. The λ_{max} for RW-AgNPs at 22.25 mg/ml was found to be 410 nm, with an absorbance value of 2.388 and indicated that the highest amount of RW-AgNPs were synthesized at this concentration. Surprisingly, the RW-ALC formed in the 22.25 mg/ml reaction had the lowest amount of RW-AgNPs deposition (**Figure 3.4(a)**), despite having the maximum absorbance (**Figure 3.4(b)**). This is evident from the pale yellow colouration. Similarly, solutions with concentrations of 25 and 19 mg/ml had λ_{max} values of 414 nm and absorbance readings of 1.902 and 1.506, respectively. However, the resulting RW-ALC were also observed to be light yellow, indicating a low amount of deposition of RW-AgNPs. The concentration of RW that resulted in the darkest hue of RW-ALC and the highest deposition of RW-AgNPs was 6.25 mg/ml. Upon examination of the SPR band at 6.25 mg/ml, it was found to have a λ_{max} of 408 nm and an absorbance of 1.036. Despite being one of the lowest absorbances recorded in this experiment, the λ_{max} of RW-AgNPs at 6.25 mg/ml exhibited the most significant blue shift, suggesting that it resulted in the formation of the smallest RW-AgNPs among all the RW concentrations. After careful consideration, 6.25 mg/ml was provisionally used as the optimal concentration of RW, as it produced the RW-AgNPs with the most uniform sizes, as well as the RW-ALC with the most AgNPs deposition. Nevertheless, the antibacterial activity of each RW-ALC synthesised using different RW concentrations was assessed to determine the most effective RW concentration for the synthesis of RW-ALC.

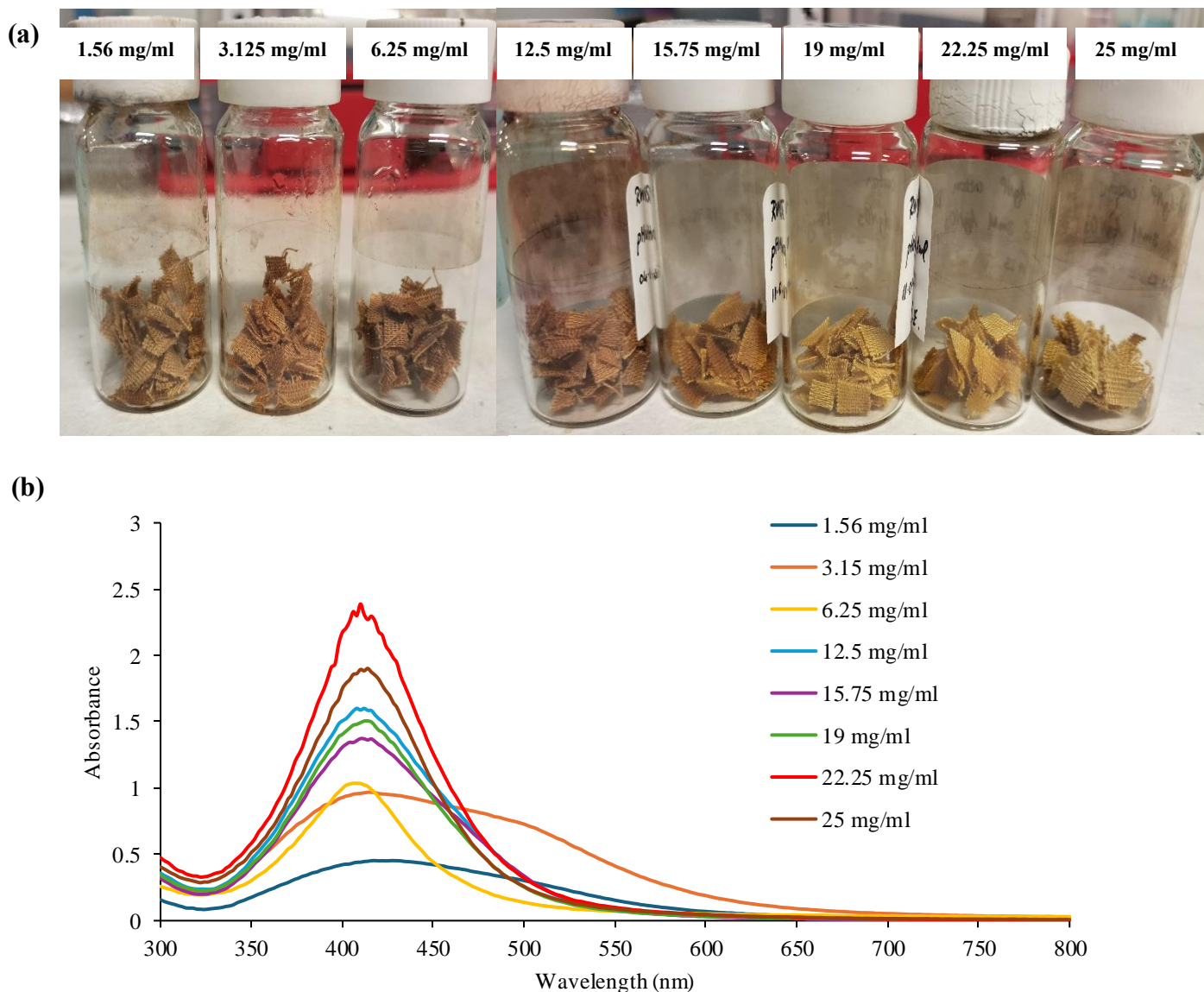


Figure 3.4: RW-ALC synthesised under hydrothermal conditions using 3 mM AgNO_3 and various concentrations of RW at pH 10. (a) RW-ALC deposited on 250 mg of cotton and (b) UV-Vis spectra of RW-AgNPs showing the effect of various RW concentrations at pH 10 with 3 mM AgNO_3 .

According to literature, lower concentrations of extract can effectively reduce Ag^+ ions (Dawadi *et al.*, 2021). However, they are unable to prevent spherical AgNPs from clumping together due to the insufficient presence of biomolecules that can act as capping or stabilizing agents. The higher concentrations of extract contain a greater number of biomolecules, which can reduce and stabilise AgNPs. Additionally, these biomolecules play a crucial role in the creation of various sizes and shapes of NPs (Dawadi *et al.*, 2021). Nevertheless, studies have indicated that excessive concentrations of plant extract can have an adverse impact on the

creation of NPs (Tyavambiza *et al.*, 2021). Another study found that higher concentrations of the plant extract led to the synthesis of NPs with more distinct UV-Vis spectra (Raza *et al.*, 2023). This study also demonstrated that increasing the concentration of RW from 1.56 to 6.25 mg/ml led to an increase in the synthesis of RW-AgNPs.

3.2 Upscaled synthesis and characterisation of RW-AgNPs and RALC

A large-scale synthesis of RW-AgNPs and RW-ALC was performed using the previously optimised conditions: 6.25 mg/ml RW, 3 mM AgNO₃, pH 10, and an ML ratio of 40. The final reaction volume was 50 ml. The resulting products were characterised using various physicochemical techniques.

3.2.1 UV-Vis spectroscopy analysis of RW-AgNPs

The UV-Vis absorption spectra of the upscaled and optimised RW-AgNPs can be seen in **Figure 3.5**. A single, narrow SPR peak was detected on the spectra, confirming the production of uniformly sized, spherical RW-AgNPs. The RW-AgNPs exhibited a maximum absorption wavelength λ_{\max} of 408 nm, with an absorbance value of 1.474. Additional analysis was performed to assess the size, morphology, polydispersity index (PDI), and zeta potential of the RW-AgNPs. This observation is in accordance with those previously reported in literature; González-Ballesteros *et al.* (2018) reported using GP of *Vitis vinifera* to synthesise AgNPs and observed an SPR band that was quite narrow and intense. Spherical nanoparticles are characterised by a single peak in the UV-Vis spectrum, while irregularly shaped AgNPs exhibit two or more peaks, depending on their symmetry (Gong *et al.*, 2018).

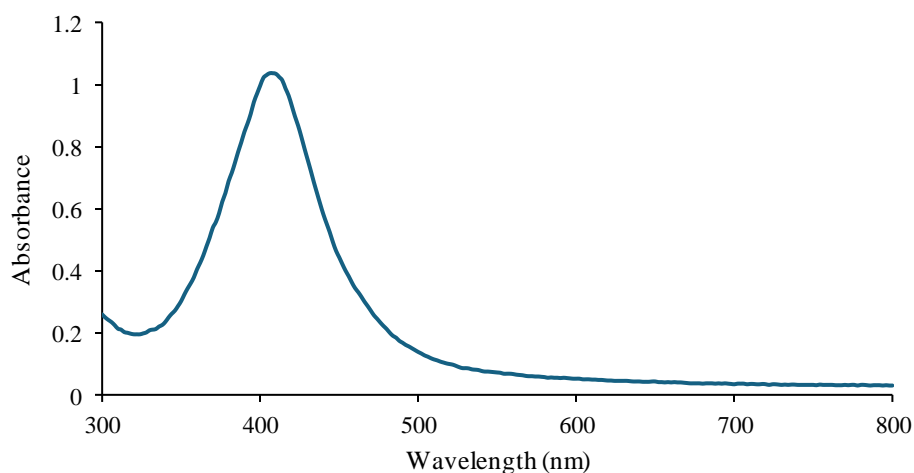


Figure 3.5 UV-Vis spectra of RW-AgNPs synthesised under hydrothermal conditions using optimal conditions (6.25 mg/ml RW at pH 10 and 3 mM AgNO₃).

3.2.2 DLS analysis of RW-AgNPs

DLS is a widely employed method for measuring the size and size distribution of particles in colloidal solutions (Dube *et al.*, 2020). It also reports on the PDI and ζ -potential of these particles. The hydrodynamic size distribution results shown in **Figure 3.6(a)** indicated that 96.1 % of the RW-AgNPs had a hydrodynamic size of 111.2 ± 48.81 nm and 3.9 % had a hydrodynamic size of 4239 ± 990.1 nm. The hydrodynamic size refers to the overall size of the NPs in a colloidal suspension, which includes both the size of the metal core and the surrounding compounds on the surface of the NPs (Simon *et al.*, 2021).

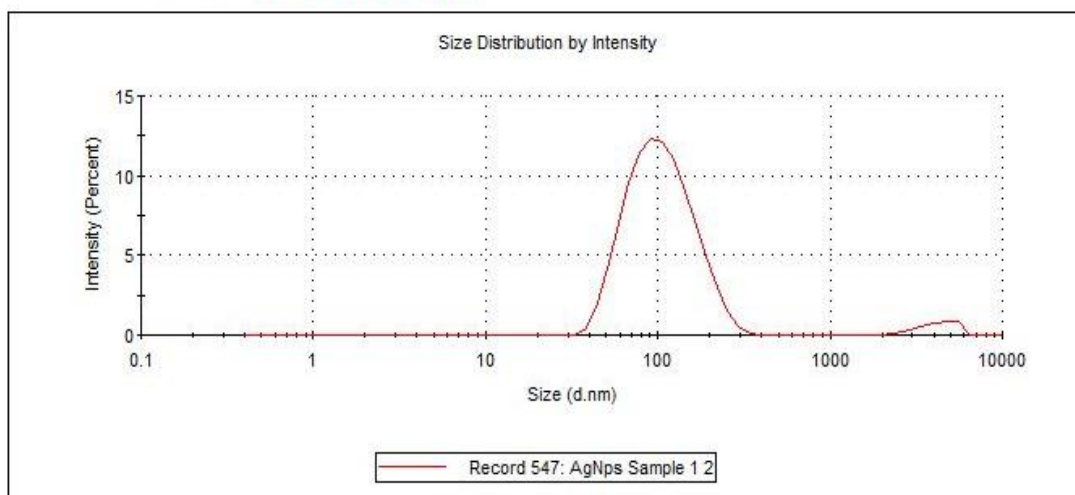
The PDI is a precise and established metric used to quantify the range of particle sizes in a solution (Babick, 2020). Values below 0.2 indicate a very narrow and almost uniform size distribution, whilst values of above 0.5 suggest a higher level of variability in size. When the PDI is more than 0.5, it indicates that the distribution is wide, and this often leads to a decrease in the reliability of the materials in use (Babick, 2020). The PDI of the RW-AgNPs was reported as 0.344 (**Figure 3.6(a)**), indicating that the NPs were mostly monodispersed. This corresponds with the AgNPs synthesised using gum arabic that had a PDI of 0.28 ± 0.03 , indicating that the AgNPs were stable and monodispersed (Fadaka *et al.*, 2022).

The ζ -potential is a measure of the surface charge of NPs, which refers to the electrical charge present on the surface of the particles. It is an important factor in determining the stability of colloidal particles (Tyavambiza *et al.*, 2021). NPs that have a ζ -potential ranging from -10 to +10 mV are classified as being electrically neutral. NPs with a ζ -potential exceeding +30 mV or falling below -30 mV are highly positively charged or highly negatively charged, respectively (Clogston and Patri, 2011). The RW-AgNPs displayed a ζ -potential of -21.3 ± 6.16 mV (**Figure 3.6(b)**), indicating that the synthesised RW-AgNPs were somewhat stable and anionic. Biogenic NPs typically exhibit a negative ζ -potential rather than a positive one. This is because the extracts contain many biomolecules that attach to the surface of the synthesised NPs that act as capping agents (Sánchez-López *et al.*, 2020). AgNPs that were synthesised utilising the aqueous extracts from two cultivars of *Pyrus communis* L. exhibited negative ζ -potential values ranging from -1.1 to -9.5 mV (Simon *et al.*, 2021). This suggested that the AgNPs had been capped with electronegative compounds, most likely the biomolecules found in the extracts. The presence of negative values also suggested the presence of powerful repulsive interactions among the AgNPs, which will effectively prevent the particles from aggregation while they are in suspension (Simon *et al.*, 2021).

(a)

	Size (d.nm):	% Intensity:	St Dev (d.nm):
Z-Average (d.nm): 94.97	Peak 1: 111.2	96.1	48.81
Pdl: 0.344	Peak 2: 4239	3.9	990.1
Intercept: 0.218	Peak 3: 0.000	0.0	0.000

Result quality : Refer to quality report



(b)

	Mean (mV)	Area (%)	St Dev (mV)
Zeta Potential (mV): -21.3	Peak 1: -21.3	100.0	6.16
Zeta Deviation (mV): 6.16	Peak 2: 0.00	0.0	0.00
Conductivity (mS/cm): 0.0371	Peak 3: 0.00	0.0	0.00

Result quality : Good

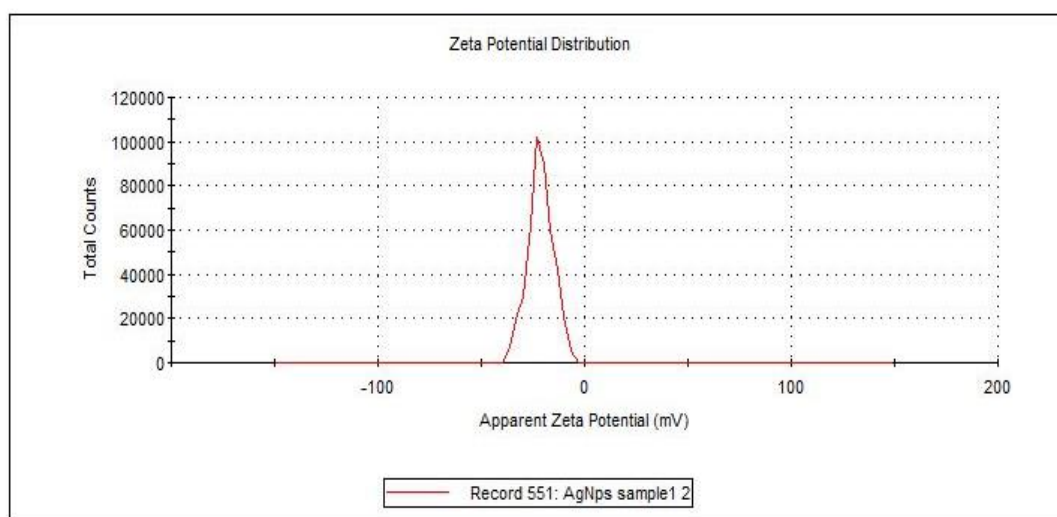


Figure 3.6: Hydrodynamic size (a) and ζ -potential (b) distribution curves of RW-AgNPs.

3.2.3 HR-TEM analysis of RW-AgNPs

HR-TEM analysis was conducted on the RW-AgNPs to determine their morphology, size, and shape. Images captured during HR-TEM analysis confirmed that the RW-AgNPs were spherical in shape and generally monodispersed (**Figure 3.7(a)**), which correlates to the single SPR band observed during UV-Vis analysis, as well as the PDI value reported during DLS analysis. The core size range of the selected RW-AgNPs was between 5-11 nm and the average core size was estimated to be 8.7 ± 1.3 nm. It is crucial to highlight the significant disparity between the hydrodynamic sizes measured by DLS analysis (111.2 ± 48.81 nm) and the core sizes detected using HR-TEM. The disparity arises because DLS analysis provides information about the hydrodynamic diameters of the particles, encompassing the metal core and the phytochemicals responsible for capping and stabilising the surface of the NPs (Tyavambiza *et al.*, 2021). On the other hand, HR-TEM assesses solely the size of the inorganic core. Therefore, the sizes obtained by DLS are frequently greater than the sizes determined by HR-TEM, as reported in literature (Souza *et al.*, 2016). In contrast to the findings of this study, most of the existing literature on biogenic AgNPs and their characterisation documents significant variability in the size and shape of the AgNPs (Dube *et al.*, 2020). This variability is attributed to the diverse biomolecules present in different plant extracts employed in the synthesis (Dube *et al.*, 2020). However, there have been reports of spherical, smooth-edged AgNPs synthesised with silk sericin solution (Harisha *et al.*, 2021) and *Camellia sinensis* extract (Rolim *et al.*, 2019). Furthermore, it has been established that AgNPs produced under hydrothermal conditions typically lead to the production of monodispersed and quasispherical NPs (Li *et al.*, 2015).

Figure 3.7 (c) displays the selected area electron diffraction (SAED) pattern of the RW-AgNPs, providing confirmation of its crystalline structure. The rings observed in the image correspond to the (111), (200), (220), and (311) crystallographic planes of silver, thus verifying the presence of the Miller indices (Alam *et al.*, 2023; Selvakumar *et al.*, 2018).

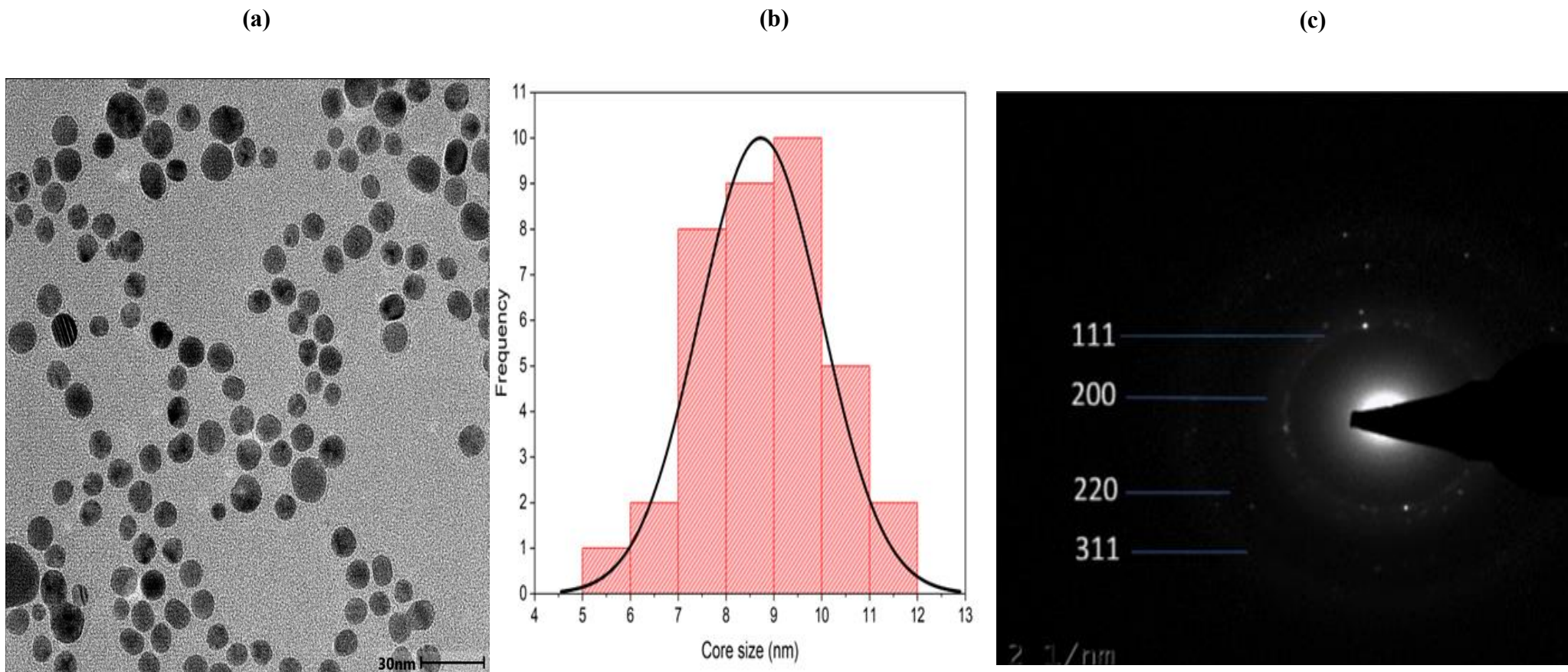


Figure 3.7: HR-TEM image analysis of RW-AgNPs. (A) TEM image (scalebar - 30 nm), (B) core size distribution, and (c) Selected area electron diffraction (SAED) pattern of the RW-AgNPs.

3.2.4 SEM analysis of RW-ALC

The *in situ*-synthesised RW-ALC were analysed by SEM and energy-dispersive X-ray (EDX) to assess the attachment of RW-AgNPs on the cotton textile's exterior layer, and the compositions of both the modified cotton fabric and the RW-ALC's exterior layer (**Figure 3.8**). The SEM micrographs of RW-ALC (**Figure 3.8 (a), (b)**) revealed the existence of spherical RW-AgNPs. A smaller number of small sized RW-AgNPs were dispersed throughout the cotton fabric, possibly due to the NPs being lost during the synthesis process. This could be attributed to the fact that the RW-AgNPs do not form chemical bonds with the cellulose present in the fabric.

The EDX spectrum exhibited a small peak for Ag (**Figure 3.9 (a)**), which typically displays an optical absorption peak around 3 keV, indicative of its distinctive SPR (Kaviya *et al.*, 2012). Furthermore, the EDX component analysis revealed that the sample consisted primarily of carbon (44.7 %) and oxygen (50.88 %), which are fundamental constituents of cellulose (Novoa *et al.*, 2022). Cellulose is found in more than 90 % of cotton textiles. The sample contained a minor amount of Ag (4.42 %), which was present due to the attachment of RW-AgNPs to the cotton. In contrast, the control cotton fabric did not show the presence of Ag. In a similar study by Novoa *et al.* (2022), SEM micrographs of cotton fabrics coated with Cys-AgNPs and bio-AgNPs displayed the existence of spherical AgNPs on the surface of the cotton. Additionally, EDX analysis detected peaks corresponding to the presence of Ag, C, and O (Novoa *et al.*, 2022).

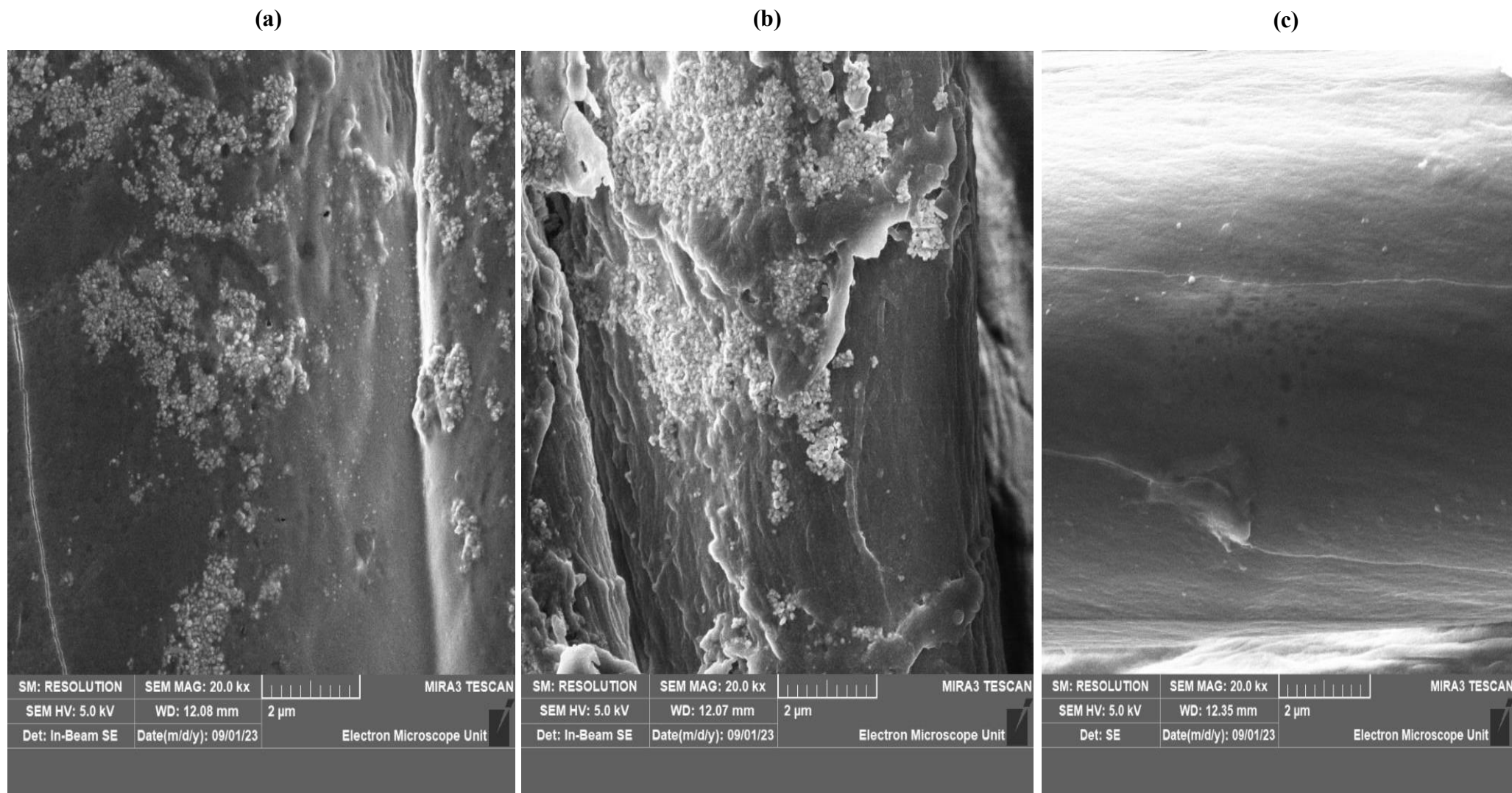


Figure 3.8: SEM analysis of the RW-ALC. (a, b); the cotton fabric covered in RW-AgNPs and the control (c).

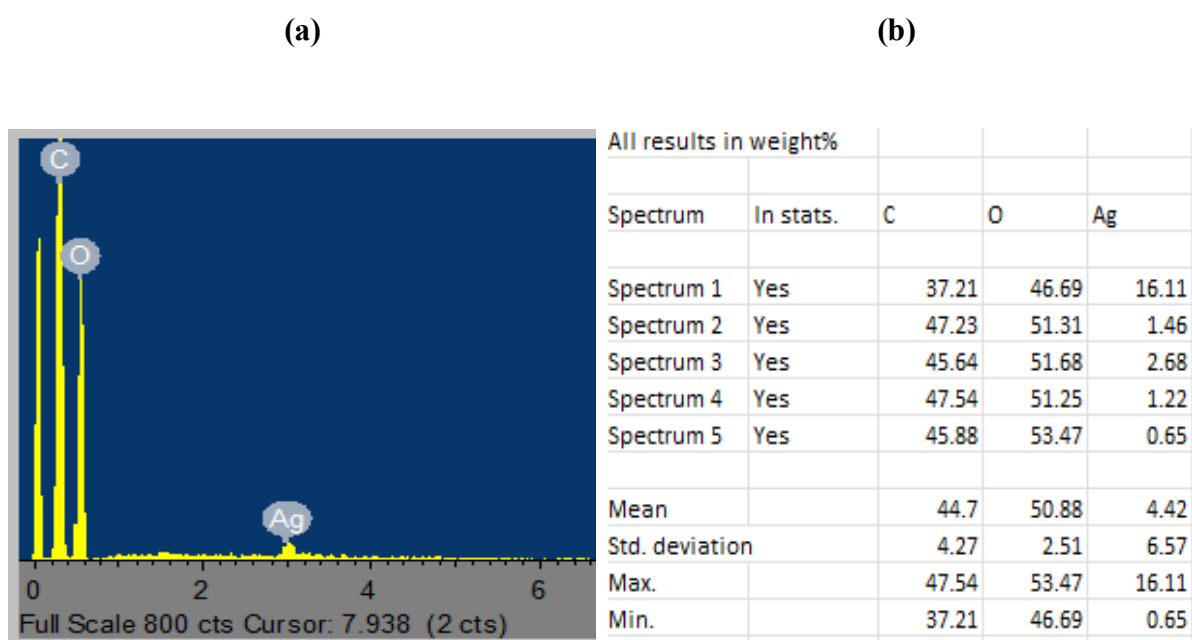


Figure 3.9: EDX spectra (a) and % weight (b) displaying the composition of the RW-ALC at pH 10 and the presence of a peak at 3 keV characteristic for Ag, as determined by the $AgL\alpha$ lines.

3.2.5 FTIR analysis of RW, RW-AgNPs and RW-ALC

The objective of the FTIR analysis was to determine the functional groups involved in the biosynthesis of RW-ALC and RW-AgNPs. The results of the analysis aid in identifying the specific phytochemicals found in RW that contributed to the reduction of $AgNO_3$ (Dube *et al.*, 2020). The absorption peaks/bands observed in the Infrared (IR) spectrum correspond to the frequencies at which the atomic bonds in the RW-AgNP and RW-ALC samples vibrate. It is pertinent to note that the IR spectrum is comprised of two primary regions: a fingerprint region including functional groups ranging from $1500-600\text{ cm}^{-1}$, and a functional group region ranging from $4000-1500\text{ cm}^{-1}$ (Jayawardena *et al.*, 2021). The functional groups have a rather stable composition across several samples, unlike the fingerprint region which contains unique functional groups for each sample. Therefore, it is highly improbable for two substances to produce identical IR spectra (Jayawardena *et al.*, 2021).

This study utilised FTIR to determine the bioactive chemicals present in the RW that may have prompted the reduction of Ag^+ to Ag^0 , as well as the capping and stabilising of the synthesised RW-AgNPs. **Figure 3.10** depicts the FTIR spectrum of RW-AgNPs, where the peaks indicated the presence of similar compounds in both RW and RW-AgNPs. The majority of the peaks exhibited a shift when comparing the RW and RW-AgNPs. This outcome is expected due to

the interaction between the Ag^+ and phytochemicals present in the RW (Lopes and Courrol, 2018). Peak values and shifts in the FTIR spectra of RW compared to the RW-AgNPs are highlighted in **Table 3.1**, along with potential functional groupings.

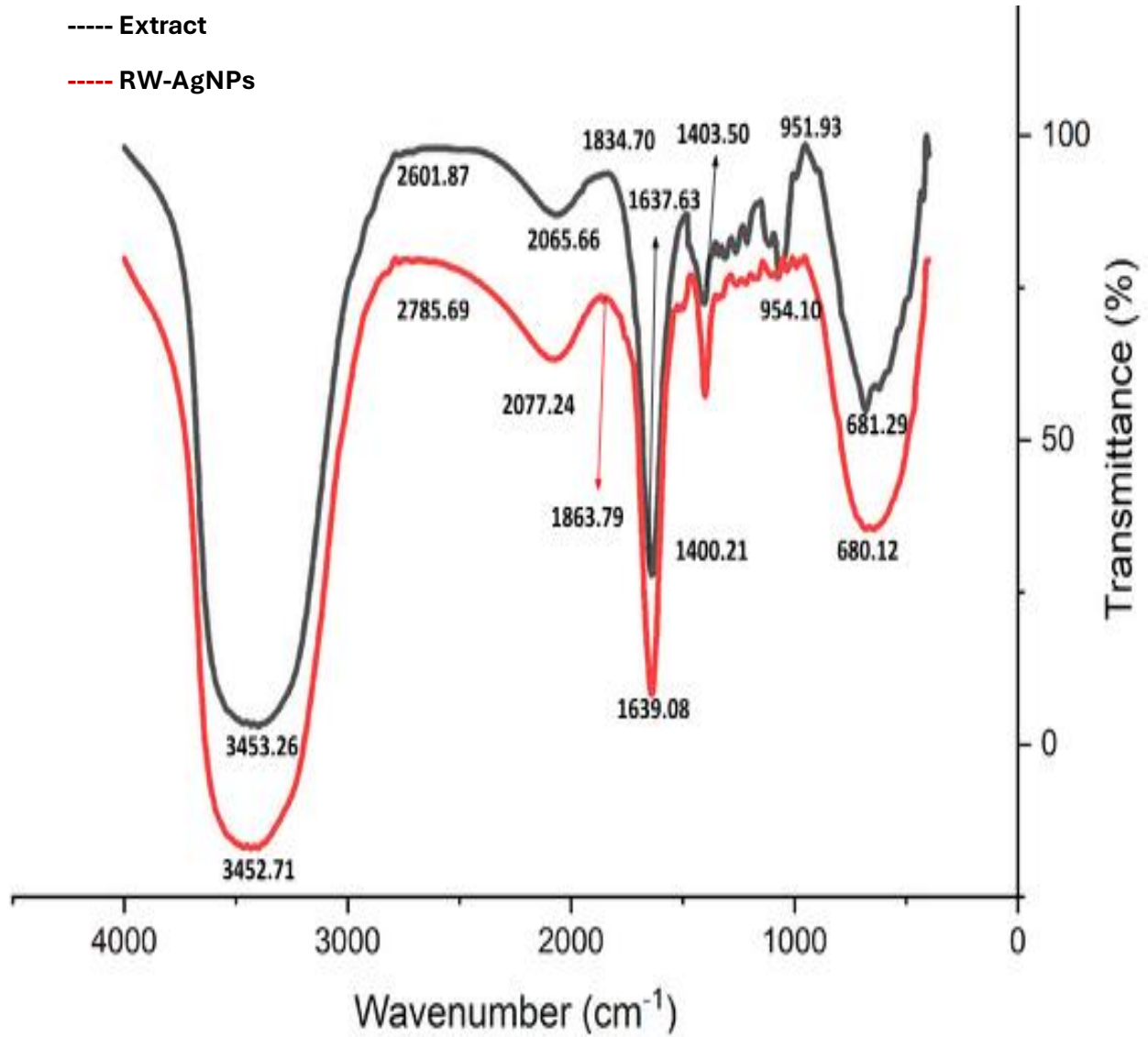


Figure 3.10: FTIR spectra of RW and RW-AgNPs.

Table 3.1: FTIR peaks and peak shifts of RW and RW-AgNPs and their respective functional groups

RW peak position (cm ⁻¹)	RW-AgNPs peak position (cm ⁻¹)	Peak shift values (cm ⁻¹)	Bond	Functional Groups
3453.26	3452.71	- 0.55	O-H stretch, N-H stretch	Alcohols, phenols, aliphatic primary amine
2601.87	2785.69	+ 183.82	C-H stretch	Aldehydes
2065.66	2077.24	+ 11.58	C-H bend	Aromatics
1637.63	1639.08	+ 1.45	C-C stretch, N-H bend	Primary amines
1403.50	1400.21	- 3.29	O-H bend	Alcohols, phenols
951.93	954.10	+ 2.17	C=C bend	Alkenes
			C-Br stretch, C-	Alkyl halides – Aliphatic bromo compounds
681.29	680.12	- 1.17	H bend	Alkynes

The shift from 3453.26 cm^{-1} in the RW to 3452.71 cm^{-1} in the RW-AgNPs indicated the stretching vibration of intermolecular polymeric bound O-H groups or N-H groups, which are characteristic of alcohols, amines, and hydroxyl groups (Dube *et al.*, 2020). The prominent peak at 2601.87 cm^{-1} in the RW migrated to 2785.69 cm^{-1} , indicating the presence of aldehydes, as a result of stretching of the C-H bonds (Ngungeni *et al.*, 2023). On the other hand, the presence of C-H bending may account for the slight troughs observed at 2065.66 and 2077.24 cm^{-1} , indicating the presence of an aromatic compound. The prominent absorption peak at 1637.63 cm^{-1} in the RW, which shifted to 1639.08 cm^{-1} in the RW-AgNPs, is most likely attributed to the elongation of C-C bonds and the bending of N-H bonds generated by primary amines (Madiehe *et al.*, 2022). The peaks detected at 1403.50 and 1400.21 cm^{-1} for RW and RW-AgNPs, respectively, were identified as O-H bending vibrations related to polyphenols (Madiehe *et al.*, 2022). The peaks at 951.93 cm^{-1} for RW and 954.10 cm^{-1} for RW-AgNPs are indicative of the presence of robust alkene groups, which arise from the bending of C=C bonds. Owing to the presence of aliphatic bromo compounds and alkynes, the absorption band at 681.29 cm^{-1} in the RW shifted to 680.12 cm^{-1} in the RW-AgNPs and was attributed to the stretching vibrations of C-Br groups and the bending vibrations of C-H groups, respectively (Dube *et al.*, 2020).

The resemblance between the two FTIR spectra, along with the minimal disparity in transmittance, indicated the presence of both NPs and the natural constituents of the extract (Riaz *et al.*, 2021). Polyphenols and proteins are presumably responsible for the swift reduction and encapsulation of Ag^+ into AgNPs in this study. The presence of polyphenols in RW, which are powerful reducing agents, likely encouraged the reduction of AgNO_3 and the subsequent formation of AgNPs (Zuas *et al.*, 2014). Previous research also provides evidence for the reduction of metal ions by the use of plant extracts (Riaz *et al.*, 2021; Zuas *et al.*, 2014).

Additionally, FTIR analysis was performed on the cotton fabrics to assess the adhesion of the RW-AgNPs with the cotton fibres. The findings of this analysis are depicted in **Figure 3.11**. Both spectra appear to be uniform, displaying the distinctive peaks of the primary functional groups found in the cellulose structure of cotton fibres. The primary functional groups of the cellulose structure can be identified by the peaks at $3323\text{--}3334\text{ cm}^{-1}$, $2913\text{--}2947\text{ cm}^{-1}$, $1141\text{--}11,667\text{ cm}^{-1}$, and $1017\text{--}1044\text{ cm}^{-1}$ (Repon *et al.*, 2021). The peak at 3329 cm^{-1} corresponds to the stretching of O-H bonds, while the peak at 2915 cm^{-1} can be related to the deformation of C-H bonds in the $-\text{CH}_2-$ group. The presence of the 1145 cm^{-1} peak suggested the occurrence of C-O stretching, whereas the 1023 cm^{-1} peak indicated the deformation of the ether linkage

(C-O-C). Based on this analysis, it is evident that there were no substantial alterations to the cotton fabrics during the *in situ* synthesis process, which is consistent with existing literature (Jain *et al.*, 2022; Repon *et al.*, 2021). Therefore, it may be inferred that treating the cotton fabric with AgNO₃ does not modify the chemical composition of the fabric, confirming that there is no chemical bonding between the cellulose chains and the AgNPs. Moreover, the deposition of AgNPs does not alter the chemical composition of the cotton fabric. Instead, it simply leads to the physical attachment or deposition of AgNPs on the surface of the fabric.

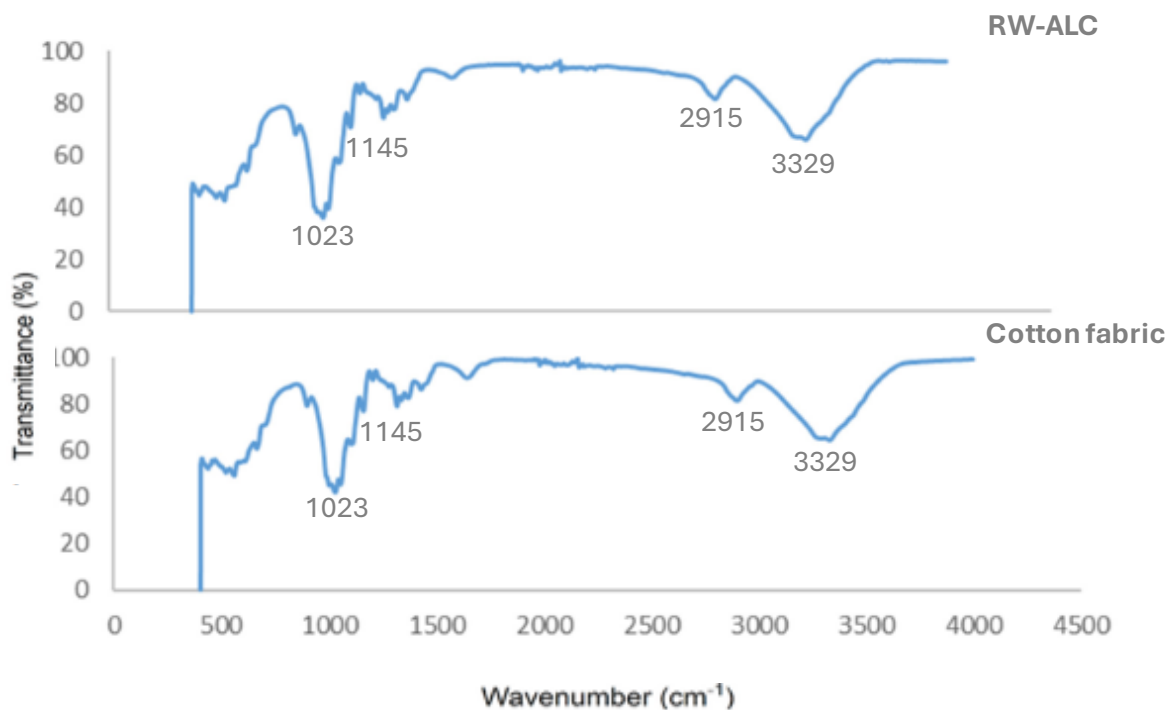


Figure 3.11: FTIR spectra of cotton fabric and RW-ALC.

3.3 Stability analysis of RW-AgNPs

The stability of NPs under different biological settings must be assessed before they can be used in any downstream biomedical applications. Thus, the stability of the RW-AgNPs was evaluated in dH₂O, PBS, MHB, and DMEM, for a duration of 48 hours. Stability analysis was performed at 37 °C to simulate biological conditions. UV-Vis analysis was used to examine any alterations in the stability of the NPs. The selection of dH₂O, PBS, MHB, and DMEM was based on their established use in the biological experiments performed in this study.

The RW-AgNPs were stable over the 48 hour period in all media, since there were no significant shifts seen in the UV-Vis absorption spectra (**Figure 3.12**). The slight decrease in absorbance is likely attributable to minimal interactions between the RW-AgNPs and the media constituents, or it may be due to pipetting errors. Notably, the SPR values remained consistent across dH₂O (416 nm), DMEM (422 nm), and MHB (418 nm), suggesting that the surface properties of the RW-AgNPs were preserved, with no evidence of aggregation, thereby indicating that the nanoparticles remained monodispersed. The presence of biomass on the surface of the AgNPs may have hindered the agglomeration of RW-AgNPs in the media, creating a steric or electrostatic barrier (Khan *et al.*, 2019). These results are in agreement with those of stability tests conducted by Dube *et al.* (2020), wherein green synthesised AgNPs were stable in various biological media.

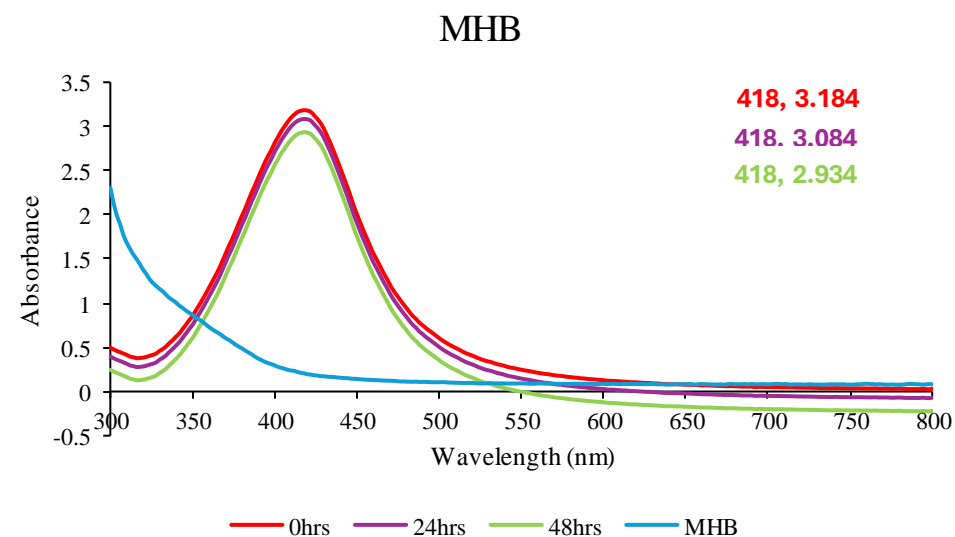
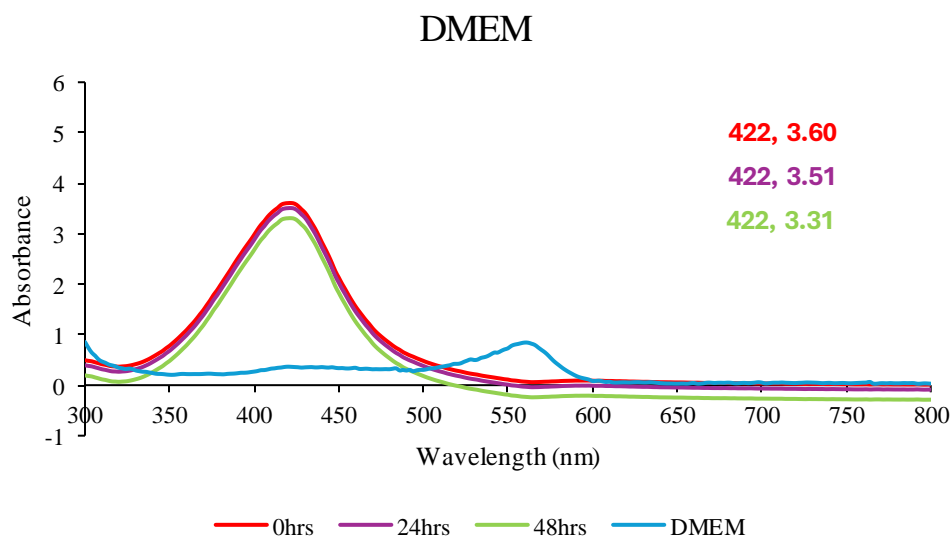
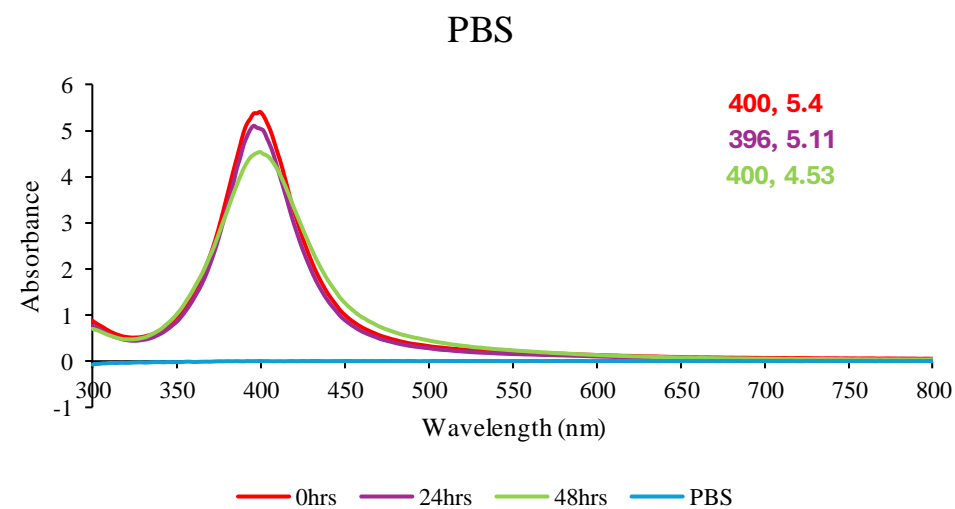
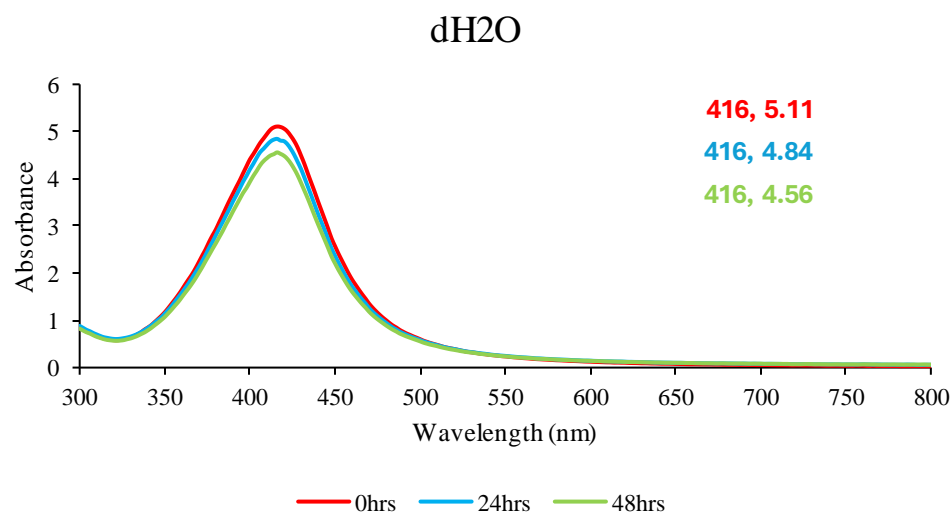


Figure 3.12: Stability of RW-AgNPs in biological media (ddH₂O, PBS, DMEM and MHB). The mixture was incubated at 37 °C for 0, 24 and 48 hrs, and analysed on a microplate reader.

3.4 Phytochemical composition and antioxidant activity of RW-AgNPs

3.4.1 TPC of RW and RW-AgNPs

The TPC of RW and RW-AgNPs were evaluated by the FC assay using Gallic acid calibration as a standard. TPC content was expressed as Gallic acid equivalents (GAE) in $\mu\text{g/ml}$ (**Figure 3.13**). Both the RW and RW-AgNPs exhibited the presence of phenolic compounds, which aligns with the findings of the FTIR analysis (**Figure 3.10**). The TPC of RW-AgNPs ($121.17 \pm 7.93 \mu\text{g GAE/ml}$) significantly surpassed the TPC of RW ($31.273 \pm 2.89 \mu\text{g GAE/ml}$) (**Table 3.2**). This finding indicates that the phenolic compound(s) found in the RW participated in reducing, stabilising, and capping the RW-AgNPs during the synthesis process. TPC were also reported in the *Vitis vinifera*-derived GP to be $54.26 \pm 1.66 \text{ GAE/g}$, while the TPC values for GP from Cabernet Franc and Chambourcin were 153.8 ± 1.83 and $92.0 \pm 2.16 \text{ GAE/g}$, respectively (Xu *et al.*, 2016). The amount of phytochemicals in plant extracts can differ based on the geographical origin of the plants, as the presence of various soil nutrients in different locations affects the composition of phytochemicals in plants (Mustarichie *et al.*, 2020).

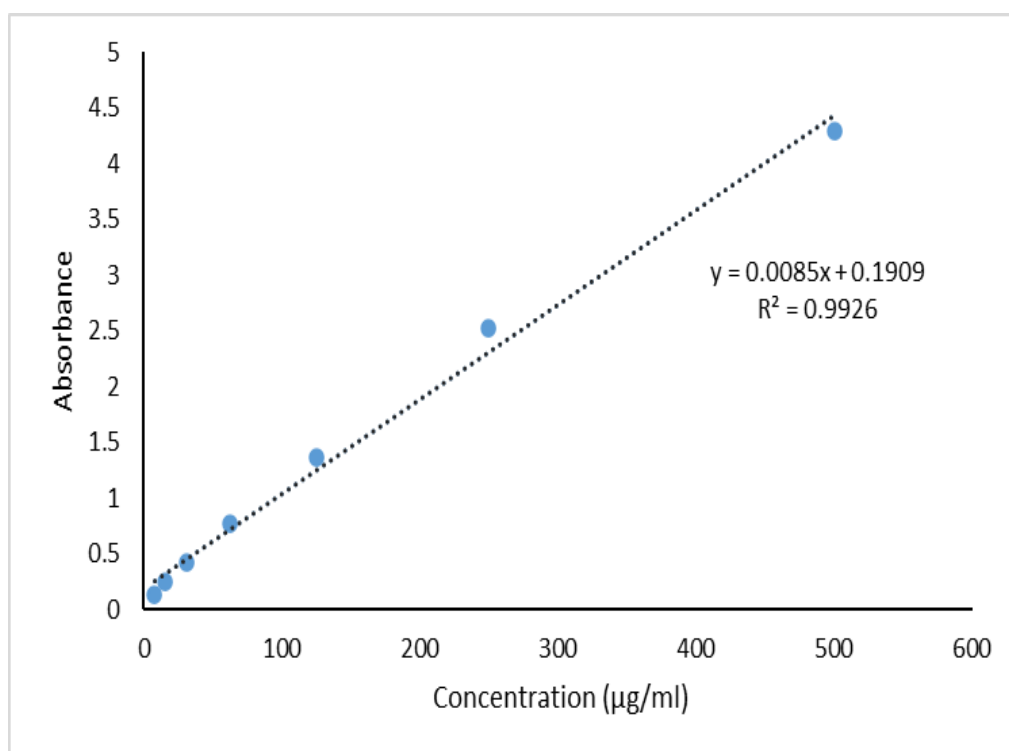


Figure 3.13: Gallic acid calibration standard curve for determining the TPC of RW and RW-AgNPs.

Table 3.2: TPC of RW and RW-AgNPs.

Samples	TPC ($\mu\text{g GAE/ml}$)
RW	31.273 ± 2.89
RW-AgNPs	121.17 ± 7.93

3.4.2 Antioxidant analysis of RW and RW-AgNPs

In addition to being effective metal chelators and reducing agents, phenolic compounds, such as flavonols, are also effective scavengers of free radicals. Phenols and flavonols have been shown to have substantial antioxidant activity due to their reducing and radical scavenger abilities (Tyavambiza *et al.*, 2022). In addition, it has been observed that MNPs have antioxidant characteristics. Utilising plant extracts rich in phytochemicals in green synthesis has the potential to generate NPs with enhanced antioxidant properties (Arumai Selvan *et al.*, 2018). The DPPH and ABTS assays were used to investigate the antioxidant capacity of the RW and RW-AgNPs.

3.4.2.1 DPPH assay

The DPPH free radical, commonly employed to assess the capacity of substances to function as free-radical scavengers and hydrogen donors, is a fast, facile, and cost-effective technique for evaluating antioxidant properties (Platzer *et al.*, 2021). The DPPH test is based on the elimination of DPPH, which is a stable free radical. DPPH is a dark-coloured crystalline substance composed of stable free-radical particles and is a widely studied antioxidant assay. When the DPPH radical is reduced and altered into DPPH-H, it changes from a dark purple colour to either colourless or bright yellow in solution (Baliyan *et al.*, 2022). Multiple plant extracts have demonstrated the ability to neutralise DPPH radical scavenging activity *in vitro* (Amrulloh *et al.*, 2021; Sridhar and Charles, 2019; Lalrinzuali *et al.*, 2015). This study assessed and compared the antioxidant properties of RW and RW-AgNPs with that of ascorbic acid, which served as the standard. RW consistently demonstrated scavenging activity above 85 % across all concentrations tested (0.78 – 100 $\mu\text{g/ml}$), and as shown in **Figure 3.14**, the activity was comparable to that of ascorbic acid. However, a significant difference was observed between the RW and ascorbic acid treatments at doses of 3.125 $\mu\text{g/ml}$ and higher. The scavenging activity of RW-AgNPs was dose-dependent, while no activity was observed at lower concentrations of 0.78 and 1.56 $\mu\text{g/ml}$. Although the RW-AgNPs exhibited substantial activity, they had inferior activity in comparison to RW and ascorbic acid. Based on these

findings, the AgNPs produced from RW exhibited hydrogen-donating properties and function as an antioxidant. The antioxidant activity of the RW and RW-AgNPs can be attributed to the presence of phytochemicals in the extract (Altemimi *et al.*, 2017). Similarly, *Aristolochia bracteolata* AgNPs exhibited significant dose-dependent DPPH radical scavenging activity. At a concentration of 100 µg/ml of AgNPs, its DPPH free radical scavenging activity was approximately 79.16 %, which was closer to the 84.60 % of ascorbic acid (positive control) (Thanh *et al.*, 2022).

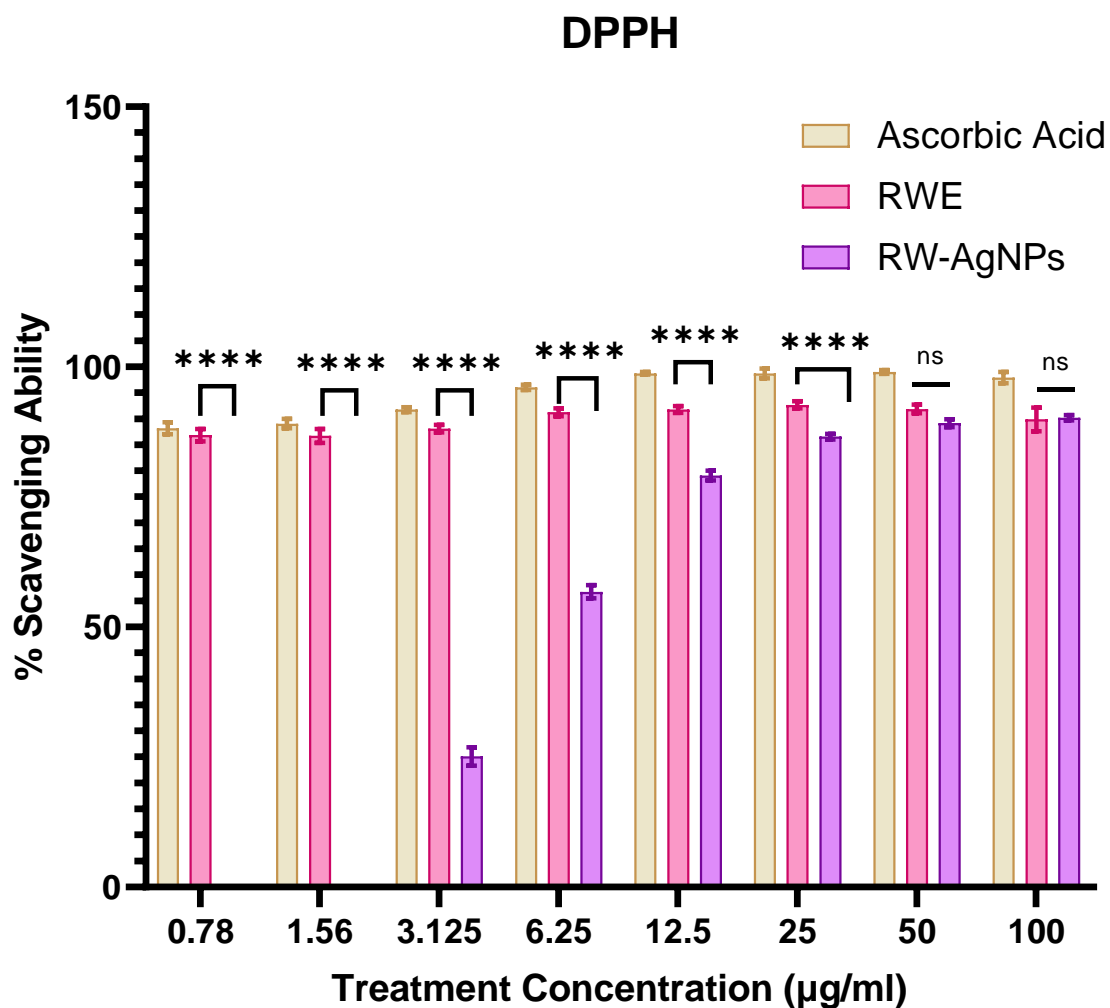


Figure 3.14: DPPH radical scavenging ability of RW, RW-AgNPs, and ascorbic acid. Data presented as mean ± SEM (n = 3). Statistical significance was determined using Two-way ANOVA where ns = non-significant and **** = p < 0.0001.

3.4.2.2 ABTS assay

ABTS is a commonly employed assay for assessing the antioxidant properties of plant extracts, food, clinical fluids, and other substances (Cano *et al.*, 2023). The ABTS assay relies on the

interaction between an antioxidant and the pre-generated ABTS•+ radical cation (Ilyasov *et al.*, 2020). The overall antioxidant activity of compounds is assessed based on their ability to reduce the dark blue ABTS •+ radical cation to colourless ABTS (Ilyasov *et al.*, 2020). The antioxidant properties of RW and RW-AgNPs were evaluated using this method; RW, RW-AgNPs, and ascorbic acid (positive control) exhibited a dose-dependent reduction of the ABTS•+ radical (**Figure 3.15**). Among the three samples, RW was the least efficacious. The antioxidant activities increased as the concentrations of the different treatments increased within the range of 0.78-100 µg/ml. RW-AgNPs demonstrated superior scavenging activity compared to the ascorbic acid. This indicated that RW-AgNPs are more potent antioxidants than ascorbic acid at these specific treatment concentrations. However, at 100 µg/ml, ascorbic acid had the highest antioxidant activity, with a scavenging activity of 95.2 %, which was much higher than the scavenging activities of RW and RW-AgNPs, which were 48.5 % and 76.5 % respectively.

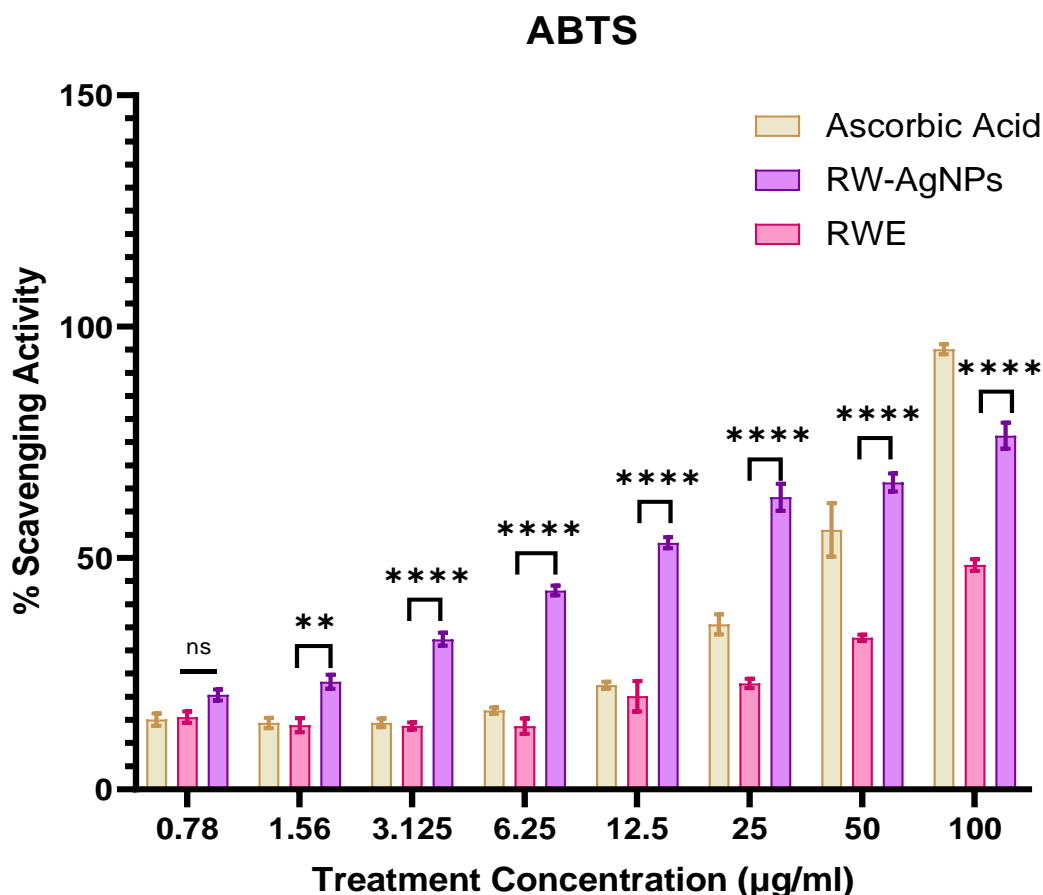


Figure 3.15: ABTS radical scavenging ability of RW, RW-AgNPs, and ascorbic acid. Data presented as mean ± SEM (n = 3). Statistical significance was determined using Two-way ANOVA where ns = non-significant, ** = p < 0.01, and **** = p < 0.0001.

Multiple studies have documented the antioxidant activity of AgNPs synthesised using green methods. Saratale *et al.* (2021) showed that bio-synthesized GP tannin-AgNPs have strong antioxidant properties, specifically in terms of their ability to scavenge stable free radical ABTS•+. The AgNPs exhibited significant ABTS free radical scavenging capabilities in a dose-dependent manner. The AgNPs exhibited an IC₅₀ value of 40.9 µg/ml. In comparison, the RW-AgNPs in this study exhibited an IC₅₀ of only 8.3 µg/ml, indicating that they have greater antioxidant properties than the GP tannin-AgNPs. Prior research findings indicated that the majority of AgNPs produced using plant extracts have greater antioxidant activity compared to the extracts themselves, which aligns with the outcomes of the current study (Mihailović *et al.*, 2023). Khuda *et al.* (2022) revealed that the % ABTS scavenging activity observed at a concentration of 1000 µg/ml was 61 % for the crude extract, 74 % for the AgNPs, and 80 % for the positive control. The IC₅₀ values for each sample were 25.45, 18.88, and 15.34 µg/ml, respectively (Khuda *et al.*, 2022).

In summary, the antioxidant assays conducted in this research showed that in addition to RW-AgNPs, the RW exhibited significant antioxidant activity. Due to its ability to scavenge free radicals and prevent lipid oxidation, the extract showed promise as a potential nutraceutical. In comparison to the crude extract, RW-AgNPs demonstrated enhanced antioxidant properties. Thus, they have the potential to be utilised in the development of a suitable formulation for the safe and efficacious treatment of various ailments. Prior research has documented the antioxidant capabilities of plant-derived AgNPs as effective agents for neutralising free radicals (Tyavambiza *et al.*, 2022). These AgNPs have several advantages over synthetic antioxidants, including enhanced bioavailability, stability, and targeted distribution.

3.5 Antibacterial activity of RW-AgNPs and RW-ALC

Conventional microbiological testing methods such as agar disc diffusion and microdilution assays were used to determine the MIC and MBC of RW-AgNPs and RW-ALC. The antibacterial activity of RW and the RW-AgNPs was evaluated against the human pathogens *S. aureus*, MRSA, *E. coli*, *E. cloacae*, *K. pneumoniae*, *P. aeruginosa*, and *A. baumannii*.

3.5.1 Disc diffusion assay using RW-ALC

The zones of inhibition (ZOI) after treatment were measured and used to assess the antibacterial efficacy of the RW-ALC synthesised during optimisation steps in **Section 2.2.1.3**. The ZOI refers to the circular region surrounding the antibacterial treatment where bacterial colonies are unable to proliferate. This area is utilised to assess the susceptibility of the bacteria to the

antibacterial therapy. The RW-ALC showed moderate antibacterial activity (**Figure 3.16**). The activity varied depending on the concentration of RW utilised to synthesise each RW-ALC. Ciprofloxacin and regular cotton fabrics were used as the positive control and negative control, respectively.

The RW-ALC appeared to be more effective against the Gram-positive bacterial strains. With MRSA, the results presented in **Figure 3.16** and **Table 3.3** demonstrated that RW-ALC effectively prevented the growth of bacteria at all concentrations tested. Comparatively, Ciprofloxacin produced an average ZOI of around 9 mm. The concentrations of 1.56 and 6.25 mg/ml RW-ALC exhibited the highest performance, with average zones of inhibition of 7.75 and 7.5 mm, respectively. For the remaining concentrations, there were no discernible ZOIs, but the region beneath the cotton showed no signs of bacterial development, suggesting that the RW-ALC prevented their growth. The outcomes for *S. aureus* were favourable, as all RW-ALC treatments resulted in ZOI exceeding 7.5 mm; 6.25 mg/ml RW-ALC was the most effective with an average ZOI of 8.2 mm, closely related to that of the positive control (Ciprofloxacin). 1.56 mg/ml RW-ALC followed closely, with an average ZOI of 8 mm. Typically, *S. aureus* is present in the bodies of healthy persons. While it does not cause infections on healthy skin, when it enters internal tissues or the bloodstream, it can lead to severe disorders like meningitis, pneumonia, endocarditis, bacteraemia, and sepsis (Nandhini *et al.*, 2022). MRSA, a strain of *S. aureus*, has developed resistance to methicillin, making it a superbug that can withstand the effects of antibiotics and medicines. This makes it a significant contributor to the transmission of infections in hospitals and communities, leading to severe repercussions and potentially fatal illnesses (Nandhini *et al.*, 2022). Developing efficient techniques to treat bacterial infections with major antibiotic resistance is of extreme importance (Hu *et al.*, 2020)

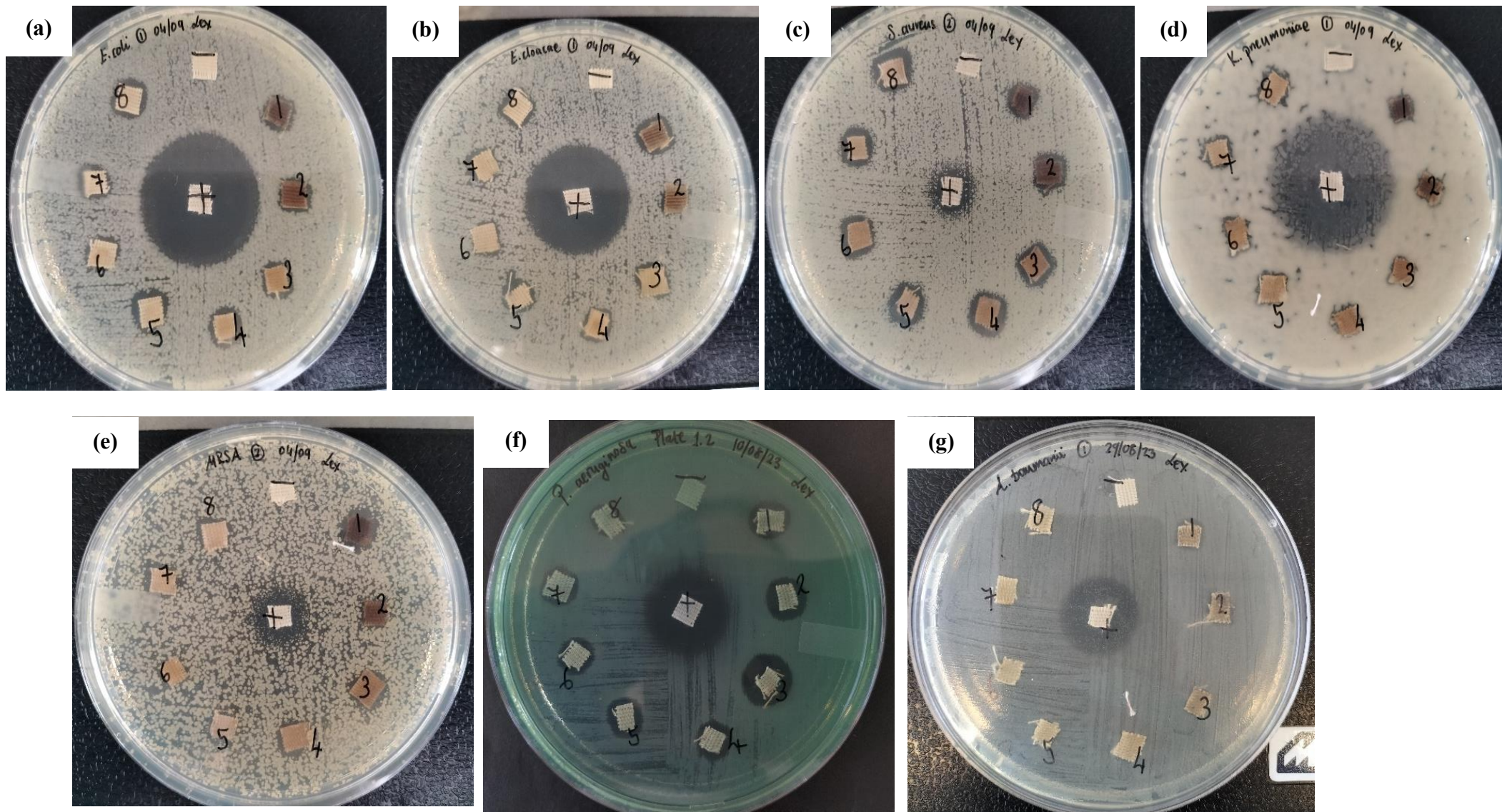


Figure 3.16: Antibacterial activity of RW-ALC using agar disc diffusion assay. Seven pathogenic bacteria were treated with RW-ALC synthesised using various concentrations of RW at pH10 and 3mM AgNO₃. += Ciprofloxacin; 1-8 = RW-ALC synthesised using 1.56 (1), 3.125 (2), 6.25 (3), 12.5 (4), 15.75 (5), 19 (6), 22.25 (7), and 25 (8) mg/ml RW. (a) *E. coli*, (b) *E. cloacae*, (c) *S. aureus*, (d) *K. pneumoniae*, (e) *MRSA*, (f) *P. aeruginosa*, (g) *A. baumannii*

Table 3.3: ZOI measurements of RW-ALC synthesised with various concentrations of RW against seven human pathogenic bacteria.

RW-ALC	<i>S. aureus</i>	MRSA	<i>E. cloacae</i>	<i>E. coli</i>	<i>K. pneumoniae</i>	<i>P. aeruginosa</i>	<i>A. baumannii</i>
ZOI ± SD (mm)							
1.56 mg/ml (1)	8.08 ± 0.88	7.75 ± 1.12	8.25 ± 0.63	7.91 ± 0.79	6.25 ± 0.61	7.17 ± 0.79	5.5 ± 0.5
3.125 mg/ml (2)	7.33 ± 0.77	5.08 ± 2.23	7 ± 0.6	7.58 ± 0.63	5.92 ± 0.63	6.67 ± 0.62	5 ± 0
6.25 mg/ml (3)	8.17 ± 0.67	7.5 ± 0.77	8.42 ± 0.67	8.41 ± 0.55	5.92 ± 0.87	7.58 ± 0.83	5 ± 0
12.5 mg/ml (4)	8 ± 1.08	6.5 ± 0.87	7.25 ± 0.71	7.58 ± 0.71	5.33 ± 0.53	6.42 ± 0.70	5 ± 0
15.75 mg/ml (5)	7.58 ± 1.09	6.17 ± 0.83	7.17 ± 0.79	7.17 ± 0.87	5.33 ± 0.44	6.42 ± 1.06	5.5 ± 0.5
19 mg/ml (6)	7 ± 0.56	4.83 ± 1.9	6 ± 0.62	6.83 ± 0.87	5.33 ± 0.5	5.25 ± 2.09	5.17 ± 0.33
22.25 mg/ml (7)	7.5 ± 1.17	6.17 ± 0.67	6.42 ± 0.81	6.42 ± .88	6 ± 1.12	6.25 ± 0.73	4.33 ± 1.74
25 mg/ml (8)	7.5 ± 0.87	6.25 ± 0.71	6.33 ± 1.32	6.67 ± 1.05	6 ± 1.12	5.58 ± 0.79	5.17 ± 0.33
Ciprofloxacin (+)	8.17 ± 1.05	9.33 ± 1.74	24.17 ± 2.44	23.83 ± 1.87	8.33 ± 0.98	9.42 ± 0.94	9.31 ± 1.72
Cotton fabric (-)	0 ± 0	0 ± 0	0 ± 0	0 ± 0	0 ± 0	0 ± 0	0 ± 0

Although the Gram-positive bacterial strains were more susceptible to the effects of the RW-ALC, the treatments also had significant activity against the Gram-negative strains. All of the RW-ALC samples showed activity against *E. coli*, with average ZOI ranging from 6.5 to 8.5. Ciprofloxacin was administered at a reduced dose of 5 µg/ml, but still resulted in significant areas of inhibition on all plates, with an average diameter of 23.8 mm. Similar to MRSA, RW-ALC at concentrations of 1.56 and 6.25 mg/ml showed the highest level of antibacterial activity, resulting in ZOIs measuring 7.9 and 8.5 mm, respectively. Similar to the previously discussed bacterial strains, *P. aeruginosa* appeared to be vulnerable to all RW-ALC treatments. The concentration of 6.25 mg/ml RW-ALC once again demonstrated superior performance, with an average ZOI of 7.5 mm. This measurement was only slightly smaller, by less than 2 mm, compared to the positive control's ZOI of 9.4 mm. *E. cloacae* exhibited susceptibility to all RW-ALC treatments, with the smallest ZOI measuring 6 mm at the 19 mg/ml RW-ALC treatment. The 6.25 mg/ml RW-ALC once again demonstrated the highest level of effectiveness, resulting in an average ZOI of 8.4 mm. Although all RW-ALC treatments demonstrated efficacy against *K. pneumoniae*, the bulk of the ZOIs ranged from 5 mm to 6 mm. However, when compared to the aforementioned bacterial strains, these results are underwhelming. 1.56 mg/ml RW-ALC exhibited the best performance in this instance, resulting in a ZOI measuring 6.25 mm. With *A. baumannii*, the RW-ALC exhibited effectiveness in all treatments. However, it only hindered bacterial growth at the specific site of treatment in all instances. Bacteria employ many strategies to acquire resistance against antibacterial agents. For instance, Cephalosporin- and carbapenem-class antibiotics have traditionally been the primary treatment for severe infections caused by *Enterobacterales*, like *K. pneumoniae* (De Oliveira *et al.*, 2020). However, their effectiveness has been undermined by the widespread acquisition of genes that encode enzymes, such as extended-spectrum β-lactamases (ESBLs) and carbapenemases. These enzymes are responsible for the development of resistance to these crucial drugs (De Oliveira *et al.*, 2020). In essence, the presence of various drug resistance mechanisms, whether naturally occurring or triggered by external factors, has led to a higher prevalence of bacterial species carrying these mechanisms in infections acquired in hospitals (De Oliveira *et al.*, 2020).

The negative control, ordinary cotton, showed no antibacterial action, since there were no ZOIs found for any of the tested bacterial strains, as anticipated. This eliminated the possibility that the cotton fabric itself possessed inherent antibacterial characteristics. The antibacterial activity shown in this experiment may be attributed completely to the RW-ALC and the RW-AgNPs.

Hebeish *et al.* (2011) conducted a similar investigation where they synthesised AgNPs from hydroxypropyl starch and then applied them to cotton fibres. Their study found that the textiles infused with AgNPs demonstrated exceptional antibacterial activities against both Gram-positive (*S. aureus*) and Gram-negative (*E. coli*) bacteria (Hebeish *et al.*, 2011). Jain *et al.* (2022) conducted an *in situ* synthesis of *Azadirachta indica*-AgNPs onto cotton fabrics under hydrothermal conditions and screened them for antibacterial activity against antibiotic-resistant Gram-positive and Gram-negative strains. They observed that the AgNP-loaded cotton fabrics had potent antibacterial activity against *Bacillus licheniformis* and moderate activity against *K. pneumoniae* and *E. coli*, while the control treatment (regular cotton) exhibited no antibacterial properties, which agrees with the observations of this study (Jain *et al.*, 2022). Based on the results of this experiment, specifically the ZOI measurements (**Table 3.3**), it was concluded that 6.25 mg/ml RW was the optimal concentration for use in the *in situ* synthesis of RW-ALC, as it produced the RW-ALC that exhibited the greatest antibacterial activity.

3.5.1.1 Effect of 2-mercaptoethanol on the antibacterial activity of RW-ALC

In order to establish that the antibacterial properties of Ag-based substances are a result of Ag's ability to bind to sulfhydryl-containing molecules, the RW-ALC were treated with 2-mercaptoethanol and then utilised in a disc diffusion assay. When Ag binds to molecules that have thiols, it prevents their antibacterial effects, which allows the bacteria to continue to grow. The RW-ALC used in this experiment was synthesised using the optimal concentration of RW, which was 6.25 mg/ml. The experiment results indicated that 2-mercaptoethanol prevented the antibacterial activity of RW-ALC against test bacterial strains (**Figure 3.17**).

The optimised RW-ALC exhibited antibacterial action against both Gram-positive and Gram-negative bacteria. The ZOI for the optimised RW-ALC, together with the RW-ALC that was preincubated with 2-mercaptoethanol are presented in **Table 3.4**. The RW-ALC treatments exhibited superior efficacy against the Gram-negative bacteria than the Gram-positive bacteria. *E. cloacae* and *A. baumannii* were most susceptible, the ZOI for *E. cloacae* was 22.17 ± 1.89 mm, while for *A. baumannii* was 23.56 ± 2.57 mm. RW-ALC also exhibited stronger antibacterial properties against the other strains; the ZOI for *P. aeruginosa*, *E. coli*, *K. pneumoniae*, *S. aureus* and MRSA were 14.67 ± 2.08 mm, 19.17 ± 3.33 mm, 17 ± 2.65 mm, 12.33 ± 1.15 mm and 13.75 ± 4.60 mm, respectively. These results indicated that the RW-ALC treatments had greater antibacterial than Ciprofloxacin at 10 µg/ml.

RW-ALC preincubated with 2-mercaptoethanol did not exhibit any antibacterial activity against all seven strains tested, confirming that thiol-containing molecules such as 2-mercaptoethanol can abrogate the antibacterial activity of the RW-AgNPs. A study conducted by Lethongkam *et al.* (2023) found that 2-mercaptoethanol and cysteine, at concentrations greater than 17.46 and 31.25 $\mu\text{g/ml}$, respectively, were able to eliminate the antibacterial effects of all the tested Ag-containing compounds against *S. aureus* and *P. aeruginosa* using a broth microdilution assay (Lethongkam *et al.*, 2023). The presence of 2-mercaptoethanol nullifies the antibacterial properties of AgNPs through various mechanisms, including surface interactions, suppression of ion release, scavenging of ROS, and changes in surface charge (Lethongkam *et al.*, 2023). The thiol group present in 2-mercaptoethanol exhibits a strong affinity for Ag, enabling it to attach to the surface of AgNPs. The binding process inactivates the nanoparticles and obstructs their active sites, which are essential for producing ROS and releasing Ag^+ . Both of these factors are important for the antibacterial effectiveness of AgNPs (Morones *et al.*, 2005).

In addition, 2-mercaptoethanol has the ability to undergo a chemical reaction with Ag^+ ions, resulting in the formation of Ag-S complexes. This reaction decreases the amount of Ag^+ that is available and reduces their toxicity towards bacterial cells (Lethongkam *et al.*, 2023). 2-mercaptoethanol reduces the dissolution of AgNPs by stabilising them, which in turn limits the release of Ag^+ responsible for antibacterial actions. 2-mercaptoethanol acts as an antioxidant and also scavenges ROS, reducing the oxidative stress that AgNPs cause on bacterial cells (Lok *et al.*, 2007). Thus, the interaction between 2-mercaptoethanol and AgNPs could affect the zeta potential of the nanoparticles, hence impacting their surface charge (Pal *et al.*, 2007). This alteration can prevent the connection between AgNPs and bacterial cell membranes, hence diminishing the NPs' capacity to bind to and infiltrate bacterial cells. The antibacterial effectiveness of RW-AgNPs was greatly deactivated by the presence of 2-mercaptoethanol through one of these mechanisms (Lethongkam *et al.*, 2023).

Table 3.4: ZOI measurements of RW-ALC before and after incubation with 2-mercaptoethanol against human pathogenic bacteria

	<i>S. aureus</i>	MRSA	<i>E. cloacae</i>	<i>E. coli</i>	<i>K. pneumoniae</i>	<i>P. aeruginosa</i>	<i>A. baumannii</i>
Zone of inhibition ± SD (mm)							
6.25 mg/ml RW-ALC	12.33 ± 1.15	13.75 ± 4.60	22.17 ± 1.89	19.17 ± 3.33	17 ± 2.65	14.67 ± 2.08	23.56 ± 2.57
2-mercaptoethanol	0 ± 0	0 ± 0	0 ± 0	0 ± 0	0 ± 0	0 ± 0	0 ± 0
Ciprofloxacin (+)	13.17 ± 3.01	11 ± 1.7	10 ± 3	17 ± 3.6	19.17 ± 1.39	12 ± 1	16.44 ± 485
Cotton fabric (-)	0 ± 0	0 ± 0	0 ± 0	0 ± 0	0 ± 0	0 ± 0	0 ± 0

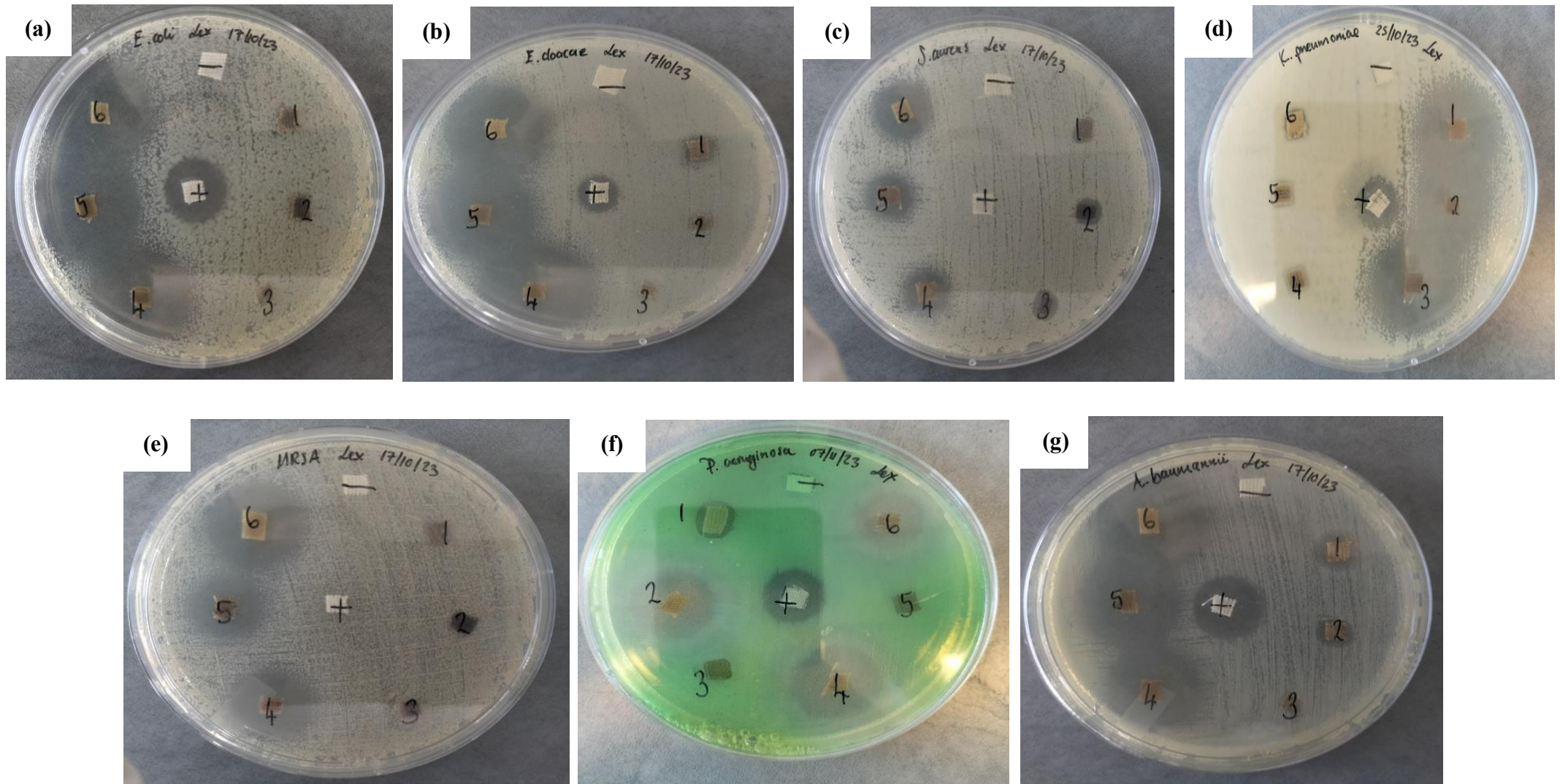


Figure 3.17: Antibacterial activity of RW-ALC using agar disc diffusion assay. Seven pathogenic bacteria were treated with RW-ALC synthesised using 6.25 mg/ml RWE (1-3), and RW-ALC preincubated with 2-mercaptoethanol (4-6). += Ciprofloxacin. (a) *E. coli*, (b) *E. cloacae*, (c) *S. aureus*, (d) *K. pneumoniae*, (e) *MRSA*, (f) *P. aeruginosa*, (g) *A. baumannii*

3.5.2 Microdilution assay using RW-AgNPs

To further evaluate the MIC and MBC of RW-AgNPs, a microdilution assay was performed against the selected strains (*S. aureus*, MRSA, *E. cloacae*, *E. coli*, *K. pneumoniae*, *P. aeruginosa*, and *A. baumannii*). The MIC is the lowest concentration of a treatment that shows no visual growth of bacteria, while the MBC is the lowest concentration of a treatment that is needed to kill 99.9 % of the bacteria (Antunes *et al.*, 2016).

RW-AgNPs displayed broad-spectrum antibacterial activity against all tested bacterial strains, as shown in **Figure 3.18**, illustrating the bactericidal properties of RW-AgNPs against the bacteria. The RW-AgNPs had dose-dependent inhibitory effects on bacterial growth and showed similar efficacy against both Gram-negative and Gram-positive bacteria, despite their variation in cell wall composition (**Table 3.5**). They were most potent against *S. aureus*, with a MIC value of 0.195 µg/ml and MBC value of 0.78 µg/ml, which are exceptionally low concentrations of RW-AgNPs required to inhibit bacterial growth and kill 99.9 % of *S. aureus*. This is particularly significant, considering that *S. aureus* is known to be resistant to numerous antibiotics, and is responsible for a variety of hospital-acquired infections and increased mortality rates (Perovic *et al.*, 2017). RW-AgNPs had a slightly lower efficacy against MRSA, as indicated by MIC and MBC values of 1.56 µg/ml and 3.125 µg/ml, respectively. This outcome was anticipated due to the fact that MRSA is a multi-resistant strain of *S. aureus* that is resistant to all β-lactam antibiotics (Nandhini *et al.*, 2022).

Table 3.5: MIC and MBC values of RW-AgNPs on seven human pathogenic bacteria.

	MIC	MBC
<i>S. aureus</i>	0.195 µg/ml	0.78 µg/ml
MRSA	1.56 µg/ml	3.125 µg/ml
<i>E. cloacae</i>	3.125 µg/ml	3.125 µg/ml
<i>E. coli</i>	0.78 µg/ml	0.78 µg/ml
<i>K. pneumoniae</i>	0.78 µg/ml	1.56 µg/ml
<i>P. aeruginosa</i>	3.125 µg/ml	6.25 µg/ml
<i>A. baumannii</i>	0.78 µg/ml	1.56 µg/ml

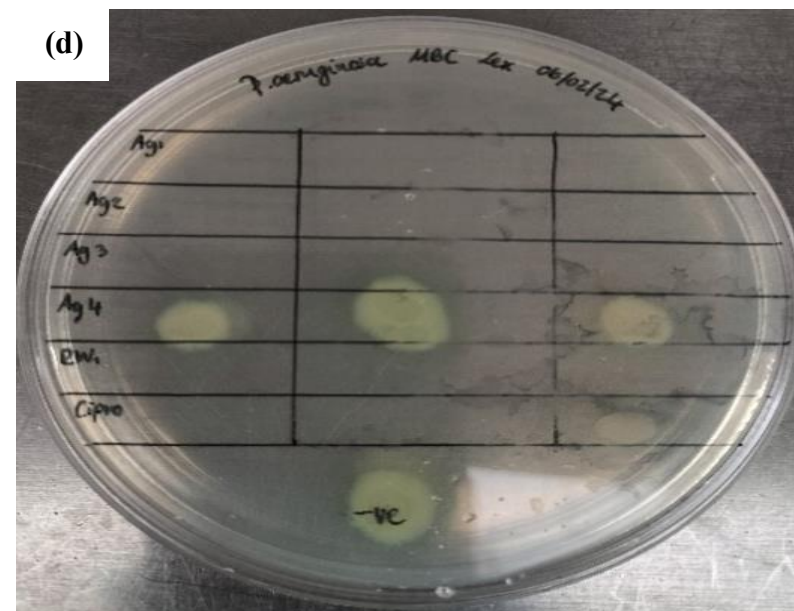
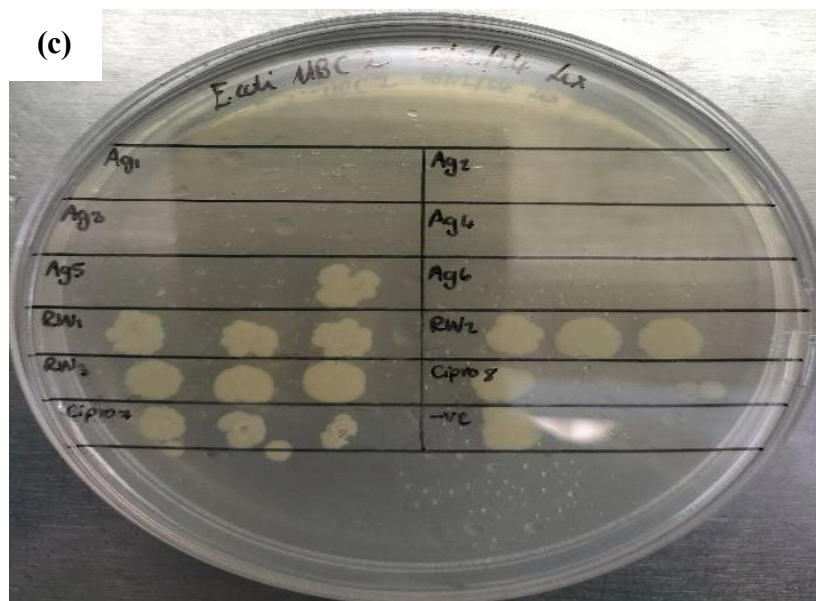
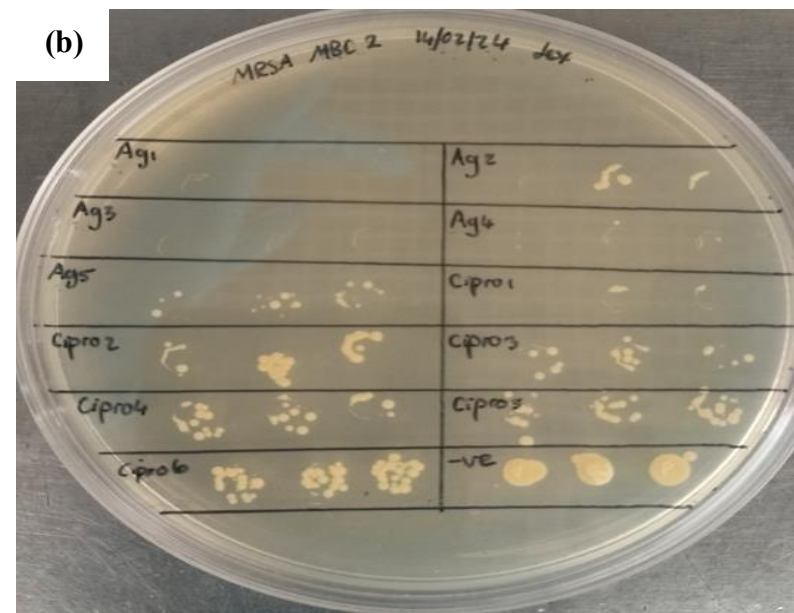
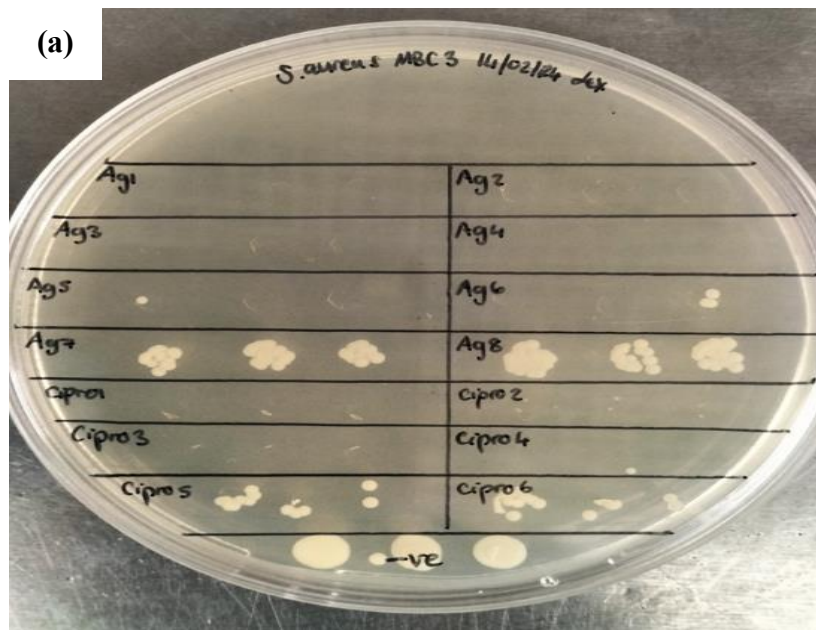


Figure 3.18: Investigation of bactericidal effects of RW-AgNPs on Gram-positive ((a) *S. aureus* and (b) MRSA) and Gram-negative ((c) *E. coli* and (d) *P. aeruginosa*) human pathogenic bacteria.

Conversely, the RW-AgNPs were least effective against *E. cloacae* and *P. aeruginosa* and exhibited a higher MIC value of 3.125 µg/ml than the other strains. The MBC was higher (6.25 µg/ml) for *P. aeruginosa*. Immunocompromised patients are vulnerable to infections by bacterial strains such as *P. aeruginosa* and *E. cloacae* (De Oliveira *et al.*, 2020). These strains have been found to produce ESBLs, which enable them to become resistant to almost all antibiotics except colistin (Balestri *et al.*, 2023). Colistin is considered the last-resort antibiotic and is highly effective against all types of bacteria (Balestri *et al.*, 2023). The inhibitory impact of RW-AgNPs was equally demonstrated on *E. coli*, *K. pneumoniae*, and *A. baumannii*, at an exceptionally low concentration of 0.78 µg/ml. The MIC and MBC values were the same for *E. coli*. However, for *K. pneumoniae* and *A. baumannii*, a concentration of RW-AgNPs that was twice as high (1.56 µg/ml) was needed to demonstrate bactericidal action. Dube *et al.* (2020) stated that a natural agent is considered a potent antibacterial agent if it has a MIC value of 1 mg/ml and below. This study demonstrated that RW-AgNPs exhibited MIC values significantly lower than 1 mg/ml, indicating their remarkable antibacterial efficacy. Consequently, these NPs can be considered as a viable alternative for the treatment of bacterial infections that necessitate urgent intervention (Dube *et al.*, 2020). The findings of this study align with a study by Arshad *et al.*, in which biogenic *Aloe vera* AgNPs demonstrated inhibitory effects on the growth of various strains, including *S. aureus*, *E. coli*, *A. baumannii*, and *P. aeruginosa* (Arshad *et al.*, 2022).

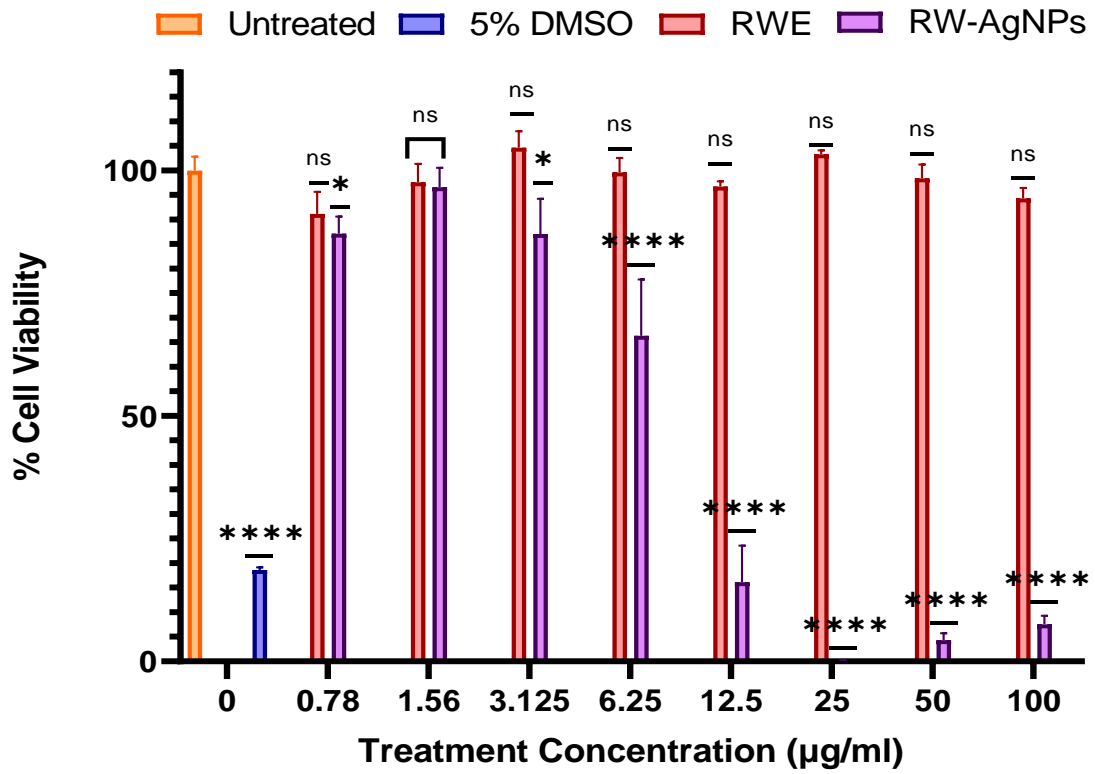
The antibacterial activity of RW-AgNPs was comparable to that of a known broad-spectrum antibiotic investigated in this study, Ciprofloxacin (**Figure 3.17; Table 3.4**). Ciprofloxacin was used at a concentration of 10 µg/ml of Ciprofloxacin for all bacteria evaluated, except for *E. coli* which was treated with 5 µg/ml. Ciprofloxacin at these dosages exhibited antibacterial activity that was comparable to – and in other strains – lower than the RW-AgNPs. The MIC and MBC values of RW-AgNPs were significantly lower than the concentrations of Ciprofloxacin employed in the agar well diffusion. This suggested that RW-AgNPs were sufficient and has the potential to produce similar antibacterial effects as Ciprofloxacin on all tested pathogens. This is an important finding from the study since it showed the broad-spectrum antibacterial activity of RW-AgNPs, which demonstrate that they can be more or equally effective as traditional antibiotic therapy.

3.6 Cytotoxicity study

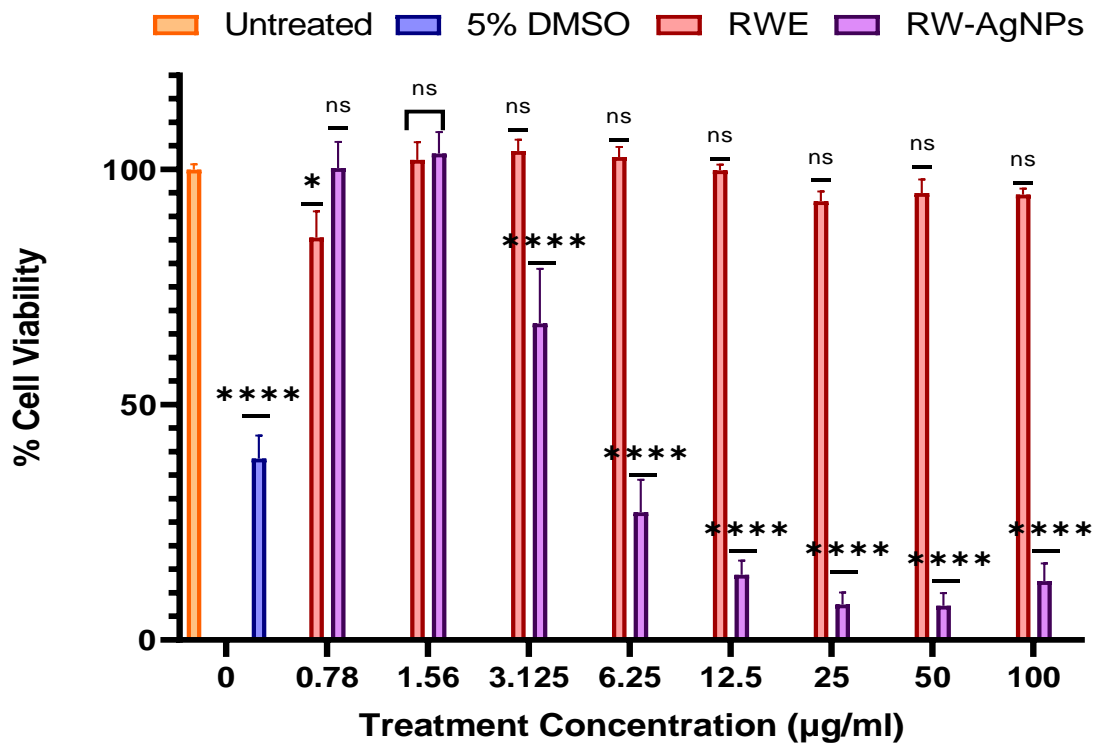
Research on the toxicity of NPs is necessary for their anticipated application in the biomedical sector. Various human cell models can be used to study the inhibitory and harmful effects of NPs (Algotiml *et al.*, 2022) on both normal and pathological cells. This is important for guiding and designing *in vivo* testing as well as possibly generating new anticancer drugs (Dadwal *et al.*, 2018). Cell-based assays are capable of quantifying several cellular characteristics such as morphology, proliferation, viability, toxicity, motility, and metabolic synthesis (Ngungeni *et al.*, 2023). These assays can be used as a reliable initial screening test for assessing the potential anti-cancer properties of NPs. The toxicity of RW-AgNPs on human cell lines was determined *in vitro* using the WST-1 assay. These cell lines included the non-cancerous KMST-6 cells as well as the malignant MCF-7, Caco-2, PC-3, Panc-1, and MIA-Paca-2 cells. The WST-1 assay operates on the idea that tetrazolium salts are enzymatically cleaved by cellular enzymes, specifically mitochondrial dehydrogenases, resulting in the formation of formazan (Morais *et al.*, 2021) as an indicator of the metabolic activity and survival of cells. Therefore, this assay allows for the evaluation of cell viability, particularly in relation to the harm that AgNPs can do to the mitochondria of the cells. The cells were treated for 24 hours with RW and RW-AgNPs at a concentration range of 0 µg/ml – 100 µg/ml, and 5 % DMSO was used as a positive control.

RW-AgNPs exhibited significant cytotoxicity against the pancreatic cell lines MIA-Paca-2 and Panc-1, with a dose-dependent response being observed between 0.78 – 25 µg/ml (**Figures 3.20A and B**). An upward shift in the trend was noted with the 50 and 100 µg/ml treatments, however, cell viability remained below 13 % in both cases. In addition, the IC₅₀ values for MIA-Paca-2 and Panc-1 cells were remarkably low at 7.9 µg/ml and 3.76 µg/ml, respectively. The IC₅₀ values mentioned here are significantly lower than the ones documented in literature. For example, Shameli Rajiri *et al.* (2020) documented an IC₅₀ value of 50 µg/ml when testing the effectiveness of green-synthesized AgNPs on Panc-1 cells (Shameli Rajiri *et al.*, 2021). In addition, *Berberis thunbergia*-AgNPs exhibited IC₅₀ values of 259 and 141 µg/ml against Panc-1 and MIA PaCa-2 cell lines, respectively (Guo *et al.*, 2022). RW did not have any significant effect on the Panc-1 and MIA-Paca-2 cells at any of the treatment concentrations.

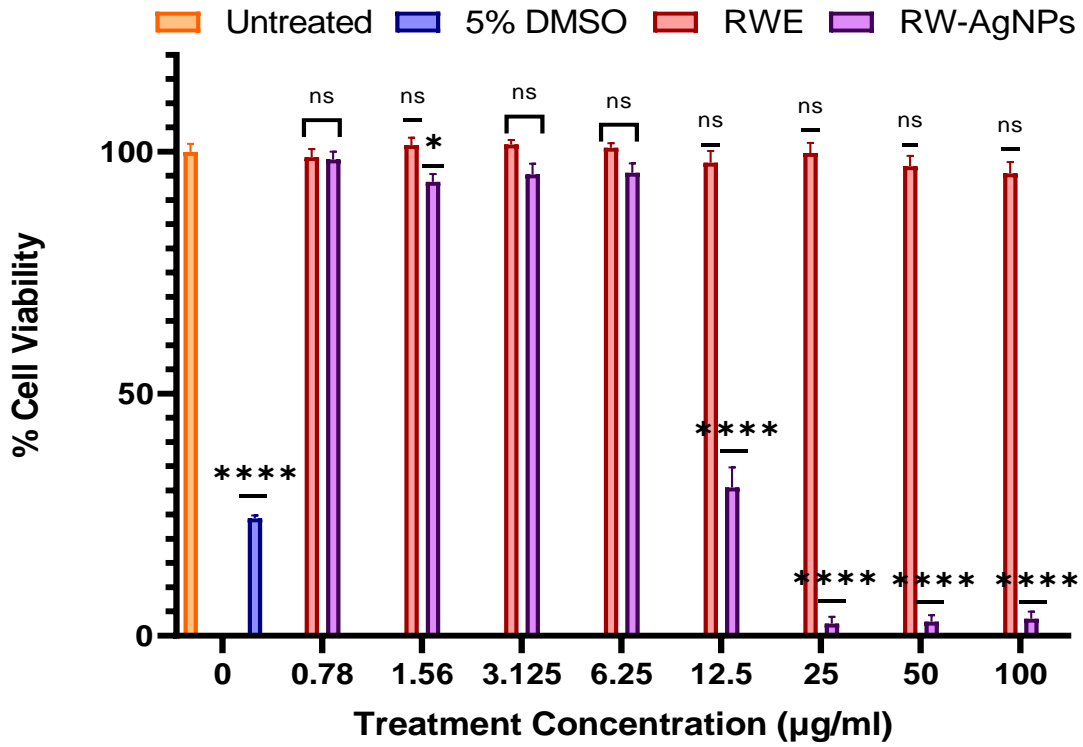
(a) MIA-PaCa-2



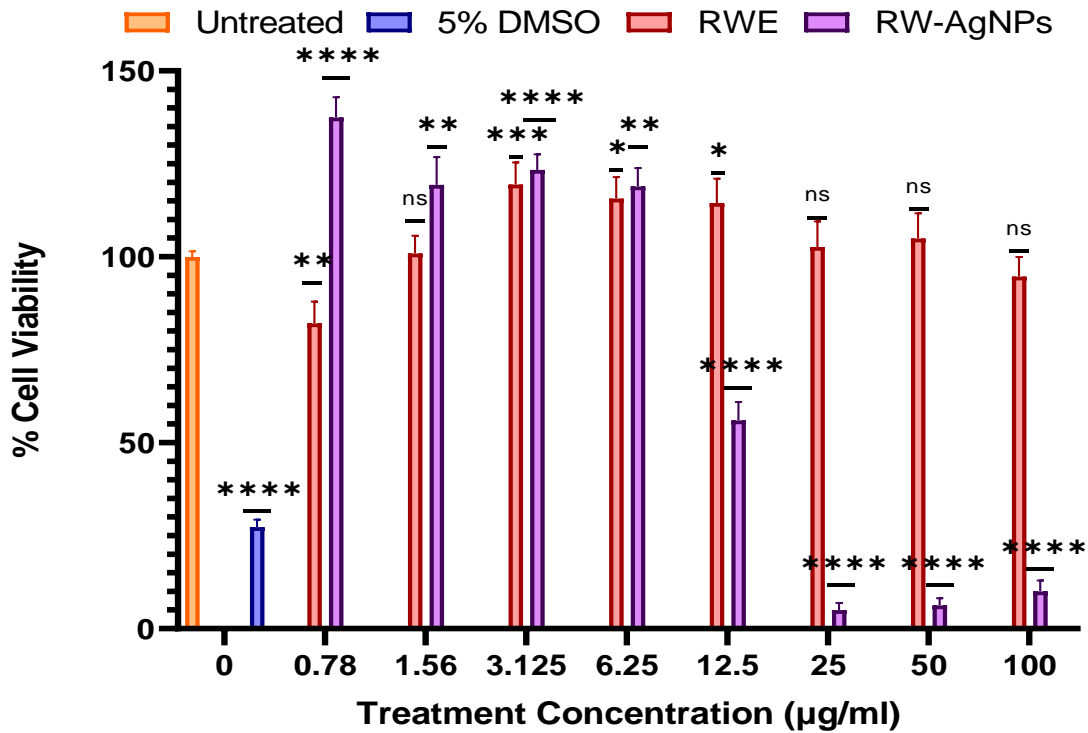
(b) Panc-1



(c) PC-3



(d) MCF-7



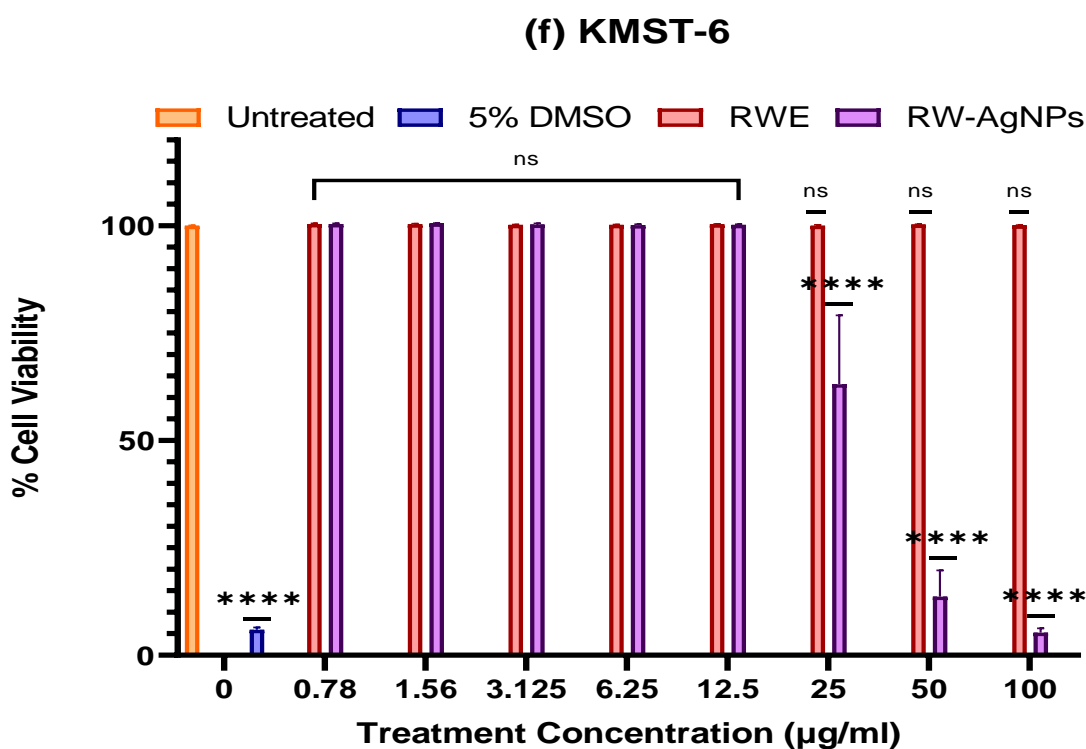
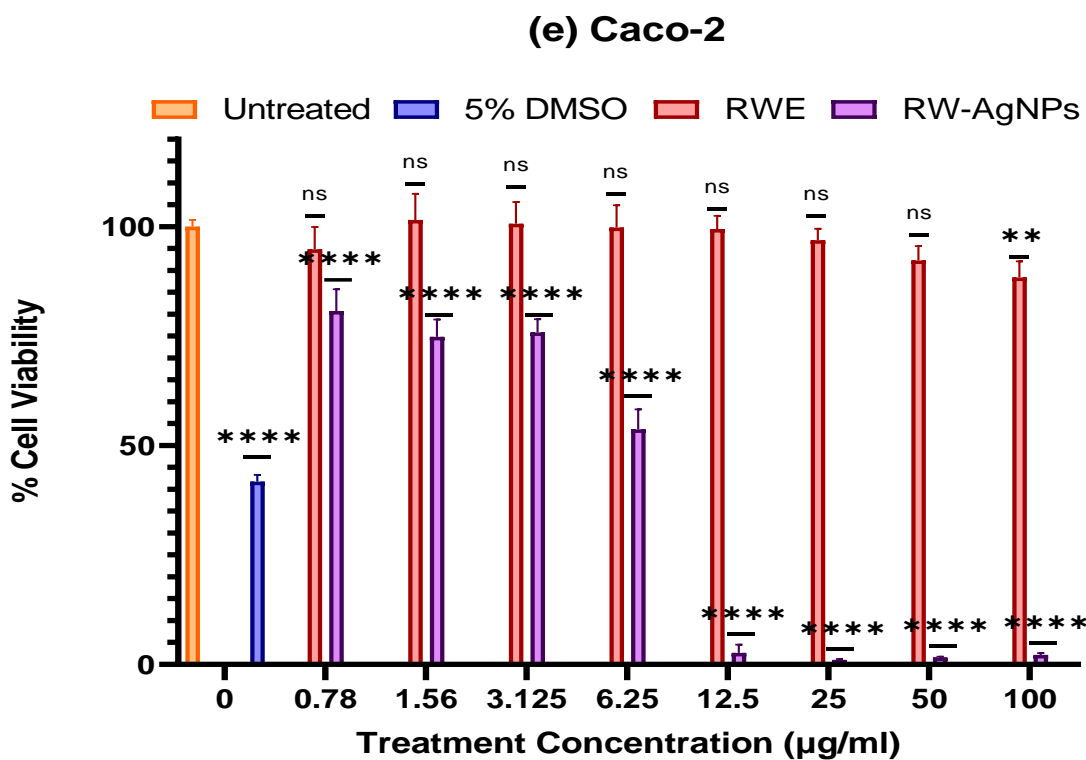


Figure 3.19: Screening of the cytotoxic effects of RW and RW-AgNPs using WST-1 assay on human cells: (a) MIA-Paca-2, (b) Panc-1, (c) PC-3, (d) MCF-7, (e) Caco-2, and (f) KMST-6. Data is presented as mean \pm SEM (n = 3). Statistical significance was determined against untreated cells using Two-way ANOVA where ns = non-significant, * = $p < 0.05$, ** = $p < 0.01$, *** = $p < 0.001$, **** = $p < 0.0001$.

There was a non-significant effect on the viability of PC-3 (prostate cancer) cells when exposed to RW-AgNPs at 6.25 µg/ml and below. Cell viability was reduced considerably to 30 % at 12.5 µg/ml, then declined to below 4 % at concentrations ranging from 25 to 100 µg/ml (**Figure 3.20C**). The IC₅₀ value was measured at 10.98 µg/ml, which exceeded the values observed in Panc-1 and MIA-Paca-2 cells, but it remained remarkably low. *Gracilaria edulis*-AgNPs exhibited cytotoxic properties against PC-3 cells, with an IC₅₀ value of 39.60 µg/ml (Priyadharshini *et al.*, 2014).

An interesting phenomenon was observed in the breast cancer MCF-7 cells, where the cells exhibited a significant increase in proliferation of up to 37 % when treated with RW-AgNPs at concentrations ranging from 0.78 to 6.25 µg/ml (**Figure 3.20D**). Furthermore, RW induced substantial cell growth at all concentrations, indicating that RW did not display any detrimental impacts on this specific cell line. The cytotoxic activity of RW-AgNPs was observed at 12.5 µg/ml, resulting in a decrease in cell viability to 55 %. Viability decreased to less than 5 % at 25 µg/ml. Similar to Panc-1 and MIA-Paca-2, there was an increase in the trend when treated with 50 and 100 µg/ml. However, the viability of the cells remained below 10 %. RW-AgNPs demonstrated substantial cytotoxicity against MCF-7 cells, as evidenced by an IC₅₀ value of only 11.47 µg/ml. Similar effects were reported for AgNPs synthesised using *Rhynchosia rufescens*, which showed strong cytotoxic effects against MCF-7 cells, with an IC₅₀ value of 26 µg/ml (Khader *et al.*, 2020).

The Caco-2 cell line, which is associated with colorectal cancer, exhibited a high susceptibility to the impact of RW-AgNPs. A significant decline in cell viability was observed even at the lowest concentration of 0.78 µg/ml. The viability of the cells was affected in a dose-dependent manner (**Figure 3.20E**). The viability of the cells was less than 3 % when exposed to 12.5 µg/ml, and the IC₅₀ value was at 6.76 µg/ml. Zein *et al.* (2020) conducted a study where they synthesised AgNPs using the extract of *Eucalyptus Camaldulensis* leaves. These AgNPs were then screened for cytotoxicity against Caco-2 cells and had an IC₅₀ value of 18 µg/ml (Zein *et al.*, 2020).

The findings of this assay indicated that RW-AgNPs had no effect on the cell viability of the non-cancerous KMST-6 cells at concentrations of 12.5 µg/ml and below (**Figure 3.20F**). However, the RW-AgNPs displayed significant toxicity towards the cells in a dose-dependent manner from 25 – 100 µg/ml, with an IC₅₀ value of 27.70 µg/ml. This outcome is favourable, as it suggests that higher concentrations of RW-AgNPs are required in order for cytotoxicity to

be observed against normal cells. In other words, these RW-AgNPs could potentially be used to target cancer cells, with minimal or no damage to normal and healthy cells. This is supported by the fact that the IC₅₀ values observed against all the cancer cell lines were significantly lower than the IC₅₀ for KMST-6 cells. This presents an opportunity for the use of RW-AgNPs as a complementary or alternative anti-cancer agent. Treatment with 5 % DMSO reduced cell viability to ≤ 40 % in all cell lines. This was expected, as previous reports have indicated that DMSO exhibits cytotoxicity to cells when used at concentrations over 1 % (Brito *et al.*, 2017).

While previous research has reported the biocompatibility of some green AgNPs (Rafique *et al.*, 2017), this current study showed that AgNPs synthesised from plant extracts, which are considered to be non-toxic in traditional medicine, have the potential to have cytotoxic effects. Similarly, RW-AgNPs demonstrated non-selectivity and induced cytotoxicity in both normal and malignant human cell lines, however, their impact was notably more pronounced on the cancerous cells.

CHAPTER 4: CONCLUSION

AMR is a major global health crisis that necessitates urgent intervention. Infections caused by antibiotic resistant bacteria are a significant contributor to mortality across all age groups. Traditional therapies for AMR infections are frequently ineffective, necessitate high or frequent doses, are linked to adverse effects, and can potentially worsen AMR. Hence, there is an urgent need for new or unconventional therapeutic approaches to combat diseases caused by antibiotic-resistant bacteria.

The primary objective of this work was to synthesize biogenic RW-AgNPs (*in situ* and *ex situ*) and examine their antibacterial properties to determine their potential as agents against AMR. The RW-AgNPs and RW-ALC inhibited bacterial growth and demonstrated cytotoxic effects towards cancer cells. The RW-AgNPs had both growth-inhibitory and bactericidal effects, with Gram-negative and Gram-positive bacteria being equally vulnerable to the antibacterial properties of the RW-AgNPs. These findings indicate that RW-AgNPs and RW-ALC could be used as promising treatments for bacterial infections caused by antibiotic-resistant bacteria. The properties were comparable to that of the broad-spectrum antibiotic Ciprofloxacin. This discovery suggested the potential of using RW-ALC as a therapeutic approach for treating infectious diseases, including chronic and infected wounds. These activities could be attributed to the strong antioxidant properties exhibited by the RW-AgNPs, possibly due to the presence of bioactive chemicals, particularly phenolics, on their surface. RW-AgNPs exhibited notable cytotoxicity against a panel of cancer cell lines (MCF-7, PC3, Caco-2, MIA-Paca-2, and Panc-1), while displaying reduced cytotoxicity towards the normal human fibroblast (KMST-6) cell line. This indicated that RW-AgNPs are suitable candidates for the treatment of bacterial infections and cancer while causing minimal harm to healthy cells.

The current study provided evidence that RW-AgNPs exhibit strong antibacterial and anticancer properties, and these activities are retained when deposited in textiles. The RW-ALC has the potential to be beneficial in the treatment of chronically infected wounds. Further work is needed to determine the mechanism of action for the antibacterial and anti-cancer effects of RW-AgNPs and confirm their biocompatibility at doses that are minimally harmful to normal cells but still lethal to pathogenic bacteria and cells. The RW-ALC could then be exploited in the development of innovative cost-effective treatments for persistent non-healing wounds, and RW-AgNPs for cancer therapy.

REFERENCES

- A., BARBA, F. J., MUNEKATA, P. E. S. & LORENZO, J. M. 2020. Physicochemical Characterization, Antioxidant Activity, and Phenolic Compounds of Hawthorn (*Crataegus* spp.) Fruits Species for Potential Use in Food Applications. *Foods*, 9, 436.
- ABOYEWA, J. A., SIBUYI, N. R. S., MEYER, M. & OGUNTIBEJU, O. O. 2021. Green Synthesis of Metallic Nanoparticles Using Some Selected Medicinal Plants from Southern Africa and Their Biological Applications. *Plants*, 10, 1929.
- AFZAL, S., RAJU, A. V., RAJU, C. S., CHONG, G., WUII, Z. & ESEYIN, O. A. 2021. Evaluation of the antimicrobial and anticancer properties of the fruits of *Synsepalum dulcificum* (Sapotaceae). *Tropical Journal of Pharmaceutical Research*, 20, 1925-1930.
- AHMED, T. & OGULATA, R. T. 2021. A Review on Silver Nanoparticles -green Synthesis, Antimicrobial Action and Application in Textiles. *Journal of Natural Fibers*, 19, 8463-8484.
- AL-OBAIDI, H., KALGUDI, R. & ZARIWALA, M. G. 2018. Fabrication of inhaled hybrid silver/ciprofloxacin nanoparticles with synergetic effect against *Pseudomonas aeruginosa*. *Eur J Pharm Biopharm*, 128, 27-35.
- ALAM, M. A., MUNNI, S. A., MOSTAFA, S., BISHWAS, R. K. & JAHAN, S. A. 2023. An investigation on synthesis of silver nanoparticles. *Asian Journal of Research in Biochemistry*, 12, 1-10.
- ALGHAMDI, S. 2021. The role of vaccines in combating antimicrobial resistance (AMR) bacteria. *Saudi Journal of Biological Sciences*, 28, 7505-7510.
- ALGOTIML, R., GAB-ALLA, A., SEOUDI, R., ABULREESH, H. H., EL-READI, M. Z. & ELBANNA, K. 2022. Anticancer and antimicrobial activity of biosynthesized Red Sea marine algal silver nanoparticles. *Scientific Reports*, 12, 2421.
- ALHARBI, N. S., KHALED, J. M., KADAIKUNNAN, S., ALOBAIDI, A. S., SHARAFADDIN, A. H., ALYAHYA, S. A., ALMANAA, T. N., ALSUGHAYIER, M. A. & SHEHU, M. R. 2019. Prevalence of *Escherichia coli* strains resistance to antibiotics in wound infections and raw milk. *Saudi Journal of Biological Sciences*, 26, 1557-1562.
- ALI, M. A., AHMED, T., WU, W., HOSSAIN, A., HAFEEZ, R., ISLAM MASUM, M. M., WANG, Y., AN, Q., SUN, G. & LI, B. 2020. Advancements in Plant and Microbe-Based

- Synthesis of Metallic Nanoparticles and Their Antimicrobial Activity against Plant Pathogens. *Nanomaterials*, 10, 1146.
- ALIREZALU, A., AHMADI, N., SALEHI, P., SONBOLI, A., ALIREZALU, K., MOUSAVI KHANEGHAH, A., BARBA, F. J., MUNEKATA, P. E. S. & LORENZO, J. M. 2020. Physicochemical Characterization, Antioxidant Activity, and Phenolic Compounds of Hawthorn (*Crataegus* spp.) *Fruits Species for Potential Use in Food Applications*. *Foods*, 9, 436.
- ALJELDAH, M. M. 2022. Antimicrobial Resistance and Its Spread Is a Global Threat. *Antibiotics*, 11, 1082.
- ALMATROUDI, A. 2020. Silver nanoparticles: Synthesis, characterisation and biomedical applications. *Open life sciences*, 15, 819-839.
- ALSHEIKH, H. M. A., SULTAN, I., KUMAR, V., RATHER, I. A., AL-SHEIKH, H., TASLEEM JAN, A. & HAQ, Q. M. R. 2020. Plant-Based Phytochemicals as Possible Alternative to Antibiotics in Combating Bacterial Drug Resistance. *Antibiotics (Basel)*, 9.
- ALTEMIMI, A., LAKHSSASSI, N., BAHARLOUEI, A., WATSON, D. G. & LIGHTFOOT, D. A. 2017. Phytochemicals: Extraction, Isolation, and Identification of Bioactive Compounds from Plant Extracts. *Plants (Basel)*, 6.
- ALVAREZ-MARTINEZ, F. J., BARRAJON-CATALAN, E. & MICOL, V. 2020. Tackling Antibiotic Resistance with Compounds of Natural Origin: A Comprehensive Review. *Biomedicines*, 8.
- AMID, A., NASRUDDIN, A., SULAIMAN, S. & OTHMAN, M. E. F. 2018. BIOSYNTHESIS OF NANOPARTICLES USING RECOMBINANT BROMELAIN. *Biological and Natural Resources Engineering Journal*, 1, 14-25.
- AMINOV, R. I. 2010. A Brief History of the Antibiotic Era: Lessons Learned and Challenges for the Future. *Frontiers in Microbiology*, 1.
- AMRULLOH, H., FATIQIN, A., SIMANJUNTAK, W., AFRIYANI, H. & ANNISSA, A. 2021. Bioactivities of nano-scale magnesium oxide prepared using aqueous extract of *Moringa oleifera* leaves as green agent. *Advances in Natural Sciences: Nanoscience and Nanotechnology*, 12, 015006.
- ANANDHAKUMAR, S., MAHALAKSHMI, V. & RAICHUR, A. M. 2012. Silver nanoparticles modified nanocapsules for ultrasonically activated drug delivery. *Materials Science and Engineering: C*, 32, 2349-2355.

- ANASTAS, P. T. & WARNER, J. C. 1998. *Green Chemistry: Theory and Practice*, Oxford University Press.
- ANEES AHMAD, S., SACHI DAS, S., KHATOON, A., TAHIR ANSARI, M., AFZAL, M., SAQUIB HASNAIN, M. & KUMAR NAYAK, A. 2020. Bactericidal activity of silver nanoparticles: A mechanistic review. *Materials Science for Energy Technologies*, 3, 756-769.
- ANTUNES, E., MMOLA, M., MEYER, M. & BEUKES, D. 2016. Assessment of the bactericidal effect of green synthesized silver nanoparticles against a panel of infectious microorganisms. *Planta Medica*, 82, P703.
- ARSHAD, H., SALEEM, M., PASHA, U. & SADAF, S. 2022. Synthesis of Aloe vera-conjugated silver nanoparticles for use against multidrug-resistant microorganisms. *Electronic Journal of Biotechnology*, 55, 55-64.
- ARUMAI SELVAN, D., MAHENDIRAN, D., SENTHIL KUMAR, R. & KALILUR RAHIMAN, A. 2018. Garlic, green tea and turmeric extracts-mediated green synthesis of silver nanoparticles: Phytochemical, antioxidant and in vitro cytotoxicity studies. *J Photochem Photobiol B*, 180, 243-252.
- ARYA, G., SHARMA, N., MANKAMNA, R. & NIMESH, S. 2019. Antimicrobial Silver Nanoparticles: Future of Nanomaterials.
- ATANASOV, A. G., WALTENBERGER, B., PFERSCHY-WENZIG, E. M., LINDER, T., WAWROSCHE, C., UHRIN, P., TEMML, V., WANG, L., SCHWAIGER, S., HEISS, E. H., ROLLINGER, J. M., SCHUSTER, D., BREUSS, J. M., BOCHKOV, V., MIHOVILOVIC, M. D., KOPP, B., BAUER, R., DIRSCH, V. M. & STUPPNER, H. 2015. Discovery and resupply of pharmacologically active plant-derived natural products: A review. *Biotechnol Adv*, 33, 1582-1614.
- AYRES, R. U. 2021. *Biotechnology and Human Health: The History and Future of Technology: Can Technology Save Humanity from Extinction?* Cham: Springer International Publishing.
- BABICK, F. 2020. Chapter 3.2.1 - Dynamic light scattering (DLS). In: HODOROABA, V.-D., UNGER, W. E. S. & SHARD, A. G. (eds.) *Characterization of Nanoparticles*. Elsevier.
- BALESTRI, A., CARDELLINI, J. & BERTI, D. 2023. Gold and silver nanoparticles as tools to combat multidrug-resistant pathogens. *Current Opinion in Colloid & Interface Science*, 66, 101710.
- BALIYAN, S., MUKHERJEE, R., PRIYADARSHINI, A., VIBHUTI, A., GUPTA, A., PANDEY, R. P. & CHANG, C.-M. 2022. Determination of Antioxidants by DPPH

- Radical Scavenging Activity and Quantitative Phytochemical Analysis of *Ficus religiosa*. *Molecules*, 27, 1326.
- BALOUIRI, M., SADIKI, M. & IBNSOUDA, S. K. 2016. Methods for in vitro evaluating antimicrobial activity: A review. *J Pharm Anal*, 6, 71-79.
- BARBIERI, R., COPPO, E., MARCHESE, A., DAGLIA, M., SOBARZO-SANCHEZ, E., NABAVI, S. F. & NABAVI, S. M. 2017. Phytochemicals for human disease: An update on plant-derived compounds antibacterial activity. *Microbiol Res*, 196, 44-68.
- BARKAT, M. A., HARSHITA, DAS, S. S., BEG, S. & AHMAD, F. J. 2020. Nanotechnology-Based Phytotherapeutics: Current Status and Challenges. In: BEG, S., BARKAT, M. A. & AHMAD, F. J. (eds.) *Nanophytomedicine: Concept to Clinic*. Singapore: Springer Singapore.
- BAYDA, S., ADEEL, M., TUCCINARDI, T., CORDANI, M. & RIZZOLIO, F. 2019. The History of Nanoscience and Nanotechnology: From Chemical-Physical Applications to Nanomedicine. *Molecules*, 25.
- BAYDA, S., ADEEL, M., TUCCINARDI, T., CORDANI, M. & RIZZOLIO, F. 2020. The History of Nanoscience and Nanotechnology: From Chemical–Physical Applications to Nanomedicine. *Molecules*, 25, 112.
- BHARDWAJ, M., YADAV, P., DALAL, S. & KATARIA, S. K. 2020. A review on ameliorative green nanotechnological approaches in diabetes management. *Biomedicine & Pharmacotherapy*, 127, 110198.
- BRENES, A., VIVEROS, A., CHAMORRO, S. & ARIJA, I. 2016. Use of polyphenol-rich grape by-products in monogastric nutrition. A review. *Animal Feed Science and Technology*, 211, 1-17.
- BRITO, R., SILVA, G., FARIAS, T., FERREIRA, P. & FERREIRA, S. 2017. Standardization of the safety level of the use of DMSO in viability assays in bacterial cells.
- BROWN, P. K., QURESHI, A. T., MOLL, A. N., HAYES, D. J. & MONROE, W. T. 2013. Silver nanoscale antisense drug delivery system for photoactivated gene silencing. *ACS Nano*, 7, 2948-59.
- BROWNE, A. J., CHIPETA, M. G., HAINES-WOODHOUSE, G., KUMARAN, E. P. A., HAMADANI, B. H. K., ZARAA, S., HENRY, N. J., DESHPANDE, A., REINER, R. C., JR., DAY, N. P. J., LOPEZ, A. D., DUNACHIE, S., MOORE, C. E., STERGACHIS, A., HAY, S. I. & DOLECEK, C. 2021. Global antibiotic consumption and usage in humans, 2000-18: a spatial modelling study. *Lancet Planet Health*, 5, e893-e904.

- BURANGE, P. J., TAWAR, M. G., BAIRAGI, R. A., MALVIYA, V. R., SAHU, V. K., SHEWATKAR, S. N., SAWARKAR, R. A. & MAMURKAR, R. R. 2021. Synthesis of silver nanoparticles by using Aloe vera and Thuja orientalis leaves extract and their biological activity: a comprehensive review. *Bulletin of the National Research Centre*, 45, 1-13.
- BURDUȘEL, A.-C., GHERASIM, O., GRUMEZESCU, A. M., MOGOANTĂ, L., FICAI, A. & ANDRONESCU, E. 2018. Biomedical Applications of Silver Nanoparticles: An Up-to-Date Overview. *Nanomaterials*, 8, 681.
- CANO, A., ETTCHETO, M., ESPINA, M., LOPEZ-MACHADO, A., CAJAL, Y., RABANAL, F., SANCHEZ-LOPEZ, E., CAMINS, A., GARCIA, M. L. & SOUTO, E. B. 2020. State-of-the-art polymeric nanoparticles as promising therapeutic tools against human bacterial infections. *J Nanobiotechnology*, 18, 156.
- CANO, A., MAESTRE, A. B., HERNÁNDEZ-RUIZ, J. & ARNAO, M. B. 2023. ABTS/TAC Methodology: Main Milestones and Recent Applications. *Processes*, 11.
- CHAND, K., CAO, D., FOUAD, D. E., SHAH, A. H., DAYO, A. Q., ZHU, K., LAKHAN, M. N., MEHDI, G. & DONG, S. 2020. Green synthesis, characterization and photocatalytic application of silver nanoparticles synthesized by various plant extracts. *Arabian Journal of Chemistry*, 13, 8248-8261.
- CHARALAMPIA, D. & KOUTELIDAKIS, A. 2016. Grape pomace: a challenging renewable resource of bioactive phenolic compounds with diversified health benefits. *Food Processing & Technology*, 3, 00065.
- CHENG, V. J., BEKHIT, A. E.-D. A., MCCONNELL, M., MROS, S. & ZHAO, J. 2012. Effect of extraction solvent, waste fraction and grape variety on the antimicrobial and antioxidant activities of extracts from wine residue from cool climate. *Food Chemistry*, 134, 474-482.
- CHERNOUSOVA, S. & EPPLE, M. 2013. Silver as Antibacterial Agent: Ion, Nanoparticle, and Metal. *Angewandte Chemie International Edition*, 52, 1636-1653.
- CHETTY, S., REDDY, M., RAMSAMY, Y., NAIDOO, A. & ESSACK, S. 2019. Antimicrobial stewardship in South Africa: a scoping review of the published literature. *JAC Antimicrob Resist*, 1, dlz060.
- CHOWDHURY, S., DE, M., GUHA, R., BATABYAL, S., SAMANTA, I., HAZRA, S. K., GHOSH, T. K., KONAR, A. & HAZRA, S. 2014. Influence of silver nanoparticles on post-surgical wound healing following topical application. *European Journal of Nanomedicine*, 6, 237-247.

- CLEMENTE, A., MORENO, N., LOBERA, M. P., BALAS, F. & SANTAMARIA, J. 2018. Versatile hollow fluorescent metal-silica nanohybrids through a modified microemulsion synthesis route. *J Colloid Interface Sci*, 513, 497-504.
- CLOGSTON, J. D. & PATRI, A. K. 2011. Zeta Potential Measurement. In: MCNEIL, S. E. (ed.) *Characterization of Nanoparticles Intended for Drug Delivery*. Totowa, NJ: Humana Press.
- CUEVA, C., MORENO-ARRIBAS, M. V., MARTIN-ALVAREZ, P. J., BILLS, G., VICENTE, M. F., BASILIO, A., RIVAS, C. L., REQUENA, T., RODRIGUEZ, J. M. & BARTOLOME, B. 2010. Antimicrobial activity of phenolic acids against commensal, probiotic and pathogenic bacteria. *Res Microbiol*, 161, 372-82.
- DADWAL, A., BALDI, A. & KUMAR NARANG, R. 2018. Nanoparticles as carriers for drug delivery in cancer. *Artif Cells Nanomed Biotechnol*, 46, 295-305.
- DAS, R. K., PACHAPUR, V. L., LONAPPAN, L., NAGHDI, M., PULICHARLA, R., MAITI, S., CLEDON, M., DALILA, L. M. A., SARMA, S. J. & BRAR, S. K. 2017. Biological synthesis of metallic nanoparticles: plants, animals and microbial aspects. *Nanotechnology for Environmental Engineering*, 2.
- DAWADI, S., KATUWAL, S., GUPTA, A., LAMICHHANE, U., THAPA, R., JAISI, S., LAMICHHANE, G., BHATTARAI, D. & PARAJULI, N. 2021. Current Research on Silver Nanoparticles: Synthesis, Characterization, and Applications. *Journal of Nanomaterials*, 2021.
- DE OLIVEIRA, D. M., FORDE, B. M., KIDD, T. J., HARRIS, P. N., SCHEMBRI, M. A., BEATSON, S. A., PATERSON, D. L. & WALKER, M. J. 2020. Antimicrobial resistance in ESKAPE pathogens. *Clinical microbiology reviews*, 33, 10.1128/cmr.00181-19.
- DELGADO-BELEÑO, Y., MARTINEZ-NUÑEZ, C. E., CORTEZ-VALADEZ, M., FLORES-LÓPEZ, N. S. & FLORES-ACOSTA, M. 2018. Optical properties of silver, silver sulfide and silver selenide nanoparticles and antibacterial applications. *Materials Research Bulletin*, 99, 385-392.
- DEY, A., MITRA, A., PATHAK, S., PRASAD, S., ZHANG, A. S., ZHANG, H., SUN, X. F. & BANERJEE, A. 2023. Recent Advancements, Limitations, and Future Perspectives of the use of Personalized Medicine in Treatment of Colon Cancer. *Technol Cancer Res Treat*, 22, 15330338231178403.

- DHAYAGUDE, A. C., DAS, A., JOSHI, S. S. & KAPOOR, S. 2018. γ -Radiation induced synthesis of silver nanoparticles in aqueous poly (N-vinylpyrrolidone) solution. *Colloids and Surfaces A: Physicochemical and Engineering Aspects*, 556, 148-156.
- DÍAZ-CRUZ, C., ALONSO NUÑEZ, G., ESPINOZA-GÓMEZ, H. & FLORES-LÓPEZ, L. Z. 2016. Effect of molecular weight of PEG or PVA as reducing-stabilizing agent in the green synthesis of silver-nanoparticles. *European Polymer Journal*, 83, 265-277.
- DIKSHIT, P. K., KUMAR, J., DAS, A. K., SADHU, S., SHARMA, S., SINGH, S., GUPTA, P. K. & KIM, B. S. 2021. Green synthesis of metallic nanoparticles: Applications and limitations. *Catalysts*, 11, 902.
- DING, Q., LIU, D., GUO, D., YANG, F., PANG, X., CHE, R., ZHOU, N., XIE, J., SUN, J., HUANG, Z. & GU, N. 2017. Shape-controlled fabrication of magnetite silver hybrid nanoparticles with high performance magnetic hyperthermia. *Biomaterials*, 124, 35-46.
- DOS SANTOS COURROL, D., REGINA BORGES LOPES, C., DA SILVA CORDEIRO, T., REGINA FRANZOLIN, M., DIAS VIEIRA JUNIOR, N., ELGUL SAMAD, R. & CORONATO COURROL, L. 2018. Optical properties and antimicrobial effects of silver nanoparticles synthesized by femtosecond laser photoreduction. *Optics & Laser Technology*, 103, 233-238.
- DREADEN, E. C., ALKILANY, A. M., HUANG, X., MURPHY, C. J. & EL-SAYED, M. A. 2012. The golden age: gold nanoparticles for biomedicine. *Chemical Society Reviews*, 41, 2740-2779.
- DRESSELHAUS, M., DRESSELHAUS, G. & EKLUND, P. 1993. Fullerenes. *Journal of materials research*, 8, 2054-2097.
- DUBE, P., MEYER, S., MADIEHE, A. & MEYER, M. 2020. Antibacterial activity of biogenic silver and gold nanoparticles synthesized from *Salvia africana-lutea* and *Sutherlandia frutescens*. *Nanotechnology*, 31, 505607.
- DUBEY, S. P., LAHTINEN, M. & SILLANPÄÄ, M. 2010. Tansy fruit mediated greener synthesis of silver and gold nanoparticles. *Process Biochemistry*, 45, 1065-1071.
- EFENBERGER-SZMECHTYK, M., NOWAK, A. & CZYZOWSKA, A. 2021. Plant extracts rich in polyphenols: antibacterial agents and natural preservatives for meat and meat products. *Crit Rev Food Sci Nutr*; 61, 149-178.
- EL-NAGGAR, M. E., SHAHEEN, T. I., ZAGHLOUL, S., EL-RAFIE, M. H. & HEBEISH, A. 2016. Antibacterial activities and UV protection of the in situ synthesized titanium oxide nanoparticles on cotton fabrics. *Industrial & Engineering Chemistry Research*, 55, 2661-2668.

- FADAKA, A. O., MEYER, S., AHMED, O., GEERTS, G., MADIEHE, M. A., MEYER, M. & SIBUYI, N. R. S. 2022. Broad Spectrum Anti-Bacterial Activity and Non-Selective Toxicity of Gum Arabic Silver Nanoparticles. *Int J Mol Sci*, 23.
- FERRAZ DA COSTA, D. C., PEREIRA RANGEL, L., QUARTI, J., SANTOS, R. A., SILVA, J. L. & FIALHO, E. 2020. Bioactive compounds and metabolites from grapes and red wine in breast cancer chemoprevention and therapy. *Molecules*, 25, 3531.
- FINESTONE, E. & WISHNIA, J. 2022. Estimating the burden of cancer in South Africa. *South African Journal of Oncology*, 6.
- FRIEDMAN, M. 2014. Antibacterial, antiviral, and antifungal properties of wines and winery byproducts in relation to their flavonoid content. *J Agric Food Chem*, 62, 6025-42.
- GAO, H., YANG, H. & WANG, C. 2017. Controllable preparation and mechanism of nano-silver mediated by the microemulsion system of the clove oil. *Results in Physics*, 7, 3130-3136.
- GEEL, J. A. & MAYET, Y. 2024. New insights into cancer epidemiology and survival in sub-Saharan Africa. *Lancet Glob Health*, 12, e897-e898.
- GIANCACCCHI, E. & FIERABRACCI, A. 2020. Insights on the Effects of Resveratrol and Some of Its Derivatives in Cancer and Autoimmunity: A Molecule with a Dual Activity. *Antioxidants (Basel)*, 9.
- GNANAJOBITHA, G., PAULKUMAR, K., VANAJA, M., RAJESHKUMAR, S., MALARKODI, C., ANNADURAI, G. & KANNAN, C. 2013. Fruit-mediated synthesis of silver nanoparticles using *Vitis vinifera* and evaluation of their antimicrobial efficacy. *Journal of Nanostructure in Chemistry*, 3, 1-6.
- GOLPOUR, M., EBRAHIMNEJAD, P., GATABI, Z. R., NAJAFI, A., DAVOODI, A., KHAJAVI, R., ALIMOHAMMADI, M. & MOUSAVI, T. 2024. Green tea-mediated synthesis of silver nanoparticles: Enhanced anti-cancer activity and reduced cytotoxicity melanoma and normal murine cell lines. *Inorganic Chemistry Communications*, 161.
- GONG, C. P., LI, S. C. & WANG, R. Y. 2018. Development of biosynthesized silver nanoparticles based formulation for treating wounds during nursing care in hospitals. *J Photochem Photobiol B*, 183, 137-141.
- GONZALEZ-BALLESTEROS, N., RODRIGUEZ-GONZALEZ, J. B. & RODRIGUEZ-ARGUELLES, M. C. 2018. Harnessing the wine dregs: An approach towards a more sustainable synthesis of gold and silver nanoparticles. *J Photochem Photobiol B*, 178, 302-309.

- GÓRNIAK, I., BARTOSZEWSKI, R. & KRÓLICZEWSKI, J. 2018. Comprehensive review of antimicrobial activities of plant flavonoids. *Phytochemistry Reviews*, 18, 241-272.
- GUJRATI, M., MALAMAS, A., SHIN, T., JIN, E., SUN, Y. & LU, Z.-R. 2014. Multifunctional cationic lipid-based nanoparticles facilitate endosomal escape and reduction-triggered cytosolic siRNA release. *Molecular pharmaceutics*, 11, 2734-2744.
- GUO, J., LI, Y., YU, Z., CHEN, L., CHINNATHAMBI, A., ALMOALLIM, H. S., ALHARBI, S. A. & LIU, L. 2022. Novel green synthesis and characterization of a chemotherapeutic supplement by silver nanoparticles containing *Berberis thunbergii* leaf for the treatment of human pancreatic cancer. *Biotechnology and Applied Biochemistry*, 69, 887-897.
- GURUNATHAN, S., HAN, J. W., KWON, D.-N. & KIM, J.-H. 2014. Enhanced antibacterial and anti-biofilm activities of silver nanoparticles against Gram-negative and Gram-positive bacteria. *Nanoscale research letters*, 9, 1-17.
- GYAWALI, R. & IBRAHIM, S. A. 2014. Natural products as antimicrobial agents. *Food Control*, 46, 412-429.
- GYSENS, I. C. & WERTHEIM, H. F. 2020. Editorial: Antimicrobial Stewardship in Low- and Middle-Income Countries. *Frontiers in Public Health*, 8.
- HADARI, H., BRIGHT, R., GARG, S., VASILEV, K., COWIN, A. J. & KOPECKI, Z. 2021. Eradication of Mature Bacterial Biofilms with Concurrent Improvement in Chronic Wound Healing Using Silver Nanoparticle Hydrogel Treatment. *Biomedicines*, 9.
- HALEEM, A., JAVAID, M., SINGH, R. P., RAB, S. & SUMAN, R. 2023. Applications of nanotechnology in medical field: a brief review. *Global Health Journal*, 7, 70-77.
- HAMDAN, S., PASTAR, I., DRAKULICH, S., DIKICI, E., TOMIC-CANIC, M., DEO, S. & DAUNERT, S. 2017. Nanotechnology-driven therapeutic interventions in wound healing: potential uses and applications. *ACS central science*, 3, 163-175.
- HAMDI, Y., ABDELJAOUED-TEJ, I., ZATCHI, A. A., ABDELHAK, S., BOUBAKER, S., BROWN, J. S. & BENKAHLA, A. 2021. Cancer in Africa: The Untold Story. *Front Oncol*, 11, 650117.
- HANH, T. T., THU, N. T., QUOC, L. A. & HIEN, N. Q. 2017. Synthesis and characterization of silver/diatomite nanocomposite by electron beam irradiation. *Radiation Physics and Chemistry*, 139, 141-146.
- HARISHA, K. S., PARUSHURAM, N., RANJANA, R., MARTIS, L. J., NARAYANA, B. & SANGAPPA, Y. 2021. Characterization and antibacterial properties of biogenic spherical silver nanoparticles. *Materials Today: Proceedings*, 42, 405-409.

- HASIBUAN, P. A. Z., TANJUNG, M., GEA, S., PASARIBU, K. M., HARAHAP, M., PERANGIN-ANGIN, Y. A., PRAYOGA, A. & GINTING, J. G. 2021. Antimicrobial and antihemolytic properties of a CNF/AgNP-chitosan film: A potential wound dressing material. *Helvion*, 7, e08197.
- HEBEISH, A., EL-NAGGAR, M., FOU DA, M. M., RAMADAN, M., AL-DEYAB, S. S. & EL-RAFIE, M. 2011. Highly effective antibacterial textiles containing green synthesized silver nanoparticles. *Carbohydrate Polymers*, 86, 936-940.
- HEBEISH, A., EL-RAFIE, M. H., EL-SHEIKH, M. A., SELEEM, A. A. & EL-NAGGAR, M. E. 2014. Antimicrobial wound dressing and anti-inflammatory efficacy of silver nanoparticles. *Int J Biol Macromol*, 65, 509-15.
- HEFNI, H. H., AZZAM, E. M., BADR, E. A., HUSSEIN, M. & TAWFIK, S. M. 2016. Synthesis, characterization and anticorrosion potentials of chitosan-g-PEG assembled on silver nanoparticles. *Int J Biol Macromol*, 83, 297-305.
- HENDI, A. 2011. Silver nanoparticles mediate differential responses in some of liver and kidney functions during skin wound healing. *Journal of King Saud University - Science*, 23, 47-52.
- HOVERSTEN, K. P., KIEMELE, L. J., STOLP, A. M., TAKAHASHI, P. Y. & VERDOORN, B. P. 2020. Prevention, Diagnosis, and Management of Chronic Wounds in Older Adults. *Mayo Clin Proc*, 95, 2021-2034.
- HU, D., ZOU, L., GAO, Y., JIN, Q. & JI, J. 2020. Emerging nanobiomaterials against bacterial infections in postantibiotic era. *VIEW*, 1, 20200014.
- HUTCHINGS, M. I., TRUMAN, A. W. & WILKINSON, B. 2019. Antibiotics: past, present and future. *Current Opinion in Microbiology*, 51, 72-80.
- ILYAS, T., CHOWDHARY, P., CHAURASIA, D., GNANSOUNOU, E., PANDEY, A. & CHATURVEDI, P. 2021. Sustainable green processing of grape pomace for the production of value-added products: An overview. *Environmental Technology & Innovation*, 23, 101592.
- ILYASOV, I. R., BELOBORODOV, V. L., SELIVANOVA, I. A. & TEREKHOV, R. P. 2020. ABTS/PP Decolorization Assay of Antioxidant Capacity Reaction Pathways. *Int J Mol Sci*, 21.
- JAHANGIRIAN, H., LEMRASKI, E. G., WEBSTER, T. J., RAFIEE-MOGHADDAM, R. & ABDOLLAHI, Y. 2017. A review of drug delivery systems based on nanotechnology and green chemistry: green nanomedicine. *Int J Nanomedicine*, 12, 2957-2978.

- JAIN, A., KONGKHAM, B., PUTTASWAMY, H., BUTOLA, B. S., MALIK, H. K. & MALIK, A. 2022. Development of Wash-Durable Antimicrobial Cotton Fabrics by In Situ Green Synthesis of Silver Nanoparticles and Investigation of Their Antimicrobial Efficacy against Drug-Resistant Bacteria. *Antibiotics*, 11, 864.
- JARA-PALACIOS, M. J., HERNANZ, D., CIFUENTES-GOMEZ, T., ESCUDERO-GILETE, M. L., HEREDIA, F. J. & SPENCER, J. P. 2015. Assessment of white grape pomace from winemaking as source of bioactive compounds, and its antiproliferative activity. *Food Chem*, 183, 78-82.
- JAYAWARDENA, H. S. N., LIYANAGE, S. H., RATHNAYAKE, K., PATEL, U. & YAN, M. 2021. Analytical Methods for Characterization of Nanomaterial Surfaces. *Analytical Chemistry*, 93, 1889-1911.
- JEBALI, A., HEKMATIMOGHADDAM, S., BEHZADI, A., REZAPOR, I., MOHAMMADI, B. H., JASEMIZAD, T., YASINI, S. A., JAVADZADEH, M., AMIRI, A. & SOLTANI, M. 2013. Antimicrobial activity of nanocellulose conjugated with allicin and lysozyme. *Cellulose*, 20, 2897-2907.
- JIANG, Q., YU, S., LI, X., MA, C. & LI, A. 2018. Evaluation of local anesthetic effects of Lidocaine-Ibuprofen ionic liquid stabilized silver nanoparticles in Male Swiss mice. *J Photochem Photobiol B*, 178, 367-370.
- JIANG, T., LI, Q., QIU, J., CHEN, J., DU, S., XU, X., WU, Z., YANG, X., CHEN, Z. & CHEN, T. 2022. Nanobiotechnology: Applications in Chronic Wound Healing. *International Journal of Nanomedicine*, 3125-3145.
- JORGE, P., MAGALHÃES, A. P., GRAINHA, T., ALVES, D., SOUSA, A. M., LOPES, S. P. & PEREIRA, M. O. 2019. Antimicrobial resistance three ways: healthcare crisis, major concepts and the relevance of biofilms. *FEMS Microbiology Ecology*, 95.
- JOUDEH, N. & LINKE, D. 2022. Nanoparticle classification, physicochemical properties, characterization, and applications: a comprehensive review for biologists. *Journal of Nanobiotechnology*, 20, 262.
- KALANTARI, K., MOSTAFAVI, E., AFIFI, A. M., IZADIYAN, Z., JAHANGIRIAN, H., RAFIEE-MOGHADDAM, R. & WEBSTER, T. J. 2020. Wound dressings functionalized with silver nanoparticles: promises and pitfalls. *Nanoscale*, 12, 2268-2291.
- KARAMI, R., MORADIPOUR, P., ARKAN, E., ZARGHAMI, R., RASHIDI, K. & DARVISHI, E. 2023. Biocompatible nano-bandage modified with silver nanoparticles based on herbal for burn treatment. *Polymer Bulletin*.

- KARTHIK, C. S., MANUKUMAR, H. M., ANANDA, A. P., NAGASHREE, S., RAKESH, K. P., MALLESHA, L., QIN, H. L., UMESHA, S., MALLU, P. & KRISHNAMURTHY, N. B. 2018. Synthesis of novel benzodioxane midst piperazine moiety decorated chitosan silver nanoparticle against biohazard pathogens and as potential anti-inflammatory candidate: A molecular docking studies. *Int J Biol Macromol*, 108, 489-502.
- KATALINIĆ, V., MOŽINA, S. S., SKROZA, D., GENERALIĆ, I., ABRAMOVIĆ, H., MILOŠ, M., LJUBENKOV, I., PISKERNIK, S., PEZO, I., TERPINC, P. & BOBAN, M. 2010. Polyphenolic profile, antioxidant properties and antimicrobial activity of grape skin extracts of 14 *Vitis vinifera* varieties grown in Dalmatia (Croatia). *Food Chemistry*, 119, 715-723.
- KAUR, A., GOYAL, D. & KUMAR, R. 2018. Surfactant mediated interaction of vancomycin with silver nanoparticles. *Applied Surface Science*, 449, 23-30.
- KAVIYA, S., SANTHANALAKSHMI, J. & VISWANATHAN, B. 2012. Biosynthesis of silver nano-flakes by *Crossandra infundibuliformis* leaf extract. *Materials Letters*, 67, 64-66.
- KHADER, S. Z. A., SYED ZAMEER AHMED, S., GANESAN, G. M., MAHBOOB, M. R., VETRIVEL, M., SANKARAPPAN, M. & MANICKAM, P. 2020. *Rhynchosia rufescens* AgNPs enhance cytotoxicity by ROS-mediated apoptosis in MCF-7 cell lines. *Environmental Science and Pollution Research*, 27, 2155-2164.
- KHAN, I., SAEED, K. & KHAN, I. 2019. Nanoparticles: Properties, applications and toxicities. *Arabian journal of chemistry*, 12, 908-931.
- KHUDA, F., JAMIL, M., ALIKHAN KHALIL, A., ULLAH, R., ULLAH, N., NAUREEN, F., ABBAS, M., SHAFIQ KHAN, M., ALI, S., MUHAMMAD UMER FAROOQI, H. & AHN, M.-J. 2022. Assessment of antioxidant and cytotoxic potential of silver nanoparticles synthesized from root extract of *Reynoutria japonica* Houtt. *Arabian Journal of Chemistry*, 15, 104327.
- KJ, P. 2017. Multi-functional silver nanoparticles for drug delivery: A review. *Int. J. Curr. Pharm. Rev. Res*, 9, 1-5.
- KOLAHALAM, L. A., KASI VISWANATH, I. V., DIWAKAR, B. S., GOVINDH, B., REDDY, V. & MURTHY, Y. L. N. 2019. Review on nanomaterials: Synthesis and applications. *Materials Today: Proceedings*, 18, 2182-2190.
- KONOP, M., DAMPS, T., MISICKA, A. & RUDNICKA, L. 2016. Certain Aspects of Silver and Silver Nanoparticles in Wound Care: A Minireview. *Journal of Nanomaterials*, 2016, 7614753.

- KUMAR, M., CURTIS, A. & HOSKINS, C. 2018. Application of Nanoparticle Technologies in the Combat against Anti-Microbial Resistance. *Pharmaceutics*, 10.
- KURŠVIETIENĖ, L., STANEVIČIENĖ, I., MONGIRDIENĖ, A. & BERNATONIENĖ, J. 2016. Multiplicity of effects and health benefits of resveratrol. *Medicina*, 52, 148-155.
- KUSHWAHA, A., GOSWAMI, L. & KIM, B. S. 2022. Nanomaterial-based therapy for wound healing. *Nanomaterials*, 12, 618.
- LALRINZUALI, K., VABEIRYUREILAI, M., JAGETIA, G. & LALAWMPUII, P. 2015. Free radical scavenging and antioxidant potential of different extracts of *Oroxylum indicum* in vitro. *Advances in Biomedicine and Pharmacy*, 2, 120-130.
- LAMBRECHTS, I. A., THIPE, V. C., KATTI, K. V., MANDIWANA, V., KALOMBO, M. L., RAY, S. S., RIKHOTSO, R., JANSE VAN VUUREN, A., ESMEAR, T. & LALL, N. 2022. Targeting Acne Bacteria and Wound Healing In Vitro Using *Plectranthus aliciae*, Rosmarinic Acid, and Tetracycline Gold Nanoparticles. *Pharmaceutics*, 15, 933.
- LANGEVELD, W. T., VELDHUIZEN, E. J. & BURT, S. A. 2014. Synergy between essential oil components and antibiotics: a review. *Crit Rev Microbiol*, 40, 76-94.
- LARESE, F. F., D'AGOSTIN, F., CROSERI, M., ADAMI, G., RENZI, N., BOVENZI, M. & MAINA, G. 2009. Human skin penetration of silver nanoparticles through intact and damaged skin. *Toxicology*, 255, 33-7.
- LEMIECH-MIROWSKA, E., KIERSNOWSKA, Z. M., MICHALKIEWICZ, M., DEPTA, A. & MARCZAK, M. 2021. Nosocomial infections as one of the most important problems of healthcare system. *Ann Agric Environ Med*, 28, 361-366.
- LETHONGKAM, S., GLASER, J., AMMANATH, A. V., VORAVUTHIKUNCHAI, S. P. & GOTZ, F. 2023. In vitro and in vivo comparative analysis of antibacterial activity of green-synthesized silver nanoparticles. *Biotechnol J*, 18, e2300186.
- LI, Y.-F., GAN, W.-P., JIAN, Z., LU, Z.-Q., CHAO, Y. & GE, T.-T. 2015. Hydrothermal synthesis of silver nanoparticles in Arabic gum aqueous solutions. *Transactions of Nonferrous Metals Society of China*, 25, 2081-2086.
- LIU, L., WANG, S., ZHANG, B., JIANG, G. & YANG, J. 2022. Supercritical hydrothermal synthesis of nano-ZrO₂: Influence of technological parameters and mechanism. *Journal of Alloys and Compounds*, 898, 162878.
- LLOR, C. & BJERRUM, L. 2014. Antimicrobial resistance: risk associated with antibiotic overuse and initiatives to reduce the problem. *Ther Adv Drug Saf*, 5, 229-41.

- LOBANOVSKA, M. & PILLA, G. 2017. Focus: drug development: Penicillin's discovery and antibiotic resistance: lessons for the future? *The Yale journal of biology and medicine*, 90, 135.
- LOK, C.-N., HO, C.-M., CHEN, R., HE, Q.-Y., YU, W.-Y., SUN, H., TAM, P. K.-H., CHIU, J.-F. & CHE, C.-M. 2007. Silver nanoparticles: partial oxidation and antibacterial activities. *JBIC Journal of Biological Inorganic Chemistry*, 12, 527-534.
- LOPES, C. R. B. & COURROL, L. C. 2018. Green synthesis of silver nanoparticles with extract of *Mimusops coriacea* and light. *Journal of Luminescence*, 199, 183-187.
- LUNA-HERNÁNDEZ, E., CRUZ-SOTO, M. E., PADILLA-VACA, F., MAURICIO-SÁNCHEZ, R. A., RAMIREZ-WONG, D., MUÑOZ, R., GRANADOS-LÓPEZ, L., OVALLE-FLORES, L. R., MENCHACA-ARREDONDO, J. L., HERNÁNDEZ-RANGEL, A., PROKHOROV, E., GARCÍA-RIVAS, J. L., ESPAÑA-SÁNCHEZ, B. L. & LUNA-BÁRCENAS, G. 2017. Combined antibacterial/tissue regeneration response in thermal burns promoted by functional chitosan/silver nanocomposites. *Int J Biol Macromol*, 105, 1241-1249.
- MADIEHE, A. M., MOABELO, K. L., MODISE, K., SIBUYI, N. R., MEYER, S., DUBE, A., ONANI, M. O. & MEYER, M. 2022. Catalytic reduction of 4-nitrophenol and methylene blue by biogenic gold nanoparticles synthesized using *Carpobrotus edulis* fruit (sour fig) extract. *Nanomaterials and Nanotechnology*, 12, 18479804221108254.
- MAGIORAKOS, A. P., SRINIVASAN, A., CAREY, R. B., CARMELI, Y., FALAGAS, M. E., GISKE, C. G., HARBARTH, S., HINDLER, J. F., KAHLMETER, G., OLSSON-LILJEQUIST, B., PATERSON, D. L., RICE, L. B., STELLING, J., STRUELENS, M. J., VATOPOULOS, A., WEBER, J. T. & MONNET, D. L. 2012. Multidrug-resistant, extensively drug-resistant and pandrug-resistant bacteria: an international expert proposal for interim standard definitions for acquired resistance. *Clinical Microbiology and Infection*, 18, 268-281.
- MAHMUD, F., UJ, K., KRISHNASAMY, D., CHEBWOGEN, S., RAMESH, V., WIJEKOON, H., SENEVIRATHNE, N. G. R. H. & MANI, M. 2023. A REVIEW ON SILVER NANOPARTICLES AND ITS ROLE IN TREATING DISEASES: ANTICANCER ACTIVITY OF AGNPS. *International Research Journal of Modernization in Engineering Technology and Science*, 5, 2582-5208.
- MAKAROV, V. V., LOVE, A. J., SINITSYNA, O. V., MAKAROVA, S. S., YAMINSKY, I. V., TALIANSKY, M. E. & KALININA, N. O. 2014. "Green" nanotechnologies: synthesis of metal nanoparticles using plants. *Acta Naturae*, 6, 35-44.

- MALIK, P., SHANKAR, R., MALIK, V., SHARMA, N. & MUKHERJEE, T. K. 2014. Green Chemistry Based Benign Routes for Nanoparticle Synthesis. *Journal of Nanoparticles*, 2014, 302429.
- MALIK, S., MUHAMMAD, K. & WAHEED, Y. 2023. Nanotechnology: A Revolution in Modern Industry. *Molecules*, 28.
- MATTIUZZI, C. & LIPPI, G. 2019. Current Cancer Epidemiology. *J Epidemiol Glob Health*, 9, 217-222.
- MAUTER, M. S. & ELIMELECH, M. 2008. Environmental applications of carbon-based nanomaterials. *Environmental science & technology*, 42, 5843-5859.
- MAYLA, A. & GOHAR, Y. 2010. HUMAN ASSOCIATED MYCOPLASMA.
- MAZAYEN, Z. M., GHONEIM, A. M., ELBATANONY, R. S., BASALIOUS, E. B. & BENDAS, E. R. 2022. Pharmaceutical nanotechnology: from the bench to the market. *Future Journal of Pharmaceutical Sciences*, 8, 12.
- MEDINA, M. A., OZA, G., SHARMA, A., ARRIAGA, L., HERNÁNDEZ HERNÁNDEZ, J. M., ROTELLO, V.M. & RAMIREZ, J. T. 2020. Triple-negative breast cancer: a review of conventional and advanced therapeutic strategies. *International journal of environmental research and public health*, 17, 2078.
- MIHAI, M. M., DIMA, M. B., DIMA, B. & HOLBAN, A. M. 2019. Nanomaterials for wound healing and infection control. *Materials*, 12, 2176.
- MIHAILOVIĆ, V., SREĆKOVIĆ, N., NEDIĆ, Z. P., DIMITRIJEVIĆ, S., MATIĆ, M., OBRADOVIĆ, A., SELAKOVIĆ, D., ROSIĆ, G. & KATANIĆ STANKOVIĆ, J. S. 2023. Green Synthesis of Silver Nanoparticles Using *Salvia verticillata* and *Filipendula ulmaria* Extracts: Optimization of Synthesis, Biological Activities, and Catalytic Properties. *Molecules*, 28, 808.
- MISHRA, M., KUMAR, H. & TRIPATHI, K. 2008. Diabetic delayed wound healing and the role of silver nanoparticles. *Dig J Nanomater Bios*, 3, 49-54.
- MODY, V. V., SIWALE, R., SINGH, A. & MODY, H. R. 2010. Introduction to metallic nanoparticles. *Journal of Pharmacy and bioallied sciences*, 2, 282-289.
- MOHAMMADLOU, M., JAFARIZADEH-MALMIRI, H. & MAGHSOUDI, H. 2017. Hydrothermal green synthesis of silver nanoparticles using *Pelargonium/Geranium* leaf extract and evaluation of their antifungal activity. *Green Processing and Synthesis*, 6, 31-42.
- MOHARIL, R. B., DIVE, A., KHANDEKAR, S. & BODHADE, A. 2017. Cancer stem cells: An insight. *J Oral Maxillofac Pathol*, 21, 463.

- MORAIS, M., MACHADO, V., DIAS, F., PALMEIRA, C., MARTINS, G., FONSECA, M., MARTINS, C. S. M., TEIXEIRA, A. L., PRIOR, J. A. V. & MEDEIROS, R. 2021. Starch-Capped AgNPs' as Potential Cytotoxic Agents against Prostate Cancer Cells. *Nanomaterials*, 11, 256.
- MORONES, J. R., ELECHIGUERRA, J. L., CAMACHO, A., HOLT, K., KOURI, J. B., RAMÍREZ, J. T. & YACAMAN, M. J. 2005. The bactericidal effect of silver nanoparticles. *Nanotechnology*, 16, 2346-53.
- MPOFU, N. S., MWASIAGI, J. I., MECHA, C. A. & NGANYI, E. O. 2023. Evaluation of solanum tuberosum potato peel waste for use as an eco-friendly antibacterial finish for cotton fabrics. *Research Journal of Textile and Apparel*.
- MUQBIL, I., BECK, F. W. J., BAO, B., SARKAR, F. H., MOHAMMAD, R. M., HADI, S. M. & AZMI, A. S. 2012. Old wine in a new bottle: the Warburg effect and anticancer mechanisms of resveratrol. *Current pharmaceutical design*, 18 12, 1645-54.
- MURRAY, C. J. L., IKUTA, K. S., SHARARA, F., SWETSCHINSKI, L., ROBLES AGUILAR, G., GRAY, A., HAN, C., BISIGNANO, C., RAO, P., WOOL, E., JOHNSON, S. C., BROWNE, A. J., CHIPETA, M. G., FELL, F., HACKETT, S., HAINES-WOODHOUSE, G., KASHEF HAMADANI, B. H., KUMARAN, E. A. P., MCMANIGAL, B., ACHALAPONG, S., AGARWAL, R., AKECH, S., ALBERTSON, S., AMUASI, J., ANDREWS, J., ARAVKIN, A., ASHLEY, E., BABIN, F.-X., BAILEY, F., BAKER, S., BASNYAT, B., BEKKER, A., BENDER, R., BERKLEY, J. A., BETHOU, A., BIELICKI, J., BOONKASIDECHA, S., BUKOSIA, J., CARVALHEIRO, C., CASTAÑEDA-ORJUELA, C., CHANSAMOUTH, V., CHAURASIA, S., CHIURCHIÙ, S., CHOWDHURY, F., CLOTAIRE DONATIEN, R., COOK, A. J., COOPER, B., CRESSEY, T. R., CRIOLLO-MORA, E., CUNNINGHAM, M., DARBOE, S., DAY, N. P. J., DE LUCA, M., DOKOVA, K., DRAMOWSKI, A., DUNACHIE, S. J., DUONG BICH, T., ECKMANNS, T., EIBACH, D., EMAMI, A., FEASEY, N., FISHER-PEARSON, N., FORREST, K., GARCIA, C., GARRETT, D., GASTMEIER, P., GIREF, A. Z., GREER, R. C., GUPTA, V., HALLER, S., HASELBECK, A., HAY, S. I., HOLM, M., HOPKINS, S., HSIA, Y., IREGBU, K. C., JACOBS, J., JAROVSKY, D., JAVANMARDI, F., JENNEY, A. W. J., KHORANA, M., KHUSUWAN, S., KISSOON, N., KOBEISSI, E., KOSTYANEV, T., KRAPP, F., KRUMKAMP, R., KUMAR, A., KYU, H. H., LIM, C., LIM, K., LIMMATHUROTSAKUL, D., LOFTUS, M. J., LUNN, M., MA, J., MANOHARAN, A., MARKS, F., MAY, J., MAYXAY, M., MTURI, N., et al. 2022.

- Global burden of bacterial antimicrobial resistance in 2019: a systematic analysis. *The Lancet*, 399, 629-655.
- MUSTARICHIE, R., SULISTYANINGSIH, S. & RUNADI, D. 2020. Antibacterial Activity Test of Extracts and Fractions of Cassava Leaves (*Manihot esculenta* Crantz) against Clinical Isolates of *Staphylococcus epidermidis* and *Propionibacterium acnes* Causing Acne. *International Journal of Microbiology*, 2020, 1975904.
- NANDHINI, P., KUMAR, P., MICKYMARAY, S., ALOTHAIM, A. S., SOMASUNDARAM, J. & RAJAN, M. 2022. Recent Developments in Methicillin-Resistant *Staphylococcus aureus* (MRSA) Treatment: A Review. *Antibiotics*, 11, 606.
- NDIKAU, M., NOAH, N. M., ANDALA, D. M. & MASIKA, E. 2017. Green Synthesis and Characterization of Silver Nanoparticles Using *Citrullus lanatus* Fruit Rind Extract. *Int J Anal Chem*, 2017, 8108504.
- NG, K. K. & ZHENG, G. 2015. Molecular interactions in organic nanoparticles for phototheranostic applications. *Chemical reviews*, 115, 11012-11042.
- NGUNGENI, Y., J. A. A., MOABELO, K. L., SIBUYI, N. R. S., MEYER, S., ONANI, M. O., MEYER, M. & MADIEHE, A. M. 2023. Anticancer, Antioxidant, and Catalytic Activities of Green Synthesized Gold Nanoparticles Using Avocado Seed Aqueous Extract. *ACS Omega*, 8, 26088-26101.
- NOVOA, C. C., TORTELLA, G., SEABRA, A. B., DIEZ, M. C. & RUBILAR, O. 2022. Cotton Textile with Antimicrobial Activity and Enhanced Durability Produced by L-Cysteine-Capped Silver Nanoparticles. *Processes*, 10, 958.
- OBIDIRO, O., BATTOGTOKH, G. & AKALA, E. O. 2023. Triple Negative Breast Cancer Treatment Options and Limitations: Future Outlook. *Pharmaceutics*, 15.
- OH, W.-K., YOON, H. & JANG, J. 2010. Size control of magnetic carbon nanoparticles for drug delivery. *Biomaterials*, 31, 1342-1348.
- OKKEH, M., BLOISE, N., RESTIVO, E., DE VITA, L., PALLAVICINI, P. & VISAI, L. 2021. Gold nanoparticles: can they be the next magic bullet for multidrug-resistant bacteria? *Nanomaterials*, 11, 312.
- OLIVEIRA, D. A., SALVADOR, A. A., SMANIA, A., JR., SMANIA, E. F., MARASCHIN, M. & FERREIRA, S. R. 2013. Antimicrobial activity and composition profile of grape (*Vitis vinifera*) pomace extracts obtained by supercritical fluids. *J Biotechnol*, 164, 423-32.
- OMRAN, B., NASSAR, H., FATTHALLAH, N., HAMDY, A., ELSHATOURY, E. & EL-GENDY, N. 2017. Waste upcycling of *Citrus sinensis* peels as a green route for the

- synthesis of silver nanoparticles. *Energy Sources, Part A: Recovery, Utilization, and Environmental Effects*, 40, 1-10.
- OVAIS, M., KHALIL, A. T., AYAZ, M., AHMAD, I., NETHI, S. K. & MUKHERJEE, S. 2018. Biosynthesis of Metal Nanoparticles via Microbial Enzymes: A Mechanistic Approach. *International Journal of Molecular Sciences*, 19.
- OVAIS, M., KHALIL, A. T., RAZA, A., KHAN, M. A., AHMAD, I., ISLAM, N. U., SARAVANAN, M., UBAID, M. F., ALI, M. & SHINWARI, Z. K. 2016. Green synthesis of silver nanoparticles via plant extracts: beginning a new era in cancer theranostics. *Nanomedicine*, 12, 3157-3177.
- PAL, S., TAK, Y. K. & SONG, J. M. 2007. Does the antibacterial activity of silver nanoparticles depend on the shape of the nanoparticle? A study of the Gram-negative bacterium *Escherichia coli*. *Appl Environ Microbiol*, 73, 1712-20.
- PALADINI, F. & POLLINI, M. 2019. Antimicrobial Silver Nanoparticles for Wound Healing Application: Progress and Future Trends. *Materials*, 12, 2540.
- PAN, K. & ZHONG, Q. 2016. Organic nanoparticles in foods: fabrication, characterization, and utilization. *Annual Review of Food Science and Technology*, 7, 245-266.
- PARK, Y. 2014. New paradigm shift for the green synthesis of antibacterial silver nanoparticles utilizing plant extracts. *Toxicol Res*, 30, 169-78.
- PARVEEN, K., BANSE, V. & LEDWANI, L. Green synthesis of nanoparticles: Their advantages and disadvantages. AIP conference proceedings, 2016. AIP Publishing.
- PATRA, J. K. & BAEK, K.-H. 2014. Green Nanobiotechnology: Factors Affecting Synthesis and Characterization Techniques. *Journal of Nanomaterials*, 2014.
- PATRA, S., MUKHERJEE, S., BARUI, A. K., GANGULY, A., SREEDHAR, B. & PATRA, C. R. 2015. Green synthesis, characterization of gold and silver nanoparticles and their potential application for cancer therapeutics. *Mater Sci Eng C Mater Biol Appl*, 53, 298-309.
- PAUL, S., CHUGH, A. & GANDHI, R. 2010. Assessing the Role of Ayurvedic 'Bhasms' as Ethno-nanomedicine in the Metal Based Nanomedicine Patent Regime. *J Intellectual Property Rights*, 16.
- PEROVIC, O., SINGH-MOODLEY, A., GOVENDER, N. P., KULARATNE, R., WHITELAW, A., CHIBABHAI, V., NAICKER, P., MBELLE, N., LEKALAKALA, R., QUAN, V., SAMUEL, C. & VAN SCHALKWYK, E. 2017. A small proportion of community-associated methicillin-resistant *Staphylococcus aureus* bacteraemia,

- compared to healthcare-associated cases, in two South African provinces. *Eur J Clin Microbiol Infect Dis*, 36, 2519-2532.
- PETROV, P. D., YONCHEVA, K., GANCHEVA, V., KONSTANTINOV, S. & TRZEBICKA, B. 2016. Multifunctional block copolymer nanocarriers for co-delivery of silver nanoparticles and curcumin: Synthesis and enhanced efficacy against tumor cells. *European Polymer Journal*, 81, 24-33.
- PLATZER, M., KIESE, S., HERFELLNER, T., SCHWEIGGERT-WEISZ, U., MIESBAUER, O. & EISNER, P. 2021. Common Trends and Differences in Antioxidant Activity Analysis of Phenolic Substances Using Single Electron Transfer Based Assays. *Molecules*, 26.
- POUDEL, B. K., SOE, Z. C., RUTTALA, H. B., GUPTA, B., RAMASAMY, T., THAPA, R. K., GAUTAM, M., OU, W., NGUYEN, H. T., JEONG, J. H., JIN, S. G., CHOI, H. G., YONG, C. S. & KIM, J. O. 2018. In situ fabrication of mesoporous silica-coated silver-gold hollow nanoshell for remotely controllable chemo-photothermal therapy via phase-change molecule as gatekeepers. *Int J Pharm*, 548, 92-103.
- PRESTINACI, F., PEZZOTTI, P. & PANTOSTI, A. 2015. Antimicrobial resistance: a global multifaceted phenomenon. *Pathogens and Global Health*, 109, 309-318.
- PRIYADHARSHINI, R. I., PRASANNARAJ, G., GEETHA, N. & VENKATACHALAM, P. 2014. Microwave-Mediated Extracellular Synthesis of Metallic Silver and Zinc Oxide Nanoparticles Using Macro-Algae (*Gracilaria edulis*) Extracts and Its Anticancer Activity Against Human PC3 Cell Lines. *Applied Biochemistry and Biotechnology*, 174, 2777-2790.
- RAFIQUE, M., SADAF, I., RAFIQUE, M. S. & TAHIR, M. B. 2017. A review on green synthesis of silver nanoparticles and their applications. *Artif Cells Nanomed Biotechnol*, 45, 1272-1291.
- RAHIM, K., SALEHA, S., ZHU, X., HUO, L., BASIT, A. & FRANCO, O. L. 2017. Bacterial Contribution in Chronicity of Wounds. *Microbial Ecology*, 73, 710-721.
- RAI, M., INGLE, A. P., GUPTA, I. & BRANDELLI, A. 2015. Bioactivity of noble metal nanoparticles decorated with biopolymers and their application in drug delivery. *Int J Pharm*, 496, 159-72.
- RAI, M., KON, K., INGLE, A., DURAN, N., GALDIERO, S. & GALDIERO, M. 2014. Broad-spectrum bioactivities of silver nanoparticles: the emerging trends and future prospects. *Appl Microbiol Biotechnol*, 98, 1951-61.

- RAMEZANPOUR, M., LEUNG, S. S., DELGADO-MAGNERO, K. H., BASHE, B. Y., THEWALT, J. & TIELEMAN, D. P. 2016. Computational and experimental approaches for investigating nanoparticle-based drug delivery systems. *Biochim Biophys Acta*, 1858, 1688-709.
- RAPPUOLI, R., BLOOM, D. E. & BLACK, S. 2017. Deploy vaccines to fight superbugs. *Nature*, 552, 165-167.
- RAZA, F., ZAFAR, H., AZAD, A. & SULAIMAN, M. 2023. Factors Influencing the Green Synthesis of Metallic Nanoparticles Using Plant Extracts: A Comprehensive Review. *Pharmaceutical Fronts*, 05, e117-e131.
- REPON, M. R., ISLAM, T., SADIA, H. T., MIKUČIONIENĖ, D., HOSSAIN, S., KIBRIA, G. & KASEEM, M. 2021. Development of Antimicrobial Cotton Fabric Impregnating AgNPs Utilizing Contemporary Practice. *Coatings*, 11.
- RIAZ, M., MUTREJA, V., SAREEN, S., AHMAD, B., FAHEEM, M., ZAHID, N., JABBOUR, G. & PARK, J. 2021. Exceptional antibacterial and cytotoxic potency of monodisperse greener AgNPs prepared under optimized pH and temperature. *Sci Rep*, 11, 2866.
- RIEHMANN, K., SCHNEIDER, S. W., LUGER, T. A., GODIN, B., FERRARI, M. & FUCHS, H. 2009. Nanomedicine--challenge and perspectives. *Angew Chem Int Ed Engl*, 48, 872-97.
- RIGO, C., FERRONI, L., TOCCO, I., ROMAN, M., MUNIVRANA, I., GARDIN, C., CAIRNS, W. R., VINDIGNI, V., AZZENA, B. & BARBANTE, C. 2013a. Active silver nanoparticles for wound healing. *International journal of molecular sciences*, 14, 4817-4840.
- RIGO, C., FERRONI, L., TOCCO, I., ROMAN, M., MUNIVRANA, I., GARDIN, C., CAIRNS, W. R., VINDIGNI, V., AZZENA, B., BARBANTE, C. & ZAVAN, B. 2013b. Active silver nanoparticles for wound healing. *Int J Mol Sci*, 14, 4817-40.
- RIVERA-RANGEL, R. D., GONZÁLEZ-MUÑOZ, M. P., AVILA-RODRIGUEZ, M., RAZO-LAZCANO, T. A. & SOLANS, C. 2018. Green synthesis of silver nanoparticles in oil-in-water microemulsion and nano-emulsion using geranium leaf aqueous extract as a reducing agent. *Colloids and Surfaces A: Physicochemical and Engineering Aspects*, 536, 60-67.
- ROLIM, W. R., PELEGRINO, M. T., DE ARAÚJO LIMA, B., FERRAZ, L. S., COSTA, F. N., BERNARDES, J. S., RODIGUES, T., BROCCHI, M. & SEABRA, A. B. 2019. Green tea extract mediated biogenic synthesis of silver nanoparticles: Characterization, cytotoxicity evaluation and antibacterial activity. *Applied Surface Science*, 463, 66-74.

- ROY, R., TIWARI, M., DONELLI, G. & TIWARI, V. 2018. Strategies for combating bacterial biofilms: A focus on anti-biofilm agents and their mechanisms of action. *Virulence*, 9, 522-554.
- SALEM, S. S. & FOUDA, A. 2021. Green Synthesis of Metallic Nanoparticles and Their Prospective Biotechnological Applications: an Overview. *Biological Trace Element Research*, 199, 344-370.
- SALVE, P., VINCHURKAR, A., RAUT, R., CHONDEKAR, R., LAKKAKULA, J., ROY, A., HOSSAIN, M. J., ALGHAMDI, S., ALMEHMADI, M., ABDULAZIZ, O., ALLAHYANI, M., DABLOOL, A. S., SARKER, M. M. R. & NUR AZLINA, M. F. 2022. An Evaluation of Antimicrobial, Anticancer, Anti-Inflammatory and Antioxidant Activities of Silver Nanoparticles Synthesized from Leaf Extract of *Madhuca longifolia* Utilizing Quantitative and Qualitative Methods. *Molecules*, 27.
- SÁNCHEZ-LÓPEZ, E., GOMES, D., ESTERUELAS, G., BONILLA, L., LOPEZ-MACHADO, A. L., GALINDO, R., CANO, A., ESPINA, M., ETTCHETO, M. & CAMINS, A. 2020. Metal-based nanoparticles as antimicrobial agents: an overview. *Nanomaterials*, 10, 292.
- SANHUEZA, L., MELO, R., MONTERO, R., MAISEY, K., MENDOZA, L. & WILKENS, M. 2017. Synergistic interactions between phenolic compounds identified in grape pomace extract with antibiotics of different classes against *Staphylococcus aureus* and *Escherichia coli*. *PLoS One*, 12, e0172273.
- SANTHOSH, S. B., RAGAVENDRAN, C. & NATARAJAN, D. 2015. Spectral and HRTEM analyses of *Annona muricata* leaf extract mediated silver nanoparticles and its Larvicidal efficacy against three mosquito vectors *Anopheles stephensi*, *Culex quinquefasciatus*, and *Aedes aegypti*. *Journal of Photochemistry and Photobiology B: Biology*, 153, 184-190.
- SARATALE, R. G., SARATALE, G. D., AHN, S. & SHIN, H. S. 2021. Grape Pomace Extracted Tannin for Green Synthesis of Silver Nanoparticles: Assessment of Their Antidiabetic, Antioxidant Potential and Antimicrobial Activity. *Polymers (Basel)*, 13.
- SARKAR, S. & DAS, R. 2018. Shape effect on the optical properties of anisotropic silver nanocrystals. *Journal of Luminescence*, 198, 464-470.
- SELVAKUMAR, P., SITHARA, R., VIVEKA, K. & SIVASHANMUGAM, P. 2018. Green synthesis of silver nanoparticles using leaf extract of *Acalypha hispida* and its application in blood compatibility. *Journal of Photochemistry and Photobiology B: Biology*, 182, 52-61.

- SERRA, A. T., MATIAS, A. A., NUNES, A. V. M., LEITÃO, M. C., BRITO, D., BRONZE, R., SILVA, S., PIRES, A., CRESPO, M. T., SAN ROMÃO, M. V. & DUARTE, C. M. 2008. In vitro evaluation of olive- and grape-based natural extracts as potential preservatives for food. *Innovative Food Science & Emerging Technologies*, 9, 311-319.
- SHAMELIRAJIRI, M., AMINSALEHI, M., SHAHBANDEH, M., MALEKI, A., JONOUBI, P. & RAD, A. C. 2021. Anticancer and therapeutic potential of Delonix regia extract and silver nanoparticles (AgNPs) against pancreatic (Panc-1) and breast (MCF-7) cancer cell. *Toxicology and Environmental Health Sciences*, 13, 45-56.
- SHARMA, R., AASHIMA, NANDA, M., FRONTERRE, C., SEWAGUDDE, P., SSENTONGO, A. E., YENNEY, K., ARHIN, N. D., OH, J., AMPONSAH-MANU, F. & SSENTONGO, P. 2022. Mapping Cancer in Africa: A Comprehensive and Comparable Characterization of 34 Cancer Types Using Estimates From GLOBOCAN 2020. *Front Public Health*, 10, 839835.
- SHARON, M., SHARON, M., PANDEY, D. S. & OZA, G. 2012. *Bio-nanotechnology : Concepts and Applications*.
- SIBBALD, R. G., CONTRERAS-RUIZ, J., COUTTS, P., FIERHELLER, M., ROTHMAN, A. & WOO, K. 2007. Bacteriology, inflammation, and healing: a study of nanocrystalline silver dressings in chronic venous leg ulcers. *Adv Skin Wound Care*, 20, 549-58.
- SIDHU, A. K., VERMA, N. & KAUSHAL, P. 2022. Role of biogenic capping agents in the synthesis of metallic nanoparticles and evaluation of their therapeutic potential. *Frontiers in Nanotechnology*, 3, 801620.
- SILVA, V., IGREJAS, G., FALCO, V., SANTOS, T. P., TORRES, C., OLIVEIRA, A. M. P., PEREIRA, J. E., AMARAL, J. S. & POETA, P. 2018. Chemical composition, antioxidant and antimicrobial activity of phenolic compounds extracted from wine industry by-products. *Food Control*, 92, 516-522.
- SIMON, S., SIBUYI, N. R. S., FADAKA, A. O., MEYER, M., MADIEHE, A. M. & DU PREEZ, M. G. 2021. The antimicrobial activity of biogenic silver nanoparticles synthesized from extracts of Red and Green European pear cultivars. *Artificial Cells, Nanomedicine, and Biotechnology*, 49, 613-624.
- SIMON, S., SIBUYI, N. R. S., FADAKA, A. O., MEYER, S., JOSEPHS, J., ONANI, M. O., MEYER, M. & MADIEHE, A. M. 2022. Biomedical Applications of Plant Extract-Synthesized Silver Nanoparticles. *Biomedicines*, 10.

- SIRIWONG, S., TEETHAISONG, Y., THUMANU, K., DUNKHUNTHOD, B. & EUMKEB, G. 2016. The synergy and mode of action of quercetin plus amoxicillin against amoxicillin-resistant *Staphylococcus epidermidis*. *BMC Pharmacol Toxicol*, 17, 39.
- SMITHA, S., PHILIP, D. & GOPCHANDRAN, K. 2009. Green synthesis of gold nanoparticles using *Cinnamomum zeylanicum* leaf broth. *Spectrochimica Acta Part A: Molecular and Biomolecular Spectroscopy*, 74, 735-739.
- SOLTYS, L., OLKHOVYY, O., TATARCHUK, T. & NAUSHAD, M. 2021. Green Synthesis of Metal and Metal Oxide Nanoparticles: Principles of Green Chemistry and Raw Materials. *Magnetochemistry*, 7, 145.
- SONI, N. & DHIMAN, R. C. 2017. Phytochemical, Anti-oxidant, Larvicidal, and Antimicrobial Activities of Castor (*Ricinus communis*) Synthesized Silver Nanoparticles. *Chinese Herbal Medicines*, 9, 289-294.
- SONI, R. A., RIZWAN, M. A. & SINGH, S. 2022. Opportunities and potential of green chemistry in nanotechnology. *Nanotechnology for Environmental Engineering*, 7, 661-673.
- SOUZA, T. G., CIMINELLI, V. S. & MOHALLEM, N. D. S. A comparison of TEM and DLS methods to characterize size distribution of ceramic nanoparticles. *Journal of Physics: Conference Series*, 2016. IOP Publishing, 012039.
- SPAMPINATO, S. F., CARUSO, G. I., DE PASQUALE, R., SORTINO, M. A. & MERLO, S. 2020. The Treatment of Impaired Wound Healing in Diabetes: Looking among Old Drugs. *Pharmaceuticals (Basel)*, 13.
- SPIRESCU, V., CHIRCOV, C., GRUMEZESCU, A., VASILE, B. & ANDRONESCU, E. 2021. Inorganic Nanoparticles and Composite Films for Antimicrobial Therapies. *International Journal of Molecular Sciences*, 22, 4595.
- SRIDHAR, K. & CHARLES, A. L. 2019. In vitro antioxidant activity of Kyoho grape extracts in DPPH and ABTS assays: Estimation methods for EC50 using advanced statistical programs. *Food Chemistry*, 275, 41-49.
- SRIKAR, S. K., GIRI, D. D., PAL, D. B., MISHRA, P. K. & UPADHYAY, S. N. 2016. Green Synthesis of Silver Nanoparticles: A Review. *Green and Sustainable Chemistry*, 06, 34-56.
- SUN, Y.-S., ZHAO, Z., YANG, Z.-N., XU, F., LU, H.-J., ZHU, Z.-Y., SHI, W., JIANG, J., YAO, P.-P. & ZHU, H.-P. 2017. Risk Factors and Preventions of Breast Cancer. *International Journal of Biological Sciences*, 13, 1387-1397.

- TANG, B., KAUR, J., SUN, L. & WANG, X. 2013. Multifunctionalization of cotton through in situ green synthesis of silver nanoparticles. *Cellulose*, 20, 3053-3065.
- TANG, K. W. K., MILLAR, B. C. & MOORE, J. E. 2023. Antimicrobial Resistance (AMR). *Br J Biomed Sci*, 80, 11387.
- THANH, N. C., PUGAZHENDHI, A., CHINNATHAMBI, A., ALHARBI, S. A., SUBRAMANI, B., BRINDHADEVI, K., WHANGCHAI, N. & PIKULKAEW, S. 2022. Silver nanoparticles (AgNPs) fabricating potential of aqueous shoot extract of *Aristolochia bracteolata* and assessed their antioxidant efficiency. *Environmental Research*, 208, 112683.
- THOMFORD, N. E., SENTHEBANE, D. A., ROWE, A., MUNRO, D., SEELE, P., MAROYL, A. & DZOBO, K. 2018. Natural Products for Drug Discovery in the 21st Century: Innovations for Novel Drug Discovery. *Int J Mol Sci*, 19.
- TIWARI, G., TIWARI, R., SRIWASTAWA, B., BHATI, L., PANDEY, S., PANDEY, P. & BANNERJEE, S. K. 2012. Drug delivery systems: An updated review. *Int J Pharm Investig*, 2, 2-11.
- TOSHIMA, N. & YONEZAWA, T. 1998. Bimetallic nanoparticles—novel materials for chemical and physical applications. *New Journal of Chemistry*, 22, 1179-1201.
- TYAVAMBIZA, C., ELBAGORY, A. M., MADIEHE, A. M., MEYER, M. & MEYER, S. 2021. The antimicrobial and anti-inflammatory effects of silver nanoparticles synthesised from *Cotyledon orbiculata* aqueous extract. *Nanomaterials*, 11, 1343.
- TYAVAMBIZA, C., MEYER, M., WUSU, A. D., MADIEHE, A. M. & MEYER, S. 2022. The Antioxidant and In Vitro Wound Healing Activity of *Cotyledon orbiculata* Aqueous Extract and the Synthesized Biogenic Silver Nanoparticles. *International Journal of Molecular Sciences*, 23, 16094.
- VAN DER MEEL, R., SULHEIM, E., SHI, Y., KIESSLING, F., MULDER, W. J. & LAMMERS, T. 2019. Smart cancer nanomedicine. *Nature nanotechnology*, 14, 1007-1017.
- VARONI, E. M., LOFARO, A. F., SHARIFI-RAD, J. & IRITI, M. 2016. Anticancer molecular mechanisms of resveratrol. *Frontiers in nutrition*, 3, 8.
- VENUGOPAL, K., RATHER, H. A., RAJAGOPAL, K., SHANTHI, M. P., SHERIFF, K., ILLIYAS, M., RATHER, R. A., MANIKANDAN, E., UVARAJAN, S., BHASKAR, M. & MAAZA, M. 2017. Synthesis of silver nanoparticles (Ag NPs) for anticancer activities (MCF 7 breast and A549 lung cell lines) of the crude extract of *Syzygium aromaticum*. *J Photochem Photobiol B*, 167, 282-289.

- WANG, M., HUANG, X., ZHENG, H., TANG, Y., ZENG, K., SHAO, L. & LI, L. 2021. Nanomaterials applied in wound healing: Mechanisms, limitations and perspectives. *Journal of Controlled Release*, 337, 236-247.
- WANG, M., ZHAO, J., ZHANG, L., WEI, F., LIAN, Y., WU, Y., GONG, Z., ZHANG, S., ZHOU, J., CAO, K., LI, X., XIONG, W., LI, G., ZENG, Z. & GUO, C. 2017. Role of tumor microenvironment in tumorigenesis. *Journal of Cancer*, 8, 761-773.
- WILKINSON, L. J., WHITE, R. J. & CHIPMAN, J. K. 2011. Silver and nanoparticles of silver in wound dressings: a review of efficacy and safety. *J Wound Care*, 20, 543-9.
- WRIGHT, G. D. 2019. Unlocking the potential of natural products in drug discovery. *Microb Biotechnol*, 12, 55-57.
- XU, C., YAGIZ, Y., HSU, W. Y., SIMONNE, A., LU, J. & MARSHALL, M. R. 2014. Antioxidant, antibacterial, and antibiofilm properties of polyphenols from muscadine grape (*Vitis rotundifolia* Michx.) pomace against selected foodborne pathogens. *J Agric Food Chem*, 62, 6640-9.
- XU, Y., BURTON, S., KIM, C. & SISMOUR, E. 2016. Phenolic compounds, antioxidant, and antibacterial properties of pomace extracts from four Virginia-grown grape varieties. *Food Sci Nutr*, 4, 125-33.
- YANG, H., CHEN, T., WANG, H., BAI, S. & GUO, X. 2018. One-pot rapid synthesis of high aspect ratio silver nanowires for transparent conductive electrodes. *Materials Research Bulletin*, 102, 79-85.
- YANG, Y. & HU, H. 2015. A review on antimicrobial silver absorbent wound dressings applied to exuding wounds. *J. Microb. Biochem. Technol*, 7, 228-233.
- YANG, Y., QIN, Z., ZENG, W., YANG, T., CAO, Y., MEI, C. & KUANG, Y. 2017. Toxicity assessment of nanoparticles in various systems and organs. *Nanotechnology Reviews*, 6, 279-289.
- YIN, M., WU, J., DENG, M., WANG, P., JI, G., WANG, M., ZHOU, C., BLUM, N., ZHANG, W., SHI, H., JIA, N., WANG, X. & HUANG, P. 2021. Multifunctional Magnesium Organic Framework-Based Microneedle Patch for Accelerating Diabetic Wound Healing. *ACS Nano*, 15.
- YOU, C., LI, Q., WANG, X., WU, P., HO, J. K., JIN, R., ZHANG, L., SHAO, H. & HAN, C. 2017. Silver nanoparticle loaded collagen/chitosan scaffolds promote wound healing via regulating fibroblast migration and macrophage activation. *Sci Rep*, 7, 10489.

- ZAHEER, Z. & AAZAM, E. S. 2017. Cetyltrimethylammonium bromide assisted synthesis of silver nanoparticles and their catalytic activity. *Journal of Molecular Liquids*, 242, 1035-1041.
- ZEIN, R., ALGHORAIBI, I., SOUKKARIEH, C., SALMAN, A. & ALAHMAD, A. 2020. In-vitro anticancer activity against Caco-2 cell line of colloidal nano silver synthesized using aqueous extract of *Eucalyptus Camaldulensis* leaves. *Heliyon*, 6.
- ZHANG, L., BAO, M., LIU, B., ZHAO, H., ZHANG, Y., JI, X., ZHAO, N., ZHANG, C., HE, X. & YI, J. 2020. Effect of andrographolide and its analogs on bacterial infection: a review. *Pharmacology*, 105, 123-134.
- ZHANG, X.-F., LIU, Z.-G., SHEN, W. & GURUNATHAN, S. 2016. Silver Nanoparticles: Synthesis, Characterization, Properties, Applications, and Therapeutic Approaches. *International Journal of Molecular Sciences*, 17, 1534.
- ZHANG, X., SUN, H., TAN, S., GAO, J., FU, Y. & LIU, Z. 2019. Hydrothermal synthesis of Ag nanoparticles on the nanocellulose and their antibacterial study. *Inorganic Chemistry Communications*, 100, 44-50.
- ZHOU, Q., LV, J., REN, Y., CHEN, J., GAO, D., LU, Z. & WANG, C. 2017. A green in situ synthesis of silver nanoparticles on cotton fabrics using Aloe vera leaf extraction for durable ultraviolet protection and antibacterial activity. *Textile Research Journal*, 87, 2407-2419.
- ZUAS, O., ABIMANYU, H. & WIBOWO, W. 2014. Synthesis and characterization of nanostructured CeO₂ with dyes adsorption property. *Processing and Application of Ceramics*, 8, 39-46.
- ZUGAZAGOITIA, J., GUEDES, C., PONCE, S., FERRER, I., MOLINA-PINELO, S. & PAZ-ARES, L. 2016. Current Challenges in Cancer Treatment. *Clin Ther*, 38, 1551-66.
- ZULKIFLI, F. H., HUSSAIN, F. S. J., ZEYOHANNES, S. S., RASAD, M. & YUSUFF, M. M. 2017. A facile synthesis method of hydroxyethyl cellulose-silver nanoparticle scaffolds for skin tissue engineering applications. *Mater Sci Eng C Mater Biol Appl*, 79, 151-160.